AD743016

ADVANCED FLAME ARRESTOR MATERIALS
AND
TECHNIQUES FOR FUEL TANK PROTECTION

Quentin C. Malmberg
Edwin W. Wiggins

MCDONNELL AIRCRAFT COMPANY
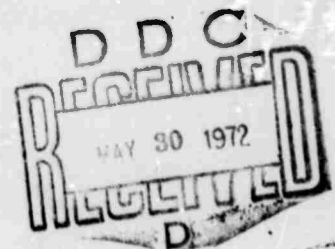
TECHNICAL REPORT AFAPL-TR-72-12

March 1972

D D C
RECEIVED
MAY 30 1972
D

Air Force Aero Propulsion Laboratory
Air Force Systems Command
Wright-Patterson Air Force Base, Ohio

160

DISCLAIMER NOTICE
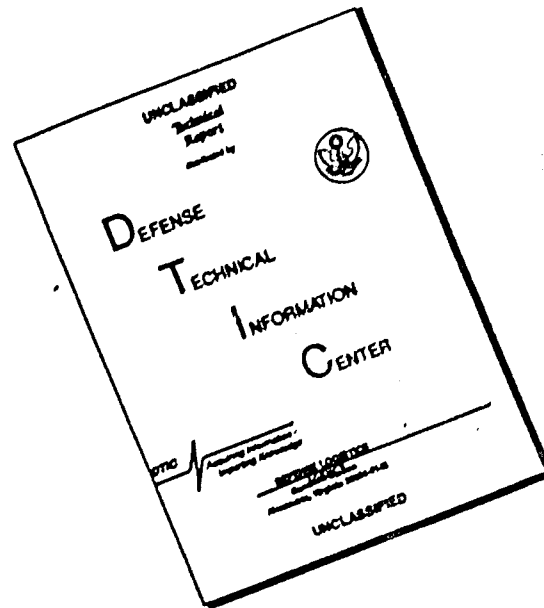
THIS DOCUMENT IS BEST QUALITY AVAILABLE. THE COPY FURNISHED TO DTIC CONTAINED A SIGNIFICANT NUMBER OF PAGES WHICH DO NOT REPRODUCE LEGIBLY.

NOTICES

When Government drawings, specifications, or other data are used for any purpose other than in connection with a definitely related Government procurement operation, the United States Government would thereby encourage no responsibility nor any obligation whatsoever; and the fact that the Government may have formulated, furnished, or in any way supplied the said drawings, specifications, or other data, is not to be regarded by any implication otherwise as in any manner licensing the holder for any other person or corporation, or conveying any rights or permission to manufacture, use, or sell any patented inventions that may in any way be related thereto.

Copies of this report should not be returned unless return is required by security considerations, contractual obligations, or notice on a specific document.

DOCUMENT CONTROL DATA - R & D

(Security classification of title, body of abstract and indexing annotation must be entered when the overall report is classified)

1. ORIGINATING ACTIVITY *(Corporate author)*	2a. REPORT SECURITY CLASSIFICATION
McDonnell Douglas Corporation P. O. Box 516 St. Louis, Missouri 63166	Unclassified
	2b. GROUP

3. REPORT TITLE

Advanced Flame Arrestor Materials and Techniques for Fuel Tank Protection

4. DESCRIPTIVE NOTES *(Type of report and inclusive dates)*
Final Technical Report - 28 December 1970 - 26 November 1971

5. AUTHOR(S) *(First name, middle initial, last name)*
Quentin C. Malmberg
Edwin W. Wiggins

6. REPORT DATE	7a. TOTAL NO. OF PAGES	7b. NO. OF REFS
	148	0

8a. CONTRACT OR GRANT NO	9a. ORIGINATOR'S REPORT NUMBER(S)
b. PROJECT NO. 3048	
c. Task 304807	9b. OTHER REPORT NO(S) *(Any other numbers that may be assigned this report)*
d. Work Unit 304807038	AFAPL-TR-72-12

10. DISTRIBUTION STATEMENT

Approved for Public Release, Distribution Unlimited

11. SUPPLEMENTARY NOTES	12. SPONSORING MILITARY ACTIVITY
	Air Force Aero Propulsion Laboratory Wright Patterson Air Force Base, Ohio 45433

13. ABSTRACT

The purpose of Phase I was to develop and test concepts for minimizing the weight and volume displacement penalties of polyurethane foam explosion arrestor suppression systems. Both structural and integral isolation concepts for arrestor voiding techniques were investigated. For fuselage tanks the integral concept of large hollow cylinders offered the greater percentage void (58%) for unpressurized tanks while the voided foam lined wall configuration was the better approach for pressurized fuselage tanks. The small six-celled wing tank egg crate pattern provided for 95 and 87% void at 0 and 2 psig initial system pressure respectively while for the large wing tank 42% void at 0, 2 and 5 psig initial system pressure was possible.

Phase II was the materials investigation portion of the program and evaluated flame arrestor effectiveness, fuel flow resistance and thermophysical properties of representative candidate materials and configuration. The most efficient of the sixteen material candidates from an arrestor effectiveness standpoint was 3M polyester Scotch Brite felt. The material thermophysical properties of thermal conductivity, specific heat, density and surface area have only a small effect on material explosion suppression performance.

Collation of data from Phase I and II was accomplished in Phase III of the program. Empirical relationships for the test data were developed through computerized regression analysis and the relative importence of the applicable variables was determined.

14 KEY WORDS	LINK A		LINK B		LINK C	
	ROLE	WT	ROLE	WT	ROLE	WT
Flame Arrestor Configurations						
Void Percent						
Polyurethane Foam						
Fuel Tank Protection						
Explosion Arrestor System						

ADVANCED FLAME ARRESTOR MATERIALS AND

TECHNIQUES FOR FUEL TANK PROTECTION

Quentin C. Malmberg
Edwin W. Wiggins

Details of illustrations in
this document may be better
studied on microfiche

Approved for public release;
distribution unlimited

FOREWORD

This report was prepared by Q. C. Malmberg and
E. W. Wiggins, Survivability/Vulnerability Design Section,
McDonnell Aircraft Company, McDonnell Douglas Corporation,
St. Louis, Missouri. The work reported herein was carried
out under Contract No. F33615-71-C-1191, Project No. 3048,
"Advanced Flame Arrestor Materials and Techniques for Fuel
Tank Protection," and was administered by the Fire Protec-
tion Branch, Air Force Aero Propulsion Laboratory, Air Force
Systems Command, Wright-Patterson Air Force Base, Ohio with
A. J. Ferrenberg as Project Engineer. The period covered
by this report is December 28, 1970 to November 26, 1971.

This report was submitted by the authors December 27,
1971.

This technical report has been reviewed and is approved.

B. P. Botteri

B. P. Botteri, Chief Fire Protection
Branch, Fuels Lubrication and Hazards
Division, Air Force Aero Propulsion
Laboratory, Weight-Patterson Air
Force Base, Ohio

ABSTRACT

The "Flame Arrestor Materials and Techniques for Fuel Tank Protection" work program was subdivided into three phases. Phases I and II involved the testing of reticulated polyurethane foam configurations and installation techniques and other candidate materials for flame arrestor effectiveness. Phase III consisted of the reduction and analysis of all the recorded data.

The purpose of Phase I was to develop and test concepts for minimizing the weight and volume displacement penalties of polyurethane foam explosion suppression systems. Both structural and integral isolation concepts for arrestor voiding techniques were investigated. These two approaches adjust weight and volume displacement penalties with respect to allowable fuel tank structural limits and system over-pressures. The structural isolation concept utilized natural aircraft structural compartmentization whereas the integral isolation concept used closed compartments within the foam itself in the form of hollow bodies. For unpressurized fuselage tanks the integral concept of large hollow cylinders offered the greater percentage void (58.5%) while the voided foam lined wall configuration was the better approach for pressurized fuselage tanks. The most effective foam configurations for small and large simulated wing tank systems were the egg crate and lined wall concepts. The small six-celled wing tank egg crate pattern provided 92 and 87% void at 0 and 2 psig initial system pressure respectively, while for the large three cell wing tank 42% void at 0, 2 and 5 psig initial system pressure was possible. Limited tests on the lined wall configuration showed 80 and 47% voiding to be possible for the small six cell and large three cell wing tank systems respectively.

Installation and fabrication techniques were addressed throughout this portion of the program and the hollow body and egg crate designs proved to be the best approach to simple installation and fabrication.

Phase II was the materials investigation portion of the program and evaluated flame arrestor effectiveness, fuel flow resistance and thermophysical properties of representative candidate materials and configurations. The most efficient of the sixteen material candidates evaluated from an arrestor effectiveness standpoint was 3M Scotch Brite. Following this came the Scott Paper Co. fire extinguishing foam and the 25 pore per inch (ppi) low density reticulated polyurethane foam materials. Fluid flow tests reversed the sequence of these materials from a pressure drop performance standpoint. Wetting agents and coatings improved arrestor effectiveness to only a small degree but showed that with the proper material configuration they could contribute significantly to reduce flame penetration. The material thermophysical properties of thermal conductivity, specific heat, density and surface area exhibited only a small effect on material explosion suppression performance.

Collation of data from Phases I and II was accomplished in Phase III of the program. Empirical relationships for the test data were developed through computerized regression analysis and the relative importance of the applicable variables was determined.

TABLE OF CONTENTS

Preceding page blank

TABLE OF CONTENTS (CONT'D)

LIST OF FIGURES

LIST OF FIGURES (CONT'D)

LIST OF TABLES

SECTION I

INTRODUCTION AND SUMMARY

Fuel tank fires and explosions are a major cause of aircraft losses in combat. Considerable research and development has been devoted to exploring fuel tank explosion protection concepts. Nitrogen dilution, chemical quenching and polyurethane foam void filler material emerge as the primary candidate systems. Of these the passive, logistics free polyurethane foam systems appears ideal. Light-weight (low density) foam and gross voiding techniques are used to reduce the weight and volume penalties encountered in contemporary foam system installations. Previous work by MCAIR, in cooperation with Scott Paper Co., successfully demonstrated a low-density reticulated polyurethane foam explosion suppression system with 80 to 90 percent voiding. This degree of voiding had only been demonstrated in tanks that were subdivided into a number of intercommunicating cells such as aircraft wing tanks which are inherently segmented by ribs and spars. Where compartmentization is not inherent as in the case of aircraft fuselage tanks, a lesser percent voiding is possible for equal allowable combustion over-pressures as evidenced by the work performed by Bureau of Mines where up to 40% voiding was achieved for single cell configurations.

Basically two types of gross voiding concepts presently exist. The first is a structural isolation design as in aircraft wing fuel tanks where the structure offers natural compartmentization with intercommunicating openings between cells. Foam is used to isolate fires to the combustion cell by acting as a flame arrestor, stopping the flame propagation to the adjacent cells. Pressure generated by the combustion process in the ignited cell is relieved through the foam and intercommunicating holes. The second variation of this concept uses hollow foam bodies to provide flame isolated compartments with walls of sufficient thickness to locally isolate fires. Combustion pressure is relieved through the foam and into isolated volumes. Both of these concepts have been investigated in Phase I of this program with an arbitrary system success criteria of 10 psi allowable combustion over-pressure.

The Phase I effort of this program was designed to improve and optimize installation concepts and techniques for foam fire and explosion suppression in simulated aircraft fuselage and wing fuel tanks. Configurations designed to accomplish these program objectives were established to provide data that would optimize the system operation from a foam void standpoint. Foam volumes were predetermined for all systems in order that test void volumes could be increased or decreased in increments of 5% of the total tank volume. Combustion tests were conducted at each void increment and the pressure and temperature in each cell of the specimen was recorded. Each configuration was tested at 0, 2 and 5 psig initial pressure with successively larger or smaller void volumes until an over-pressure from combustion of 10 psi was reached. In some cases where it was obvious that data could be successfully extrapolated, the tests were completed when sufficient data were obtained to establish a curve.

Phase II investigated material flame arrestor effectiveness with respect to combustion over-pressure and fuel flow resistance. Thermophysical properties determinations of candidate arrestor materials were conducted including thermal conductivity, specific heat, melting temperature, heat of fusion, bulk density,

1

specific fuel retention and surface area. Combustion testing was divided
into three tasks: (1) arrestor material configuration and screening tests,
(2) basic material evaluation tests and (3) coating tests. The success criterion
of the arrestors was based on a combustion over-pressure limit of 25 PSI.

All material combustion and fuel flow pressure drop tests were con-
ducted in an eight-inch diameter plexiglass tube using a material thickness
of two inches. Combustion tests were conducted at 0, 2 and 5 psig initial
system pressures and flow tests were run at 50, 100, and 150 gpm flow rates
using JP-4 as the fluid media. Thermophysical properties tests were conducted
on those materials that performed satisfactorily through at least one
set of combustion parameters.

Data from Phases I and II of the program were reduced and collated dur-
ing Phase III. Application of the data from the Phase I effort was directed
toward weight and volume displacement panalties as well as system advantages
and disadvantages for design of explosion suppression systems for both retro-
fit and new aircraft. Arrestor effectiveness data was analyzed to determine
the relationships of chemical interactions and system parameters and the
relative significance of these parameters on the performance of the material
as a flame arrestor. Empirical relationships were developed by computer
regression analysis with all applicable data included. These relationships
give direction to the future development of flame arrestor materials by
pointing to the parameter's relative effectiveness toward flame suppression.

Data from the program have lead to the following conclusions:

o The maximum void percentage obtained in these tests for the
   simulated 100 gallon aircraft fuselage fuel tank is 58.5% at
   0 psig initial system pressure using a 10 psig over-pressure
   success criterion and was accomplished using large (15 inch
   diameter) hollow foam cylinders.

o The ten percent voided foam lined wall fuselage tanks configuration
   offers the lightest weight and subsequently the largest void percent-
   age (52 and 47.5%) system of those tested for 2 and 5 psig initial
   pressure.

o Egg crate type patterns offer the greatest degree of design freedom
   as well as the most efficient flame barrier system with the greatest
   amount of void volume (92% at 0 psig, 87% at 2 psig, and 79% at 5 psig
   initial test pressures) of the configurations tested for the six-cell
   simulated aircraft wing tank.

o The egg crate voiding configuration performed to the 50% void volume
   level for the three-cell 300 gallon simulated aircraft wing tank.

o Systems with a number of small voids may not be as effective as
   those with fewer larger voids.

o All void vapor volume in the hollow body configurations tested burned
   when the system combustion over-pressure reached 5 psig from the
   initial ignition.

o Successive ignitions using the same foam are possible for fire and
   explosion suppression systems.

2

o 15 ppi foam is not as efficient as 25 ppi foam in voided
  fire and explosion suppression systems at percentages
  greater than 20%.

o The performance of hollow body configurations is hindered by
  the fact that for a projectile simulated line source ignition,
  combustion occurs simultaneously inside and outside the foam
  wall, thus burning a greater portion of combustibles within
  the foam.

o Combustion volume to foam thickness is the primary design parameter
  for gross voided foam explosion suppression systems.

o The use of other materials in a gross voided configuration for
  explosion suppression is possible.

o 3M polyester felt, "Scotch Brite," showed the best possibility
  as a substitute material of those tested.

o Where fuel flow pressure drop is an important system operation
  parameter the 25 ppi Scott reticulated polyurethane foam appeared to
  be the best material tested.

o Wetting agents are more effective in eliminating burn through than
  reducing combustion over-pressure when the relief to combustion
  volume (Vr/Vc) ratios are small.

o The thermophysical properties investigated have a negligible effect
  on the explosion suppression capabilities of the material.

o Arrestor material geometry appears to be the most important parameter
  in eliminating flame propagation with foams and felts being the best
  configurations tested.

PHASE I TEST PROGRAM

1.0   TEST SET-UP

1.1   Test Specimen

Three specimens were used throughout Phase I testing. The specimens
were (1) a 100 gallon fuselage tank, (2) a 300 gallon 6 cell wing tank,
and (3) a 300 gallon 3 cell wing tank. The three specimens were assembled
from six 30 x 24 x 15 inch elemental boxes. Each elemental box was
basically a steel angle iron frame which had match drilled sides so that
the elements could be assembled in any combination. The boxes were de-
signed with both steel and plexiglass side and cover plates capable of
withstanding 40 psig over-pressure. Plexiglass covers provided the
capability to photographically record the explosion events.

The fuselage tank was constructed by assembling two sets of frames and
panels to produce a 30 x 30 x 24 inch tank (Fig. 1). This size was selected
to meet the military standard 100 gallon fuselage test tank so that the data
generated could be compared to other similar work.

The three and six celled wing tanks were assembled from the six
elemental frames to produce 90 x 48 x 15 and 90 x 30 x 24 inch tanks
respectively, Figures 2 and 3. The three celled tank had, 55% cell to
cell intercommunication while the six celled tank was provided with only
5% cell to cell intercommunicating open area.

1.2   Instrumentation

The instrumentation consisted of strain gage type transducers, and 40
gauge cromel-alumel thermocouples in each cell of the respective specimen.
The pressure, temperature and ignition time data was recorded on oscillo-
graph traces at 15 inches per second as shown in the sample trace of Figure 4.
The thermocouple outputs were used only to monitor ignition and flame propa-
gation in that combustion temperatures exceeded their useful range.

1.3   Explosive Mixture

Premixed propane/air mixtures near stoichiometric conditions were used
as the combustible media in each test and the foam was wetted with JP-5 fuel.
This simulated explosive aircraft tank condition was used for test simplicity
in lieu of JP-4 flushing. If JP-4 had been used, stoichiometric vapor/air
conditions could have been achieved only by cooling the entire test article
below 40°F. The use of propane/air JP-5 permitted testing at all ambient
and specified initial pressure conditions. Previous tests using propane/air
proved that it produces results equivalent to JP-4/air combustion.

Preceding page blank
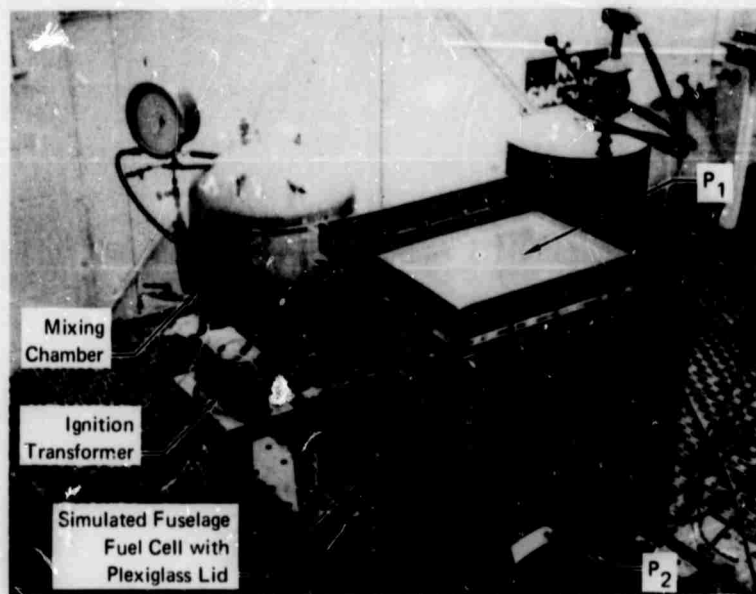
FIGURE 1 FUSELAGE FUEL CELL TEST SET UP

GP 71-239-4

Ignition
Cell

Bomb
Sampler
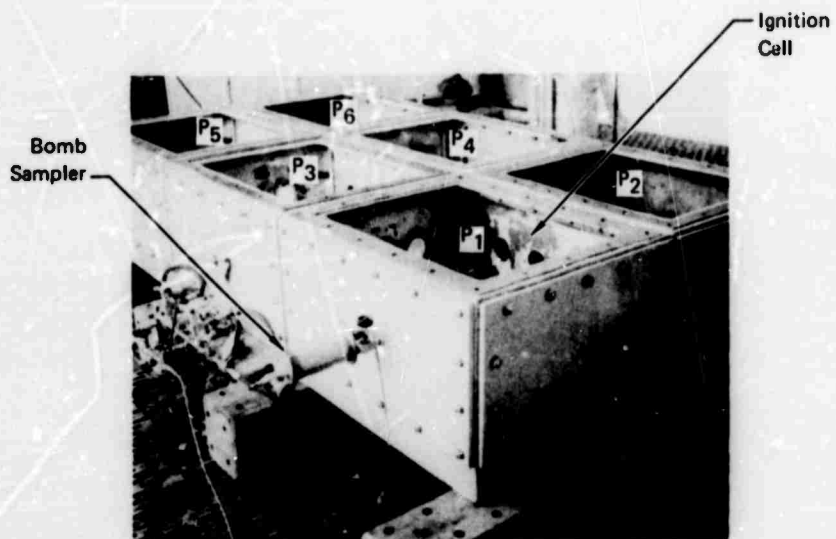
FIGURE 2 SIMULATED SIX CELL WING TANK TEST SET UP

GP71-0937-25

7
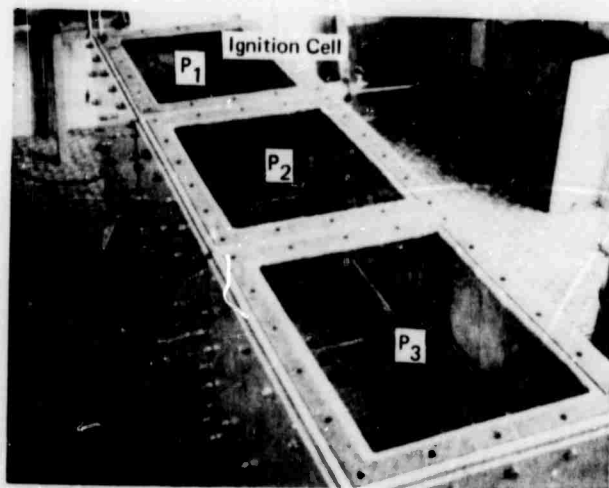
FIGURE 3 SIMULATED THREE CELL WING TANK TEST SET UP

GP71 0937 26

8

Bomb Sample Test
For Propane/Air Mixture
Combustion Effectiveness Value

96 psi

Simulated Fuselage Fuel Tank
Combustion Pressure Rise With
40% Void Lined Walled Configuration
at 0 psig Initial Pressure

T_1 T_2 T_3

7.9 psi 7.7 psi 7.7 psi

Ignition P_1 P_2 P_3 P_4 Ignition

P_1, P_2, P_3 (10 psi/inch) P_4 (25 psi/inch)

Note: Paper Speed 15 inches per second
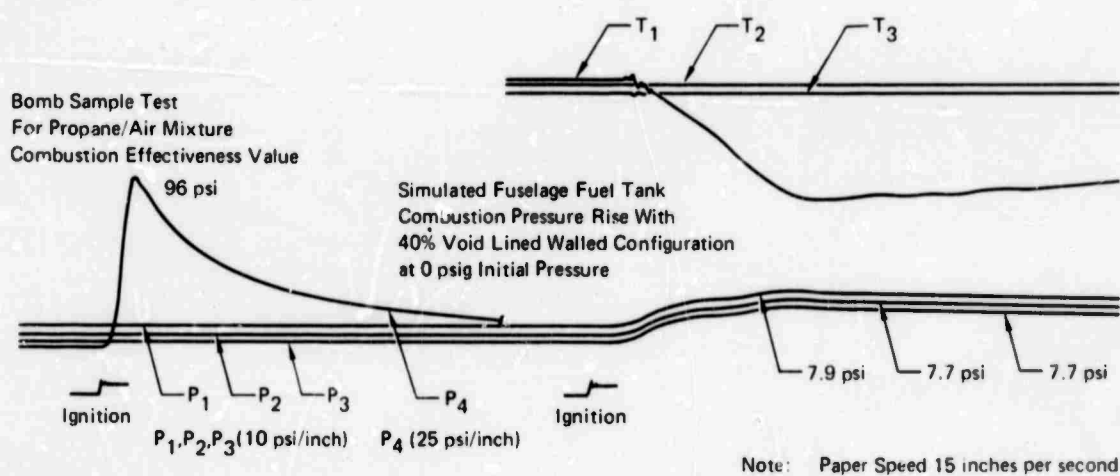
FIGURE 4 TEST PRESSURE TRACE

GP71-0237-29

9

1.4 Ignition System

The ignition system used was a standard Bureau of Mines luminous tube transformer set-up operated at 60 to 70 volts primary. The ignitor portion of the set-up was varied slightly to simulate a straight line projectile path ignition source. This was accomplished by placing the ignitor in a perforated tube which extended from wall to wall, simultaneously igniting all individual voids along its path.

2.0 TEST CONFIGURATIONS

2.1 General

The test configurations for all three specimens were designed around the structural and integral voiding concepts. The percent voiding range was based upon the MCAIR model of Arrestor Suppressed Explosions. This model relates the tank over-pressure to the ratio of relief volume to combustion volume, and the initial pressure. Using this model and the program defined success criteria of 10 psig over-pressure the initial test void was calculated and the testing proceeded from that point in ± 5% incremental void changes. Initially all test configurations were tested using 25 ppi, 1.36 lb/ft^3 reticulated polyurethane foam. After the best configuration for the fuselage tank specimen was established, 15 ppi, 1.36 lb/ft^3 reticulated polyurethane foam was tested in that configuration.

2.2 Fuselage Tank Configurations

Four fuselage foam configurations were investigated. These configurations were (a) lined walls, (b) voided lined walls, (c) large flat end hollow cylinders and (d) small flat and hemispherical ended cylinders shown in Figure 5. These configurations were varied in total void percentages as described in the following paragraphs.

2.2.1 Lined Wall Configuration

Model analysis of the lined wall configuration for initial pressures of 0, 2 and 5 psig, predicted that the maximum allowable void percentages would be 46, 43, and 39% void respectively. This variation in void percentage was adopted and predetermined thicknesses of foam to obtain 5% incremental voids from 30 to 45 percent were stacked on the specimen walls. Tests were run by removing the inner most layer of foam after each ignition.

2.2.2 Voided Lined Wall Configurations

This configuration was basically the same as the lined wall configuration with the exception that sixteen voids within the foam were included as shown in Figure 6. The total void percentage was the sum of these internal voids and the center void. The total void % for the configuration was varied from 30 to 60% using 10, 15 and 25% internal voids and 15 to 45% center voiding. The void sizes and wall thickness used are given in Table 1 and a photograph of an actual set of voided wall segments is presented in Figure 7.

10
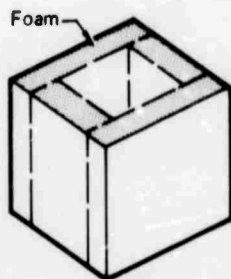
Lined Wall
Configuration A
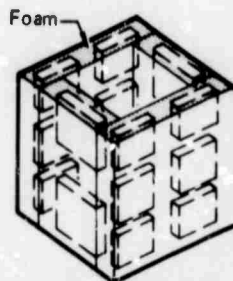
Voided Lined Wall
Configuration B
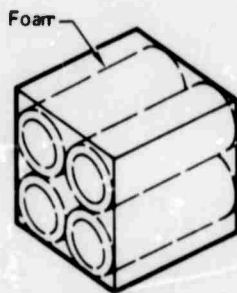
Large Diameter Hollow Cylinders
Configuration C
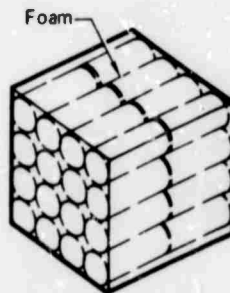
Small Diameter Hollow Cylinders
Configurations D & E

FIGURE 5 FUSELAGE FUEL TANK FOAM CONFIGURATIONS

GP71-0937-27

11
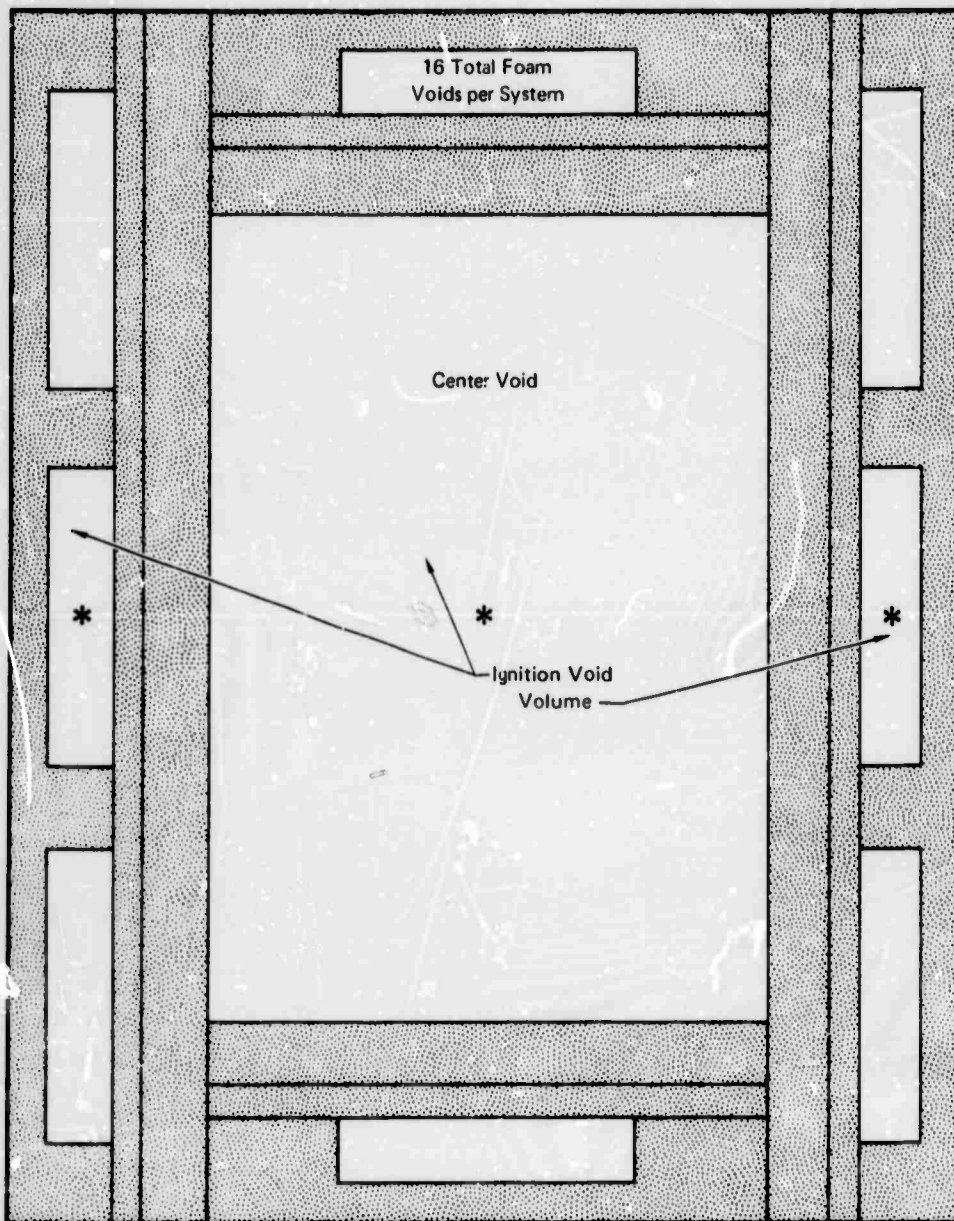
FIGURE 6   VOIDED WALL CONFIGURATION

VOIDED FOAM LINED WALL CONFIGURATION
FOAM VOID DIMENSIONS

Test No.	Foam Void Dim. (in)	(%)	Center Void Dim. (in)	(%)	Total Volume (in³)	Foam Void Outer Dim. (in)	Foam Void Inner Dim. (in)	Foam Thickness Foam Void To Center Void	Total Void (%)
1	1.6 x 7.33 x 11	10.0	30 x 15.2 x 9.2	20.5	20,500 →	30 x 28 x 22	30 x 24.8 x 19.8	4.8 in.	30.5
2	1.6 x 7.33 x 11	10.0	30 x 16.4 x 10.4	25.0		30 x 28 x 22	30 x 24.8 x 18.8	4.2 in.	35.0
3	1.6 x 7.33 x 11	10.0	30 x 17.6 x 11.6	29.9		30 x 28 x 22	30 x 24.8 x 18.8	3.6 in.	39.9
4	1.6 x 7.33 x 11	10.0	30 x 18.8 x 12.8	35.3		30 x 28 x 22	30 x 24.8 x 18.8	3.0 in.	45.3
5	1.6 x 7.33 x 11	10.0	30 x 19.8 x 13.8	40.0		30 x 28 x 22	30 x 24.8 x 18.8	2.5 in.	50.0
6	1.6 x 7.33 x 11	10.0	30 x 21.7 x 15.7	50.0		30 x 28 x 22	30 x 24.8 x 18.8	1.55 in.	60.0
7	1.6 x 7.33 x 11	10.0	30 x 19.8 x 18.8	40.0		30 x 28 x 22	30 x 24.8 x 18.8	2.50 in.	50.0
8	1.6 x 7.33 x 11	10.0	30 x 20.8 x 14.8	45.0		30 x 28 x 22	30 x 24.8 x 18.8	2.00 in.	55.0
9	1.6 x 7.33 x 11	10.0	30 x 18.8 x 12.8	35.3		30 x 28 x 22	30 x 24.8 x 18.8	3.00 in.	45.3
10	1.6 x 7.33 x 11	10.0	30 x 19.8 x 13.8	40.0		30 x 28 x 22	30 x 24.8 x 18.8	2.50 in.	50.0
11	2.4 x 7.33 x 11	15.1	30 x 18.8 x 12.8	35.3		30 x 28 x 22	30 x 23.2 x 17.2	2.20 in.	50.4
12	2.4 x 7.33 x 11	15.1	30 x 17.6 x 11.6	29.9		30 x 28 x 22	30 x 23.2 x 17.2	2.80 in.	45.0
13	2.4 x 7.33 x 11	15.1	30 x 17.6 x 11.6	29.9		30 x 28 x 22	30 x 23.2 x 17.2	2.80 in.	45.0
14	1.6 x 7.33 x 11	10.0	30 x 21.7 x 15.7	50.0		30 x 28 x 22	30 x 24.8 x 18.6	1.55 in.	60.0
15	4.0 x 7.33 x 11	25.0	30 x 13.6 x 7.6	15.0		30 x 28 x 22	30 x 20 x 14	3.20 in.	40.0
16	4.0 x 7.33 x 11	25.0	30 x 15.2 x 9.2	20.5		30 x 26 x 22	30 x 20 x 14	2.40 in.	45.5
17	4.0 x 7.33 x 11	25.0	30 x 16.4 x 10.4	25.0		30 x 23 x 22	30 x 20 x 14	1.80 in.	50.0

13
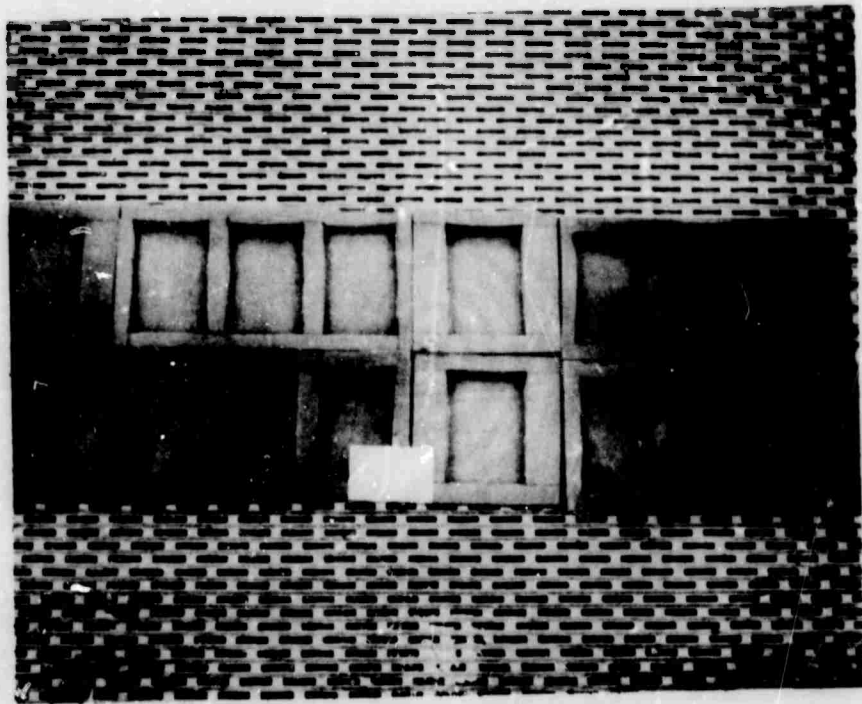
FIGURE 7   VOID WALL SEGMENTS

2.2.3 Large Diameter Hollow Cylinders (Flat Ends)

Void percentages for the 15 inch diameter 12 inch long cylinders were varied from 40 to 60%. Two sets of cylinders with varied wall and end thicknesses were used for all testing. The first set of cylinders were configured with 2.75 inch walls and 1.0 inch ends and were used for tests 1 through 6 given in Table 5. The second set was fabricated with 1.95 inch wall and ends and used for test number 7. Alteration of this set to 1.85 inch wall and end thickness was made for tests 8 through 13. Tests 11 and 12 used the first set of cylinders with 2.4 inch thick walls and ends. Figure 8 is a photograph of this configuration installed in the fuselage tank.

2.2.4 Small Diameter Hollow Cylinders

Two configurations of 7.5 inch diameter hollow cylinders were tested, flat end 24 inch long cylinders and hemispherical end 12 inch long cylinders. The void percentage range for each configuration was obtained by varying the inside diameter of the cylinders. The flat end configuration was tested from 30 to 50% total void while the hemispherical end cylinders were tested from 40 to 60% total void. Figure 9 is a photograph of the installed flat end cylinders and Figure 10 is a photograph of a hemispherical end hollow cylinder.

2.3 Wing Tank Configurations

Two tank specimens were used, a three and six cell simulated 300 gallon wing tank previously described. Lined wall and egg crate foam configurations as described for the fuselage tanks were evaluated in these specimens. In addition to these configurations 7.5 and 15 inch diameter cylinders were tested in the six cell specimen. Figures 11 and 12 are schematics of these wing tank configurations.

Extensive work was conducted on the egg crate design since both the void volume and foam wall thickness were investigated. (Table 2) The number of void volumes were varied from 4 to 24 per cell depending on the total void desired. A schematic of a typical installation is shown in Figure 13 while photographs of the six and three cell wing tank installation are presented as Figures 14 and 15.

Total voiding for these specimens was considerably higher than that of the fuselage tanks in that the relief to combustion volume for subdivided tanks is naturally much higher. The total void percentages tested for these configurations ranged from 40 to 90% for the six celled specimen and 30 to 80% for the three cell wing tank specimen.

3.0 TEST PROCEDURE

The test procedure for all three tank specimens and all foam configurations was basically the same. After the desired foam configuration was fabricated and installed in the test specimen the foam was wetted with JP-5 fuel. All excess JP-5 fuel was drained off before ignition. The specimen was then sealed and evacuated to 5 psia with a water educator in preparation for the

15
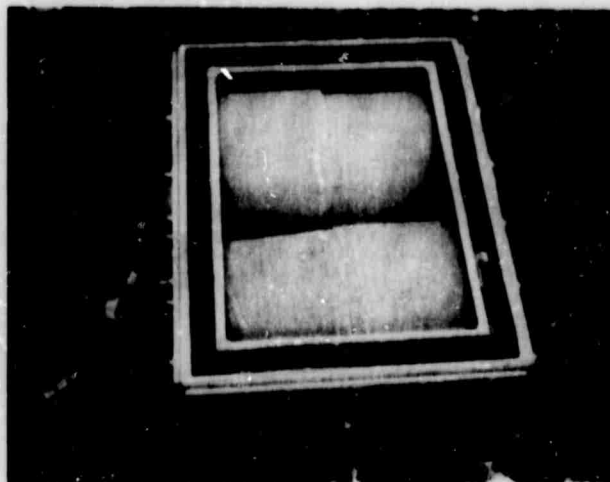
**FIGURE 8   15 INCH DIAMETER CYLINDER INSTALLATION
IN SIMULATED FUSELAGE TANK**

7.5" Dia. Cyl.
24" Long
1.45" Thick
45% Void
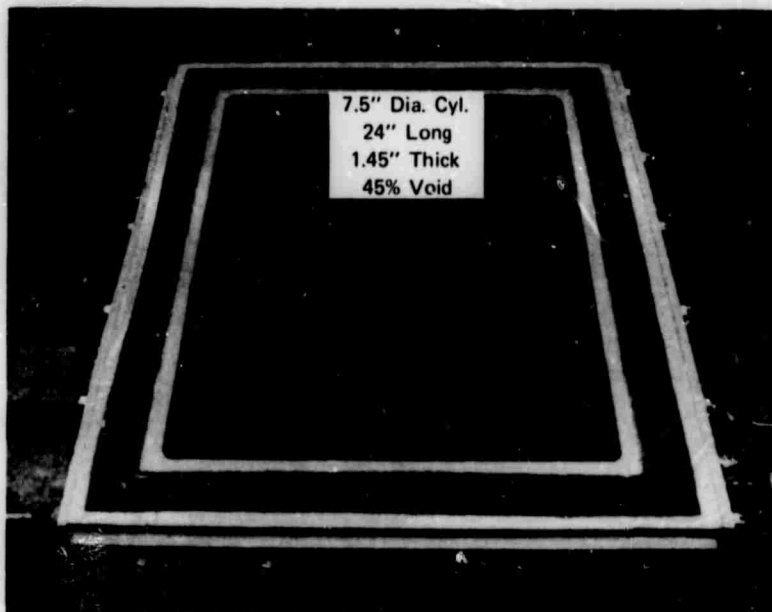
FIGURE 9   7.5 INCH DIAMETER CYLINDER INSTALLATION
IN SIMULATED FUSELAGE TANK

GP71-0937-38

17

7.5" Dia. Cyl.
Spherical Ends
12" Long
1.45" Thick
55% Void
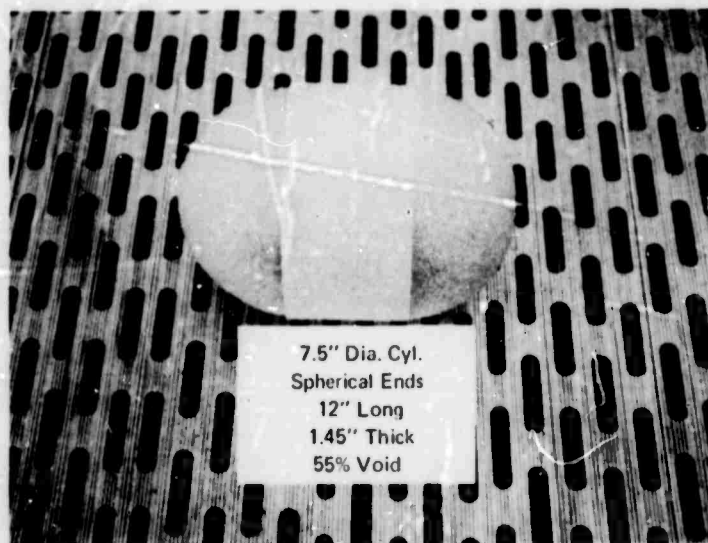
FIGURE 10 TYPICAL 7.5 INCH DIAMETER
CYLINDER WITH HEMISPHERICAL ENDS

GP71-0937-49
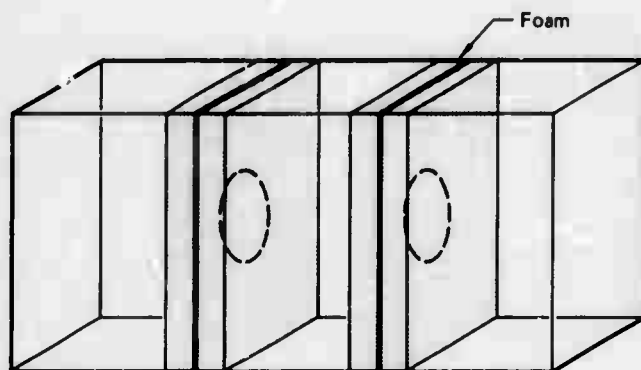
Configuration A
Lined Walls
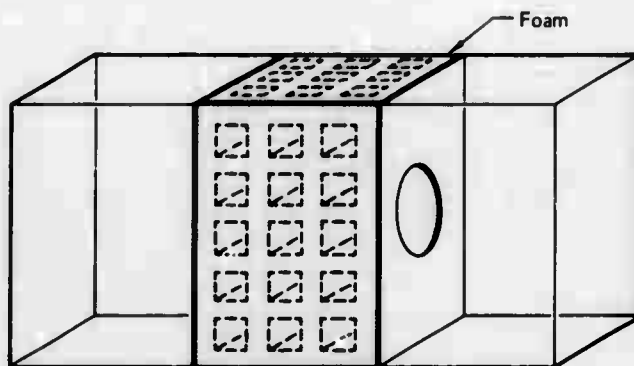
Configuration B
Egg Crate

FIGURE 11 THREE CELL WING TANK FOAM CONFIGURATIONS

GP71-0937 53

19
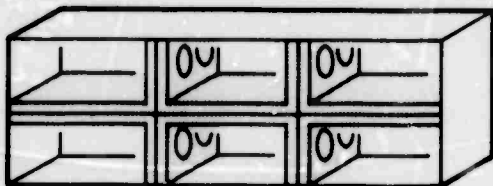
Configuration A
Lined Walls
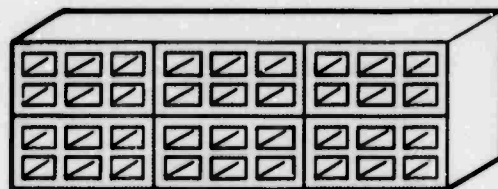
Configuration B
Egg Crate
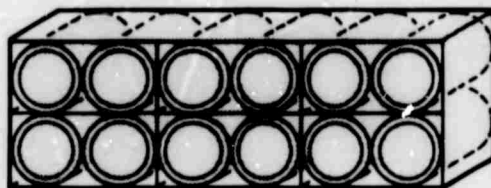
Configurations C & D
Cylinders (Large & Small)

FIGURE 12 SIX CELL WING TANK FOAM CONFIGURATIONS

GP71-0937-50

TABLE II

EGG CRATE CONFIGURATION DIMENSIONS

Test Number	Number Of Voids	Size (in)	Cell Wall Thickness (in)	Middle Section Thickness (in)	Top And Bottom Thickness (in)	Inside Wall Thickness (in)	Outside Wall Thickness (in)
1-3	24	6.25 x 5.6 x 6.2	1	1	.5	1	1
4-7	24	6.25 x 7.125 x 6.25	.5	1	.5	.5	.75
8-11	12	6.50 x 10.6 x 8.7	1	1	.5	1	1
12-14	12	7.00 x 10.9 x 9.0	1	1	None	.5	.5
15-16	4	11.0 x 14.0 x 15.0	1	None	None	.5	.5

21
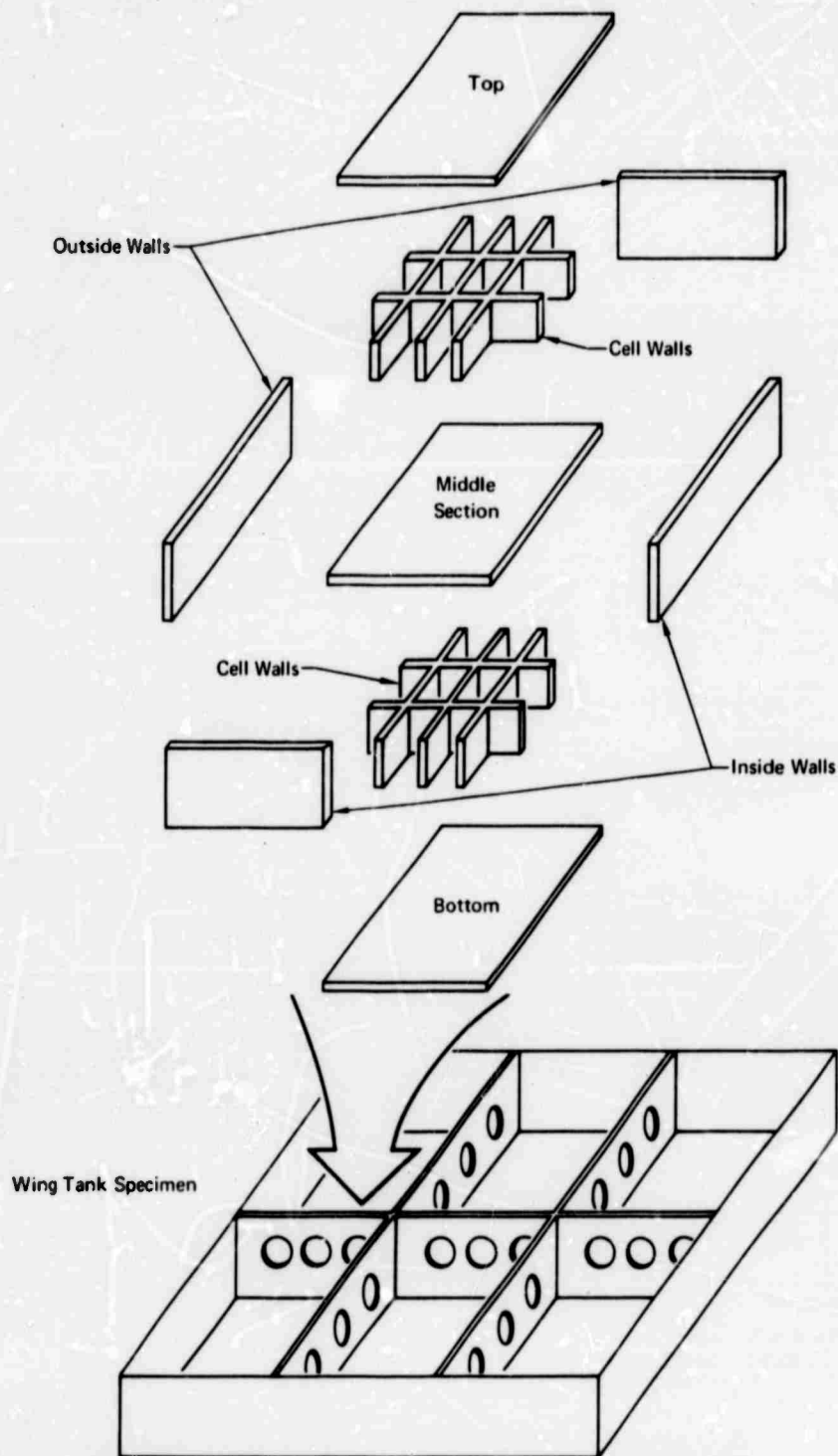
FIGURE 13 SCHEMATIC OF EGG CRATE ARRANGEMENT

Top

Outside Walls

Cell Walls

Middle Section

Cell Walls

Inside Walls

Bottom

Wing Tank Specimen

GP71-0937-51

22

25 PPI Reticulated Foam
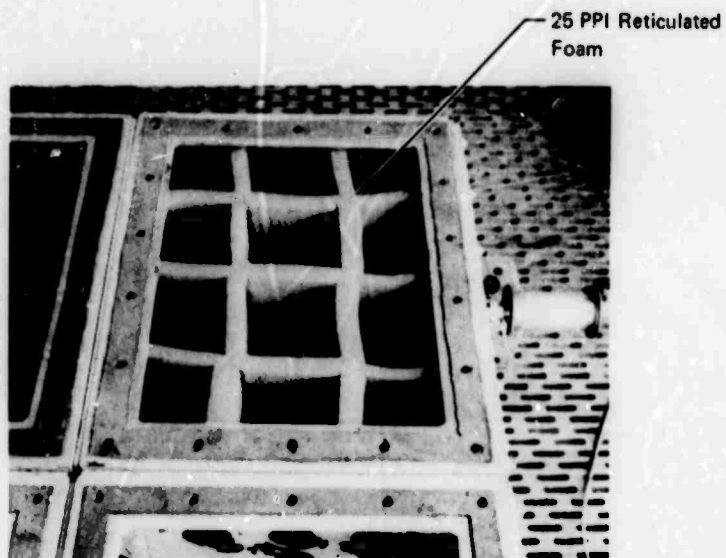
FIGURE 14 FOAM EGG CRATE INSTALLATION

GP71-0937-15

23
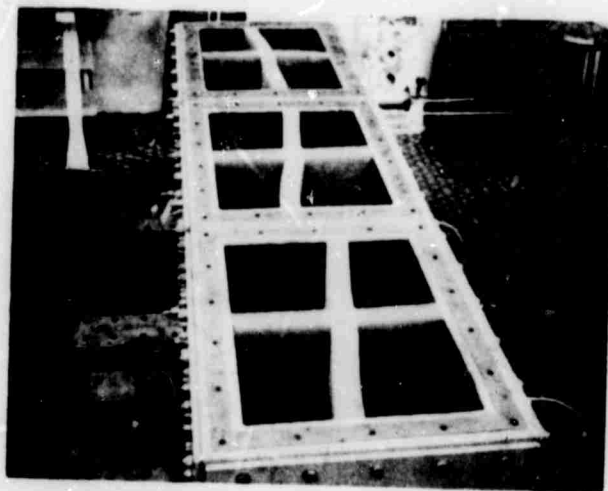
**FIGURE 15 THREE CELL WING TANK
EGG CRATE CONFIGURATION**

GP71-0937-55

24

introduction of the premixed pressurized propane/air mixture. The propane/
air mixture was made up in a separate mixing tank by introducing a pre-
determined partial pressure of propane into the tank and pressurizing the
tank with shop air to the calculated total pressure required. The mixing tank
and the specimen tank were manifolded together and brought to pressure
equilibrium via the interconnecting plumbing shown schematically in Figure 16.
After equilibrium was established the mixing tank was isolated and the test
specimen was bled down through the bomb sampler to the desired initial
pressure 0, 2 or 5 psig. The bomb sampler was then isolated from the
specimen by valving. The sample mixture was ignited and the peak pressure
recorded prior to each test. This procedure verified the explosive mixture
conditions and established the adiabatic expansion factor used in the
model and data analysis.

The ignition of the test specimen's explosive mixture immediately
followed that of the bomb sample. After the completion of this test
sequence the complete system was purged and made ready for the next test.
Foam void configurations were varied as were the initial pressures until the
resultant specimen tank over-pressure of 10 psig was exceeded and sufficient
data was obtained to define the configuration performance. Then a new con-
figuration of foam was introduced into the program.

4.0 RESULTS AND DISCUSSION OF RESULTS

All of the data for the three tank specimens and their respective foam
configurations are presented in four ways. The raw data is presented as
tables, whereas the reduced data is presented graphically (1) as physically
installed and tested (2) according to the theoretical model and (3) in
summary bar form. The graphs of the "as tested" are in the form of total
installed void percent versus peak combustion to initial absolute pressure
ratio. The total installed void percent is also the percent reduction in
weight and volume penalties for the foam system and thus of direct value
to the designer. Absolute peak combustion to initial pressure ratios are used
instead of ΔP's in that theoretical considerations predict that this approach
will normalize the data for different initial pressures thereby consolidating
the graphical data. Although this normalizing was not realized it is still
felt that the pressure ratio presentation is useful and convenient.

The second form of the data correlation presents the actual relief to
combustion volume ratio to the various observed peak combustion to initial
absolute pressure ratios. Plotting the data in the relief/combustion volume
theoretical form provided a means of monitoring the data for gross deviations
and interpretation of the results. In many cases particularly where internal
void configurations were being tested several pressure peaks were observed
on the oscillograph traces. The first observed over-pressure correlated with
the initial ignited volume whereas the intermediate peak over-pressure was
shown to correlate well with the total void volume, indicating burn through
or ignition of the secondary inner voids. Since straight line, simulated pro-
jectile ignition was used in the testing the relief volume to combustion volume
varied from one configuration to another even though the total void percent
was the same.

25

Labels in figure:
- Ignitor
- Ignition Bomb
- Test Tank Vent
- 150 PSIG Transducer
- 40 PSIG Relief Valve
- 100 PSI Gauge
- Vent
- Shop Air
- Propane
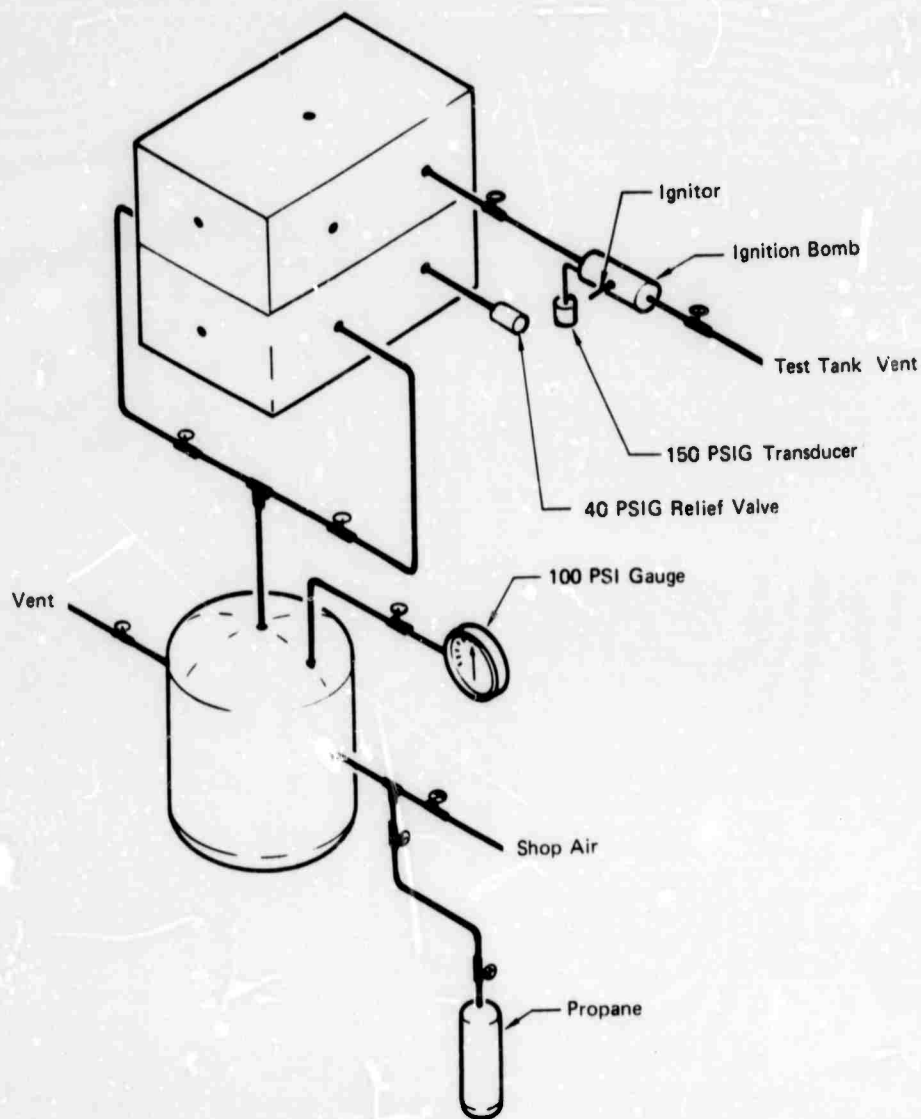
FIGURE 16 FUSELAGE TANK TEST SETUP

GP71-0937-59

The bar graphs are presented to provide a simple visual comparison of the foam voiding configuration capabilities ss compared to each other. From these graphs the superior configuration for any of the program test parameters can be easily determined as indicated by the solid bars.

4.1 Fuselage Tank Results

Tables 3 through 8, present the test conditions, configuration and combustion over-pressure data for the simulated 100 gallon fuselage tank. Only the maximum or peak combustion over-pressures are given in these tables. The average peak over-pressures were converted to absolute pressure ratios and plotted against total void volume. These plots are presented in Figures 17 through 32. The theoretical relief/combustion volume curves are presented as Figures 24 through 31.

4.1.1 Lined Wall Configuration

The lined wall foam configuration data are plotted in Figure 17 and can be seen to correlate quite well with the theoretical curve up to 40% voiding even though the initial pressures were varied from 0 to 5 psig. These same data also correlate quite well with the theoretical model parameters as shown in Figure 24. The divergence of data from that predicted theoretically is caused by penetration of the flame front into the foam. Flame penetration into arrestor materials were observed in the movies and is known to be a function of both pressure and foam pore diameter. It can be clearly seen that both parameters prevail by inspecting the three curves; theoretical, 25 and 15 pores per inch foam in Figure 18. The 25 ppi foam configuration was adopted as the base line to compare with other configurations and therefore appears in all the fuselage tank configuration graphs.

4.1.2 Voided Lined Walls

This configuration was essentially the same as the previous discussed lined wall configuration with the exception that closed "hidden" voids constituting 10, 15 and 25% of the total tank volume were incorporated in the foam liner. In all cases this additional voiding was divided into 16 individual cells of which two were included in the initial ignition volume. Consequently one-eighth of the additional voiding was negated thereby displacing the curve above the base line as seen in Figures 18 through 20. In the case of the 10% voided wall configuration the theoretical shift of 7/8 of the additional voiding was obtained out to the 45% baseline point. However in the case of the 15 and 25% voided lined wall configuration full theoretical improvement was not obtained as several of the wall voids ignited during the test. The data are good however, as can be seen in Figures 26 and 27. In these plots the peak over-pressures are plotted against the theoretical curve parameters and are seen to correlate. In addition the initial or intermediate pressures are plotted against the initial combustion relief volumes where applicable and maximum pressure against the assumed total void combustion volume to relief volume. The latter plot correlates well with the theoretical curve and therefore it can be

concluded that all inner voids are burning, but on a delayed basis. The size of the center void volume, in addition to wall thickness, affects the performance of this approach. This is to be expected in that as previously discussed the larger the center void volume the greater the resultant heat flux, pressure and depth of penetration. Graphically this can be observed in Figures 19 and 20 for the 15% and 25% voided wall configuration. The center void volume in the 15% voided lined wall configuration was greater than that of the 25% voided wall configuration for the same total void %, therefore flame penetration and burning of the voids within the foam occurs sooner for the 15% configuration. This did not occur with the 10% voided foam liner since the foam thickness to combustion volume was greater. These results would lead to the conclusion that an optimum void volume to foam thickness exists and that if all voids were uniform the optimum total voiding could be reached. This optimum configuration would be an egg crate configuration with more and more voids as the tank volume got larger. This relationship is further supported by results from other configurations and larger cell tests to be discussed.

4.1.3 Large Diameter Hollow Cylinders

This configuration was quite successful. The small number of voids and the resulting greater foam thickness to combustion volume can probably be credited with the success. There were four internal voids of which two in addition to the void external to the cylinders were initially ignited. The expected improvement in voiding performance was realized at zero psig initial pressure as can be seen from Figure 21. At higher initial pressures however the depth of flame penetration caused all of the internal voids to burn as evidenced in Figures 21 and 23. When all the voids burned the configuration reverted to the baseline performance.

4.1.4 Small Diameter Hollow Cylinders

Two configurations of hollow 7.5 inch diameter cylinders were tested. Flat end twenty four inch long and hemispherical end twelve inch long cylinders of four wall thicknesses were run. Figures 22 and 23 show the performance of these two configurations. It is quite apparent that the shorter hemispherical end cylinders were superior. Of interest here is the divergence from predicted performance. The different initial pressures gave different curves which plot below the baseline. Some explanation of the pressure phenomena can be gained by looking at Figures 29 and 30. In these it is quite obvious that nearly all the flat end cylinders were penetrated as were all but three test conditions for the smaller hemispherical end cylinders. The flat end cylinders had a smaller initial combustion volume and yet performed more poorly. The principal difference was the flat end cylinders had small external combustion volume channels which tend to slow flame speed. This slow flame freely penetrates the foam. One explanation for the data below the baseline is the fact that in the positive initial pressure tests where this is evident, higher resulting combustion pressure occurs thus the flame penetrates into the foam from both sides and subsequently burns more vapor. This effect was discussed when the baseline was established. (Paragraph 4.1.1)

28

4.1.5 Fuselage Tank Summary

Figure 32 summarized the results of all the fuselage configurations
tested. The three bar graphs for 0, 2 and 5 psig show that the large
hollow cylinders are best for 0 psig tankage while the 10% voided lined
wall configuration is better for the 2 and 5 psig initial tank pressure system.
These results might well be different for larger or smaller tanks in that
the combustion volume has a direct proportional effect in system resultant
pressure rise. Further, the multicell two or three tier egg crate configuration
not investigated might well out perform either of the two best candidates
thus far evolved as the geometry of this configuration allows for greater
void percentages while keeping the combustion volumes small.

4.2 Six Cell Wing Tank Results

The tank specimen used in the following series of tests contained six
cells each of 50 gallon capacity. There were four foam configurations tested.
The results and test parameters are presented in Tables 9 through 12. The
test configurations were lined walls, egg crates, and small and large hollow
cylinders. Figures 33 through 39 percent the data in graphical form.

4.2.1 Six Cell Lined Wall

The lined wall system was given only a cursory investigation since
previous MCAIR tests revealed that this design used in an 80% void configuration
in a relatively small scale test fixture produced excellent results. Testing
for this configuration was limited to an 80% void arrangement at 0, 2 and 5 psig
initial pressure to determine the applicability to larger size wing tanks.
The limit of cell size to voiding for this configuration is still now known and
should be further investigated.

4.2.2 Six Cell Egg Crate Configuration

Extensive work was conducted on the egg crate design since both the
void volume and foam wall thickness had to be optimized. Table 10 contains
the data for this configuration while Figures 33 and 36 present the results
in graphical form. It can be seen that this configuration works best with
one inch foam separation walls. This thickness is characteristic of the
25 ppi foam. Smaller pores would require less thickness while larger pores
would require a greater thickness. The percent void allowable for the 10
psig over-pressure criteria was found to be 90, 87, and 70 for 0, 2 and 5 psig
initial system pressures.

4.2.3 Six Cell Large Hollow Cylinders

Figures 34 and 37 present the results for this configuration while
Table 11 contains the data. The performance here matched that of the
fuselage tank tests. While only two points were established for the wing
tank they correlated well with the fuselage tank results as shown in Figure 34.

4.2.4 Six Cell Small Hollow Cylinders

Figures 35 and 38 present the results for this configuration while the data are contained in Table 12. From Figure 35 it can be seen that three curves, one for each initial pressure test condition, were obtained. The smaller 7.5 inch diameter cylinders in this size tankage performed better than the 15 inch diameter cylinders. Equivalent results however were obtained in the fuselage tank at greater void percentages.

4.2.5 Six Cell Configuration Summary

In general for the six cell 300 gallon wing tank it can be concluded that the egg crate followed by the lined wall configuration were the better designs (See Figure 39). The hollow bodies are more sensitive to initial pressure and when flame penetration into the inner voids occurs greater than the theoretical minimum pressure results. This latter fact is probably due to a pumping action where the outside ignition pushes some combustibles into the foam followed by internal ignition pushing it back out to be further reacted. This action does not occur with the lined wall or egg crate design since there is no external/internal voiding. The lined wall and egg crate configurations act in one direction resulting in data that falls very near to the theoretical predictions.

4.3 Three Cell Wing Tank Results

Tests for this segment of the program were carried out in a three cell 300 gallon specimen. Two foam configurations were tested the results of which are presented in Tables 13 and 14. The configurations tested were lined wall and egg crate. The data are graphically presented in Figures 40 through 44.

4.3.1 Three Cell Lined Wall

Only ambient pressure system tests were conducted with the lined wall configuration as the performance resulted in only a 47° void system. The degradation of performance of this configuration in the three celled specimen is due to the larger combustion volumes with respect to foam and relief volumes. It is interesting to note that this void percent is the predicted value for the equivalent size fuselage tank.

4.3.2 Three Cell Egg Crate Configuration

The egg crate configuration performed to a 42% void at the 0, 2 and 5 psig initial system pressure. Once again the larger voids in the three celled specimen for the egg crate configuration dictated the limit of performance. In only one case did the flame fail to penetrate the walls of the egg crate voids. From Figure 43 it is obvious that for the remaining tests all available void volume was ignited as the calculated data for combustion of all voids plot within testing tolerances of the theoretical curve.

4.3.3 Three Cell Configuration Summary

Tests in the three cell specimen reveal that lined wall and egg crate foam configuration perform equally well. (See Figure 44). The larger initial ignition volumes substantially reduce the void possibilities because of the reduction of V_r/V_c when considering V_c equal to ignition volume only. Reducing the size of the voids does not increase the total possible system void if a one inch minimum foam wall thickness is maintained.

SECTION III

CONCLUSIONS AND RECOMMENDATIONS

5. CONCLUSIONS

The Phase I tests of this program have shown that aircraft fuel tank fire and explosion suppression may be readily accomplished by the use of voided reticulated polyurethane foam systems. Fuel tank size and shape as well as foam configuration have proven to dictate to a degree the amount of voiding possible when using the program success criterion of 10 psi combustion over-pressures.

o The largest percentage void (58.5%) for 100 gallon fuselage tanks at 0 psig initial pressure, was obtained using fifteen inch diameter hollow foam cylinders.

o The greatest amount of voiding in fuselage tanks was obtained with the 10% voided lined wall configuration with 52 and 47.5 percent total void for the 2 and 5 psig initial pressure.

o The 80% void, lined wall foam configuration was successfully tested at 0, 2 and 5 psig initial pressures in the 300 gallon, six cell simulated wing tank.

o The six cell wing tank egg crate pattern performed within 10 psi maximum combustion over-pressure to 92% void at 0 psig initial system pressures.

o The lined wall foam configuration performed satisfactorily up to 45% for the three cell 300 gallon simulated wing tank.

o The egg crate configuration for the three cell simulated wing tank specimen provided 40%, 30% and 50% maximum void with 0, 2 and 5 psig initial system pressure respectively.

o No special installation techniques were required for any of the foam designs tested. The hollow body configurations were assembled with adhesive prior to installation while the lined wall and egg crate patterns were held in place within the respective tank by cutting the pieces oversize and compressing them in place.

6.0 RECOMMENDATIONS

It is recommended that further testing of the lined wall and egg crate configurations be conducted using actual aircraft tanks and a gunfire ignition source. Further it is recommended that tests be conducted to determine the maximum and minimum opening between cells to determine their effect on the void concept. Hollow spheres should be tested in future work as this configuration appears to be promising and quite adaptable to system retrofit.

Preceding page blank

33

TABLE III

FUSELAGE FUEL TANK SYSTEM TEST DATA
LINED WALL CONFIGURATION

Test	Config.	Description	Foam Pore Size (ppi)	Foam Density (lb/ft³)	Foam Void	Total Void	Amb. Pressure (psia)	Initial System Pressure (psia)	Bomb Sample Ignition Pressure Rise (psig)	Simulated Fuel Tank Ignition Pressure ΔP_1	ΔP_2	ΔP_3
1	A	Lined Walls Center Cavity	25	1.35	0	27.1	14.13	14.13	95.25	4.25	4.40	4.40
2	A	Lined Walls Center Cavity	25	1.35	0	35.0	14.31	14.31	95.3	6.00	6.30	6.10
3	A	Lined Walls Center Cavity	25	1.35	0	39.8	14.37	14.37	95.0	7.70	7.70	7.60
4	A	Lined Walls Center Cavity	25	1.35	0	44.8	14.37	14.37	96.1	16.10	13.70	14.30
5	A	Lined Walls Center Cavity	25	1.35	0	35.0	14.33	16.33	78.4	7.57	7.62	7.74
6	A	Lined Walls Center Cavity	25	1.35	0	39.8	14.19	16.19	102.5	9.72	9.72	9.93
7	A	Lined Walls Center Cavity	25	1.35	0	30.0	14.13	19.13	125.5	7.04	7.00	7.09
8	A	Lined Walls Center Cavity	25	1.35	0	35.0	14.48	19.48	123.8	8.78	8.86	8.88
9	A	Lined Walls Center Cavity	25	1.35	0	40.0	14.48	19.48	136.9	13.90	13.75	14.05
10	A	Lined Walls Center Cavity	25	1.35	0	30.0	14.52	16.52	108.2	6.08	6.22	6.08
11	A	Lined Walls Center Cavity	25	1.35	0	35.0	14.52	16.52	116.8	7.56	7.70	7.82

TABLE IV

FUSELAGE FUEL TANK SYSTEM TEST DATA

VOIDED FOAM WALL CONFIGURATION

Test	Config.	Description	Foam Pore Size (PPI)	Foam Density (lb/ft3)	Foam Void (%)	Total Void (%)	Amb. Pressure (psia)	Initial System Pressure (psia)	Bomb Sample Ignition Pressure Rise (psig)	Simulated Fuselage Fuel Tank Ignition Pressure (psig)		
										ΔP_1	ΔP_2	ΔP_3
1	B	Voided Lined Wall With Center Cavity	25	1.4	10	30.5	14.46	14.46	95.6	3.04	3.21	3.18
2	B	Voided Lined Wall With Center Cavity	25	1.4	10	35.0	14.40	14.40	103.5	4.25	4.16	4.31
3	B	Voided Lined Wall With Center Cavity	25	1.4	10	39.9	14.40	14.40	100.3	5.34	5.34	5.32
4	B	Voided Lined Wall With Center Cavity	25	1.4	10	45.3	14.40	14.40	103.8	6.84	6.82	6.86
5	B	Voided Lined Wall With Center Cavity	25	1.4	10	50.0	14.40	14.40	97.8	8.40	8.25	—
6	3	Voided Lined Wall With Center Cavity	25	1.4	10	60.0	14.36	14.36	90.0	12.25	12.25	12.37
7	B	Voided Lined Wall With Center Cavity	25	1.4	10	50.0	14.33	16.33	101.1	9.15	9.14	9.32
8	B	Voided Lined Wall With Center Cavity	25	1.4	10	55.0	14.30	16.30	103.2	12.13	12.10	12.20

TABLE IV CONT.

Test	Config.	Description	Foam Pore Size (PPi)	Foam Density (lb/ft³)	Foam Void (%)	Total Void (%)	Amb. Pressure (psia)	Initial System Pressure (psia)	Bomb Sample Ignition Pressure Rise (psig)	Simulated Fuselage Fuel Tank Ignition Pressure (psig)		
										ΔP_1	ΔP_2	ΔP_3
9	B	Voided Lined Wall With Center Cavity	25	1.4	10	45.3	14.30	19.30	—	9.18	9.14	9.26
10	B	Voided Lined Wall With Center Cavity	25	1.4	10	50.0	14.52	19.52	—	11.31	11.30	11.42
11	B	Voided Lined Wall With Center Cavity	25	1.4	15	50.4	14.54	14.54	101.8	13.32	13.30	13.60
12	B	Voided Lined Wall With Center Cavity	25	1.4	15	45.0	14.62	14.62	95.0	6.94	6.84	6.96
13	B	Voided Lined Wall With Center Cavity	25	1.4	15	45.0	14.62	16.62	114.5	10.48	10.50	10.74
14	B	Voided Lined Wall With Center Cavity	25	1.4	10	60.0	14.42	14.42	100.5	23.80	23.70	23.90
15	B	Voided Lined Wall With Center Cavity	25	1.4	25	40.0	14.36	14.36	91.5	4.73	4.76	4.73
16	B	Voided Lined Wall With Center Cavity	25	1.4	25	45.5	14.33	14.38	97.2	7.04	7.04	7.18
17	B	Voided Lined Wall With Center Cavity	25	1.4	25	50.0	14.52	14.52	100.0	10.60	10.50	10.60

TABLE V

FUSELAGE FUEL TANK SYSTEM TEST DATA

FLAT END CYLINDERS (15 INCH DIA.)

Test	Config.	Description	Foam Pore Size (µµ)	Foam Density (lb/ft³)	Propane/Air Vol (%)	Total Void (%)	Amb. Pressure (psia)	Initial System Pressure (psia)	Bomb Sample Ignition Pressure Rise (psig)	Simulated Fuselage Fuel Tank Ignition Pressure (psig) ΔF_1	ΔF_2	ΔF_3
1	C	Cylinders (15" dia 12" long 2.75" wall 1" flat ends)	25	1.36	4.78	45	14.44	14.44	100.0	4.33	4.29	4.43
2	C		25	1.36	4.24	45	14.36	14.36	98.6	4.41	4.46	4.34
3	C	Same Set of Cyls. Used for Tests 1 Thru 6	25	1.36	3.74	45	14.34	14.34	94.0	3.71	3.86	3.82
4	C		25	1.36	2.97	45	14.29	14.29	79.5	0.50	0.50	0.50
5	C		25	1.36	5.52	45	14.29	14.29	94.2	4.30	4.22	4.42
6	C		25	1.35	4.80	45	14.34	16.34	118.8	16.20	14.25	14.58

37

TABLE V (CONTINUED)

Test	Config.	Description	Foam Pore Size (ppi)	Foam Density (lb/ft³)	Propane/Air Vol (%)	Total Void (%)	Amb. Pressure (psia)	Initial System Pressure (psia)	Bomb Sample Ignition Pressure Rise (psig)	Simulated Fuselage Fuel Tank Ignition Pressure (psig)		
										ΔP_1	ΔP_2	ΔP_3
7	C	Cylinders (15 in. dia. 12 in. long 1.95 in. wall 1 in. flat ends)	25	1.36	4.79	55	14.50	14.50	103.5	7.26	7.36	7.25
8	C	Cylinders (15 in. dia. 12 in. long 1.85 in. wall 1.85 in.flat ends)	25	1.36	4.79	50	14.50	14.50	100.8	4.60	4.60	4.70
9	C	Cylinders (15 in. dia. 12 in. long 1.85 in. wall 1.85 in.flat ends)	25	1.36	4.78	50	14.54	16.54	116.4	14.90	15.00	15.20
10	C	Cylinders (15 in. dia. 12 in. long 1.85 in. wall 1.65 in.flat ends)	25	1.36	4.78	50	14.50	14.50	100.5	4.86	5.00	-
11	C	Cylinders (15 in. dia. 12 in. long 2.4 in. wall 2.4 in.flat ends)	25	1.36	4.79	40	14.42	14.42	101.5	8.80	8.74	-
12	C	Cylinders (15 in. dia. 12 in. long 2.4 in. wall 2.4 in.flat ends)	25	1.36	4.78	40	14.42	14.42	100.0	8.80	8.90	-

TABLE V (CONTINUED)

Test	Config.	Description	Foam Pore Size (ppi)	Foam Density (lb/ft³)	Propane/Air Vol (%)	Total Void (%)	Amb. Pressure (psia)	Initial System Pressure (psia)	Bomb Sample Ignition Pressure Rise (psig)	Simulated Fuselage Fuel Tank Ignition Pressure (psig)		
										ΔP_1	ΔP_2	ΔP_3
13	C	Cylinders (15 in. dia. 12 in. long 1.85 in. wall 1.85 in.flat ends)	25	1.36	4.78	50	14.38	14.42	100.0	4.60	4.60	-
14	C	Cylinders (15 in. dia. 12 in. long 1.375 in. wall 1.375 in. flat ends)	25	1.36	4.78	60	14.33	14.33	99.4	20.35	20.30	21.85

39

TABLE VI

FUSELAGE FUEL TANK SYSTEM TEST DATA

FLAT END CYLINDERS (7.5 INCH DIA.)

Test	Config.	Description	Foam Pore Size (ppi)	Foam Density (lb/ft³)	Propane/Air Vol (%)	Total Void (%)	Amb. Pressure (psia)	Initial System Pressure (psia)	Bomb Sample Ignition Pressure Rise (psig)	Simulated Fuselage Fuel Tank Ignition Pressure (psig)		
										ΔP_1	ΔP_2	ΔP_3
1	D	Cylinders (7.5 in. dia. 24 in. long 1.45 in. wall 1.45 in. flat ends)	23	1.36	4.78	45	14.23	14.23	98.0	7.10	7.10	—
2	D	Cylinders (7.5 in. dia. 24 in. long 1.25 in. wall 1.25 in. flat ends)	23	1.36	4.78	50	14.27	14.27	98.0	9.88	9.79	10.52
3	D	Cylinders (7.5 in. dia. 24 in. long 1.65 in. wall 1.65 in. flat ends)	23	1.36	4.78	40	14.42	14.42	99.0	7.49	8.48	8.10
4	D	Cylinders (7.5 in. dia. 24 in. long 1.65 in. wall 1.65 in. flat ends)	23	1.36	4.78	40	14.42	14.42	95.0	8.08	7.85	8.55
5	D	Same as Test No. 1	23	1.36	4.78	45	14.48	14.48	103.0	8.55	8.45	9.30
6	D	Same as Test No. 1	23	1.36	4.78	45	14.46	16.46	113.0	12.70	12.60	13.73
7	D	Same as Test No. 1	23	1.36	4.78	45	14.42	19.42	140.5	13.60	13.60	14.60
8	D	Same as Test No. 1	23	1.36	4.78	45	14.42	19.42	151.0	17.70	19.40	—
9	D	Same as Test No. 2	23	1.36	4.78	50	14.44	16.44	—	18.90	13.40	—
10	D	Same as Test No. 2	23	1.36	4.78	50	14.44	19.44	135.0	24.90	25.60	—
11	D	Same as Test No. 3	23	1.36	4.78	40	14.40	16.40	115.0	14.70	16.10	—

TABLE VI (CONT'D)

Test	Config.	Description	Foam Pore Size (PPi)	Foam Density (lb/ft³)	Propane/Air Vol (%)	Total Void (%)	Amb. Pressure (psia)	Initial System Pressure (psia)	Bomb Sample Ignition Pressure Rise (psig)	Simulated Fuselage Fuel Tank Ignition Pressure (psig)		
										ΔF_1	ΔF_2	ΔF_3
12	D	Same as Test No. 3	23	1.36	4.78	40	14.36	19.36	139.0	17.10	17.10	—
13	D	Cylinders (7.5 in. dia. 24 in. long 2.15 in. wall 2.15 in flat ends)	23	1.36	4.78	30	14.39	14.39	102.0	6.20	6.35	—
14	D	Same as Test No.13	23	1.36	4.78	30	14.39	16.39	112.0	10.20	11.00	—
15	D	Same as Test No.13	23	1.36	4.78	30	14.39	19.39	143.0	12.40	13.70	—
16	D	Cylinders (7.5 in. dia. 24 in. long 2.15 in. wall 2.15 in. flat ends)	23	1.36	4.79	30	14.44	14.44	98.4	3.81	4.00	3.86
17	D	Same as Test No. 16	23		4.79	30	14.44	14.44	113.6	8.40	9.00	8.70
18	D	Same as Test No. 16	23		4.78	30	14.44	14.44	97.2	3.70	4.00	3.70
19	D	Same as Test No. 16	23		4.79	30	14.44	14.44	98.2	3.70	3.90	3.90
20	D	Same as Test No. 16	23		4.78	30	14.44	19.44	132.5	11.30	11.80	11.70

TABLE VII

FUSELAGE FUEL TANK SYSTEM TEST DATA

HEMISPHERICAL END CYLINDERS (7.5 INCH DIA.)

Test	Config.	Description	Foam Pore Size (ppi)	Foam Density (lb/ft³)	Propane/Air Vol (%)	Total Void (%)	Amb. Pressure (psia)	Initial System Pressure (psia)	Bomb Sample Ignition Pressure Rise (psig)	Simulated Fuselage Fuel Tank Ignition Pressure (psig)		
										ΔP_1	ΔP_2	ΔP_3
1	B	Cylinders (7.5 in. dia. 12 in. long 1.75 in. wall 1.75 in ends)	25	1.36	4.79	50	14.56	14.56	97.8	10.07	9.44	—
2	E	Same as Test No. 1	25	1.36	4.78	50	14.56	16.56	119.0	17.10	18.00	—
3	E	Same as Test No. 1	25	1.36	4.79	50	14.56	19.56	134.0	25.90	27.10	—
4	E	Cylinders (7.5 in. dia. 12 in. long 2.45 in. wall 2.45 in. ends)	25	1.36	4.78	40	14.60	14.60	94.5	6.68	7.00	6.68
5	E	Same as Test No. 4	25	1.36	4.77	40	14.60	16.60	111.0	8.10	8.50	8.26
6	E	Same as Test No. 4	25	1.36	4.77	40	14.60	19.60	137.5	12.65	13.00	12.75
7	E	Cylinders (715 in. dia. 12 in. long 1.25 in. wall 1.25 in ends)	25	1.36	4.78	60	14.40	14.40	97.0	15.12	15.10	14.55
8	E	Same as Test No. 7	25	1.36	4.78	60	14.40	16.40	112.2	21.95	21.50	21.10
9	E	Same as Test No. 7	25	1.36	4.78	60	14.40	19.40	137.3	32.25	31.90	31.00

42

TABLE VIII

FUSELAGE FUEL TANK SYSTEM TEST DATA

VOIDED FOAM WALL CONFIGURATION (15 PPI FOAM)

Test	Config.	Description	Foam Pore Size	Foam Density (lb/ft^3)	Foam Void (%)	Total Void (%)	Amb. Pressure (psia)	Initial System Pressure (psia)	Bomb Sample Ignition Pressure Rise (psig)	Simulated Fuselage Fuel Tank Ignition Pressure (psig)		
										$\triangle P_1$	$\triangle P_2$	$\triangle P_3$
1	B	Voided Lined Wall With Center Cavity	12	1.38	10	30.5	14.42	14.42	94.8	11.3	11.6	11.2
2	B	Voided Lined Wall With Center Cavity	12	1.38	10	35.0	14.42	14.42	99.5	19.5	19.8	19.2
3	B	Voided Lined Wall With Center Cavity	12	1.38	10	40.0	14.42	14.42	100.0	25.8	26.3	25.6
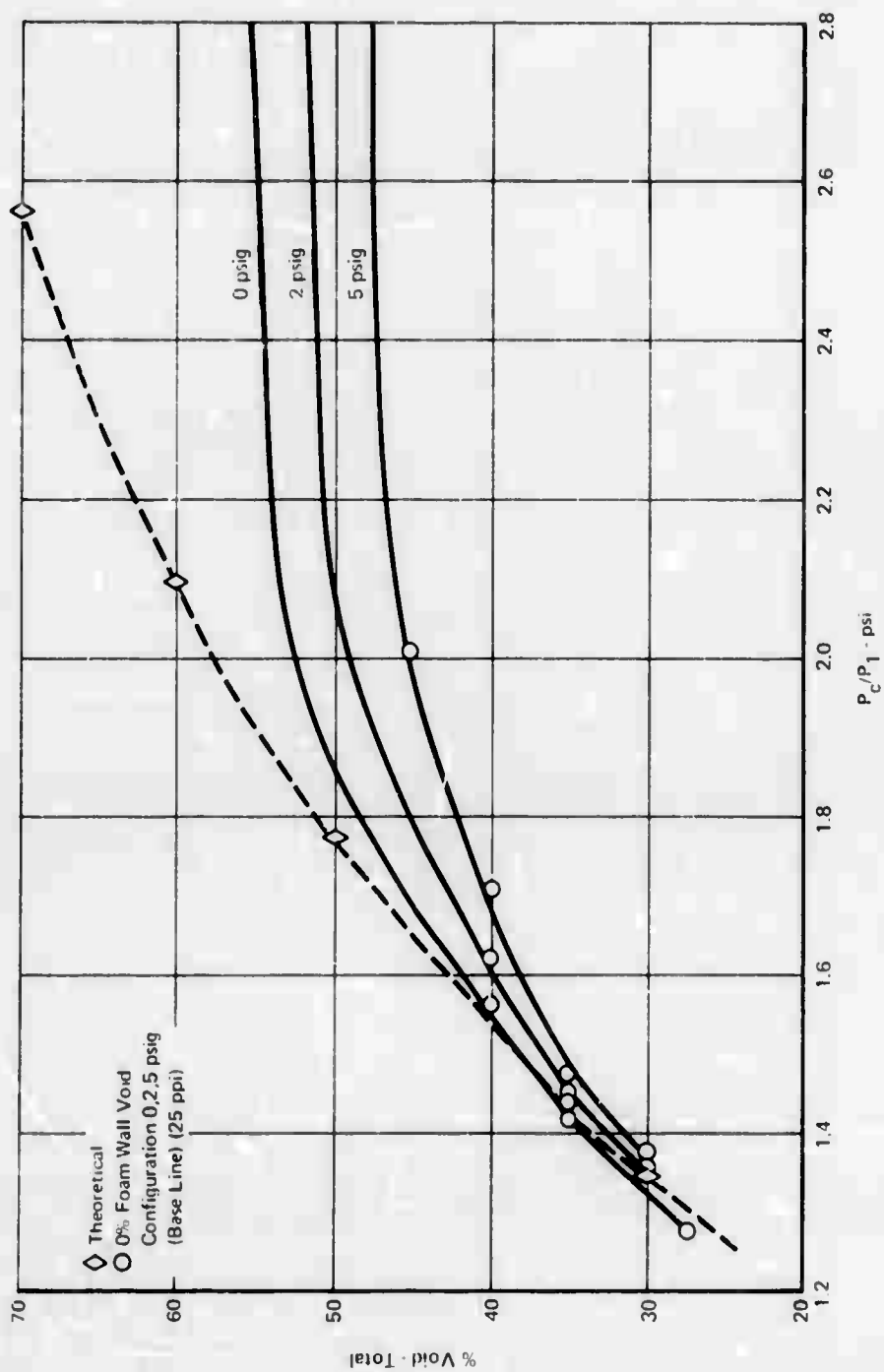
FIGURE 17 0% FOAM WALL VOID CONFIGURATION
BASE LINE

GP71 0937 28

44
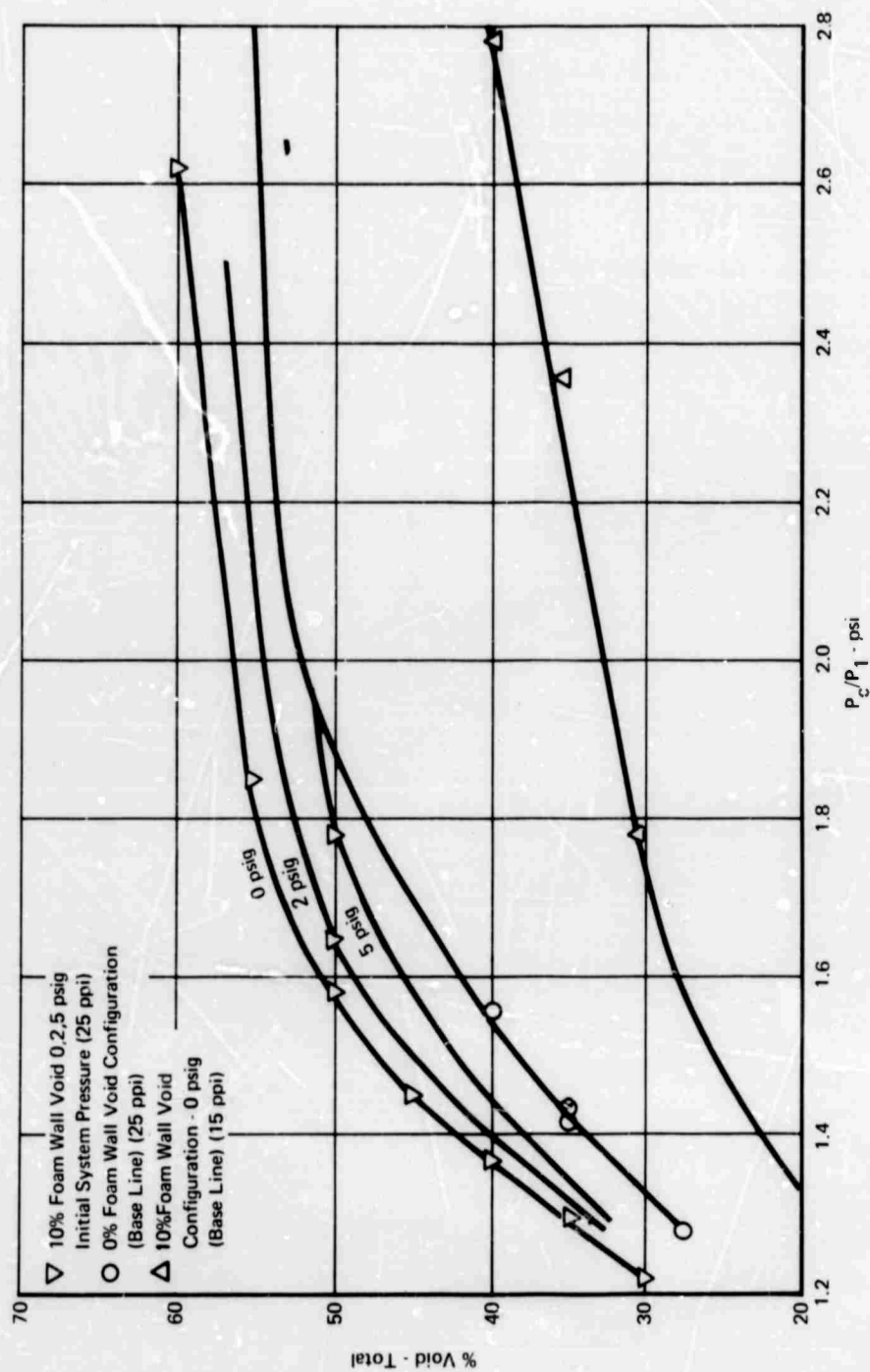
FIGURE 18 10% FOAM WALL VOID CONFIGURATION

GP71-0937-30

45
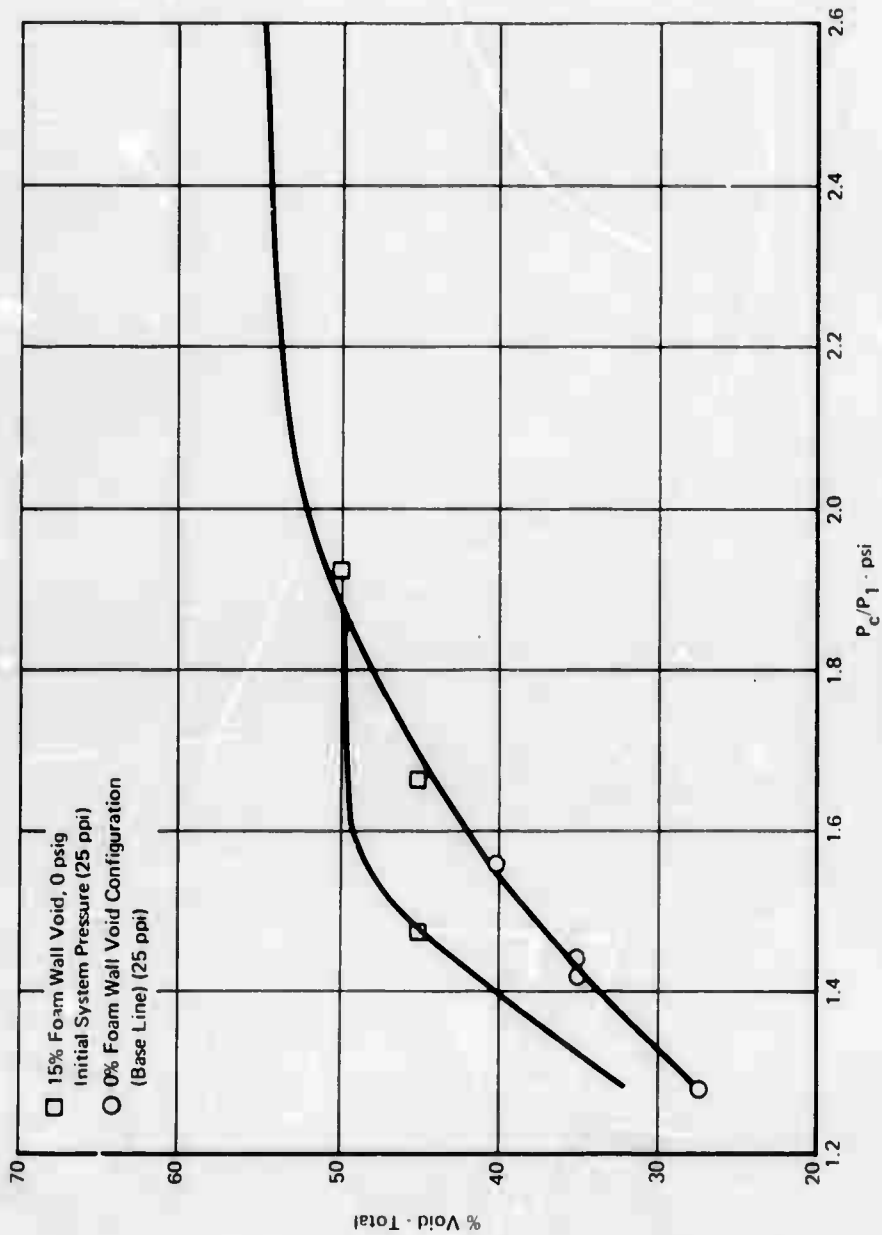
FIGURE 19 15% FOAM WALL VOID CONFIGURATION

□ 15% Foam Wall Void, 0 psig
Initial System Pressure (25 ppi)

O 0% Foam Wall Void Configuration
(Base Line) (25 ppi)

P_c/P_1 - psi

% Void - Total

· GP71 0937 31

46
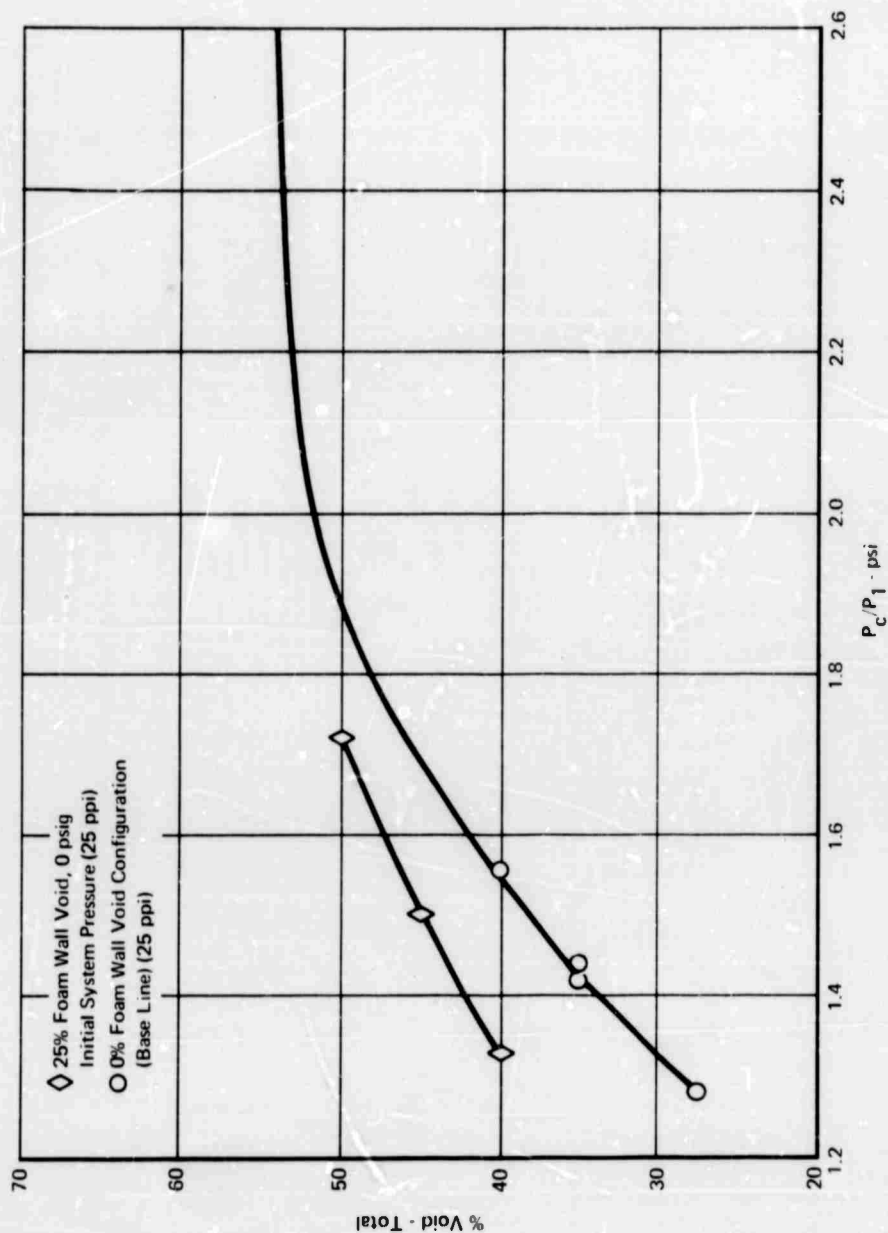
FIGURE 20 25% FOAM WALL VOID CONFIGURATION

GP71 0937 32

47
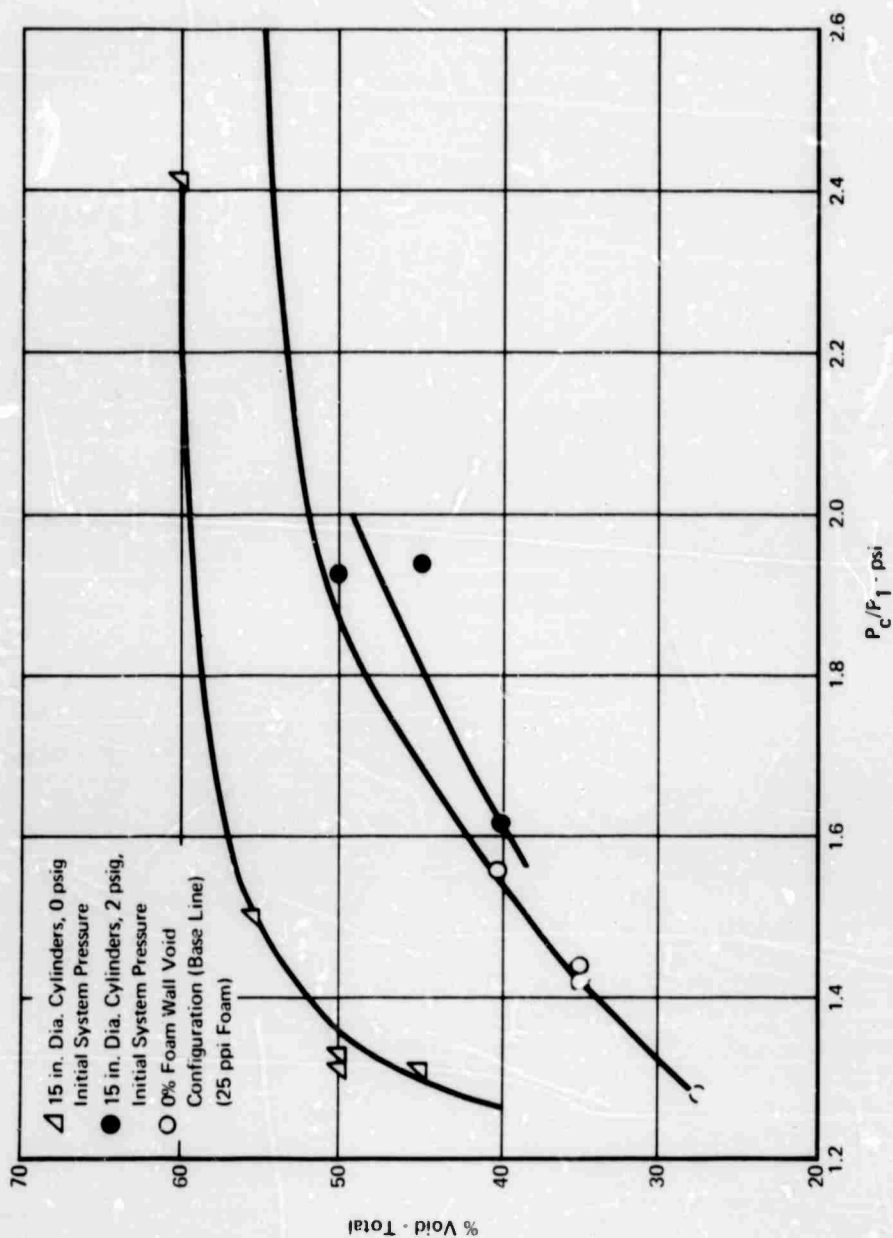
FIGURE 21 15 INCH DIAMETER CYLINDER CONFIGURATION

GP71 0937 35

48
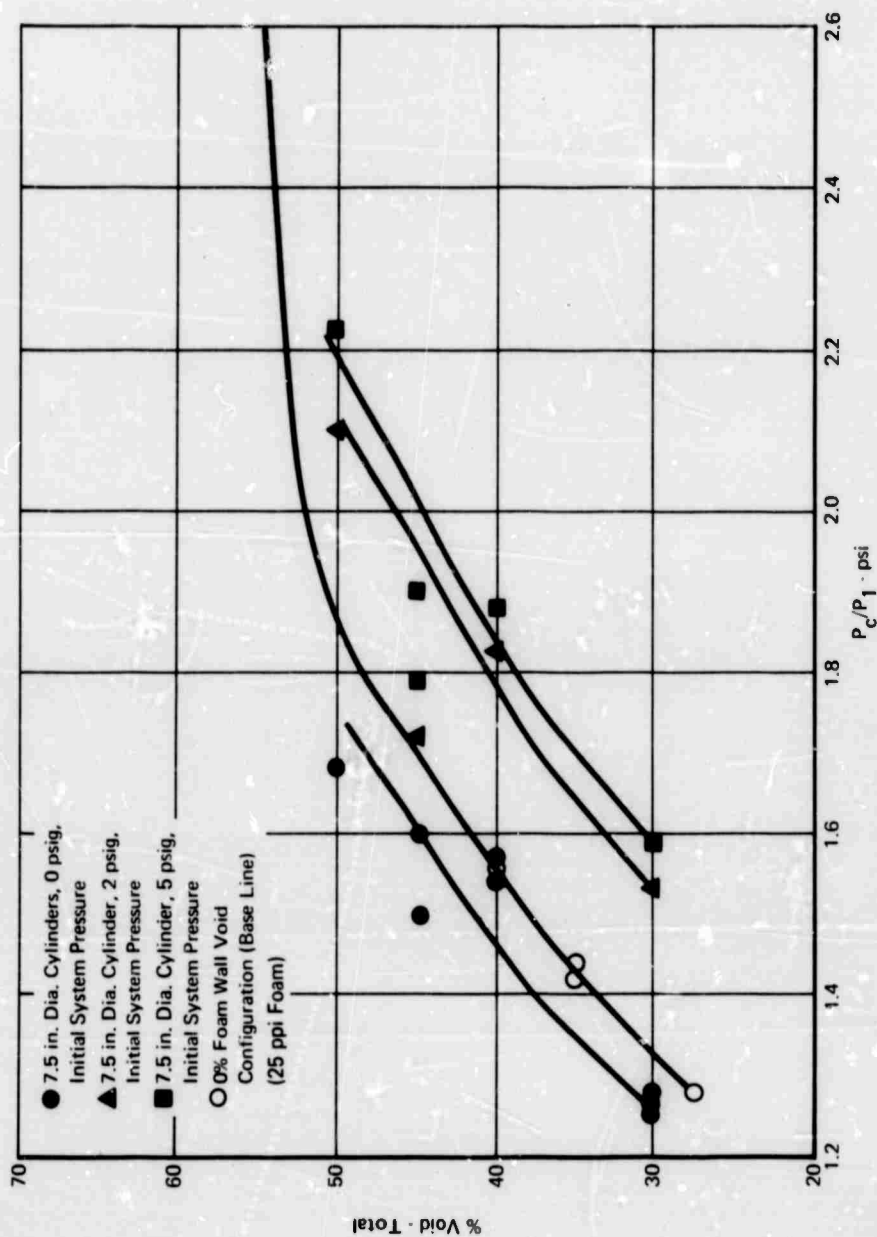
FIGURE 22 7.5 INCH DIAMETER CYLINDERS FLAT END CONFIGURATION

GP71 0937 37

49
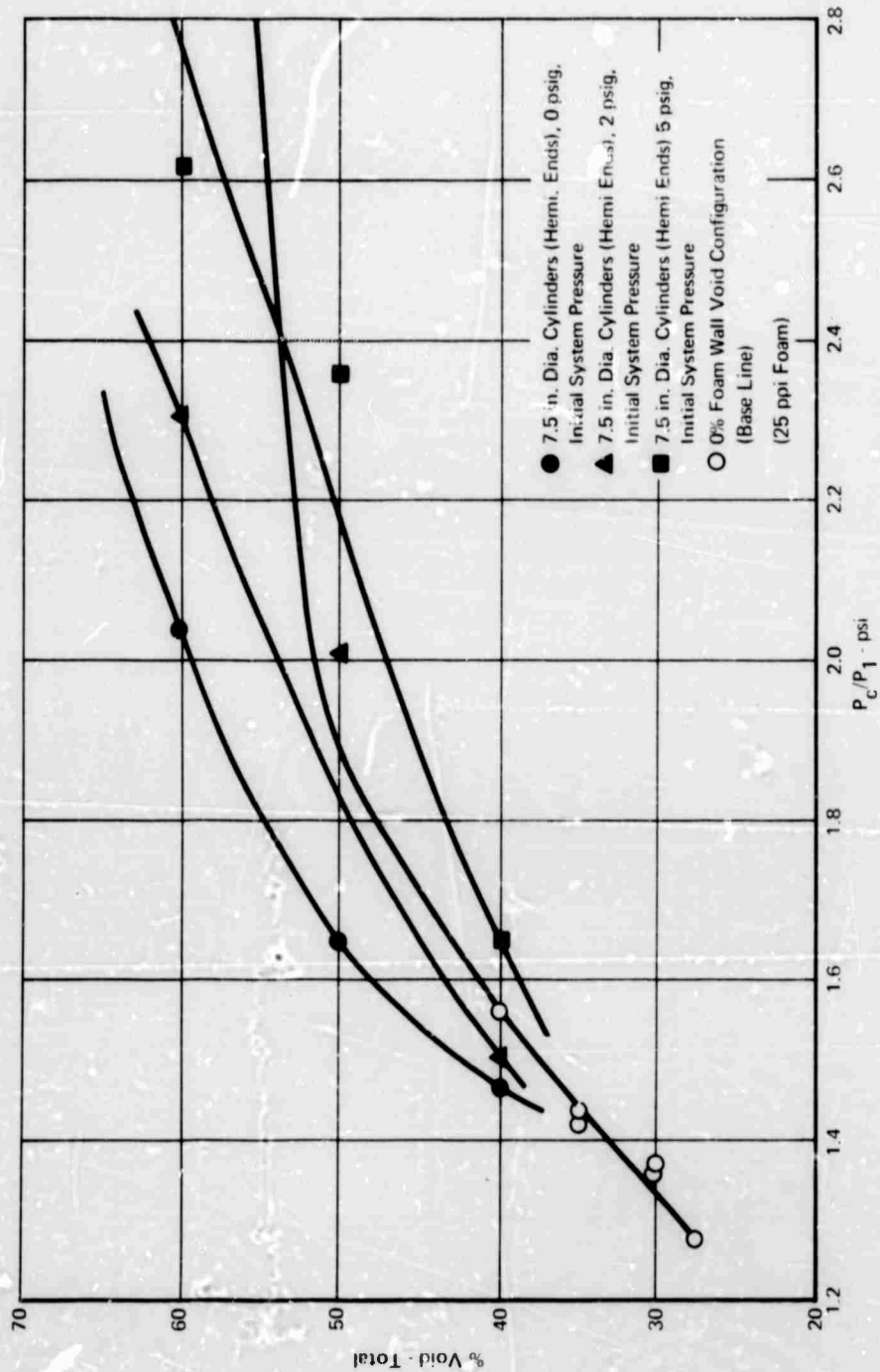
FIGURE 23 7.5 INCH DIAMETER CYLINDERS (HEMI. END) CONFIGURATION

- ● 7.5 in. Dia. Cylinders (Hemi. Ends), 0 psig.
  Initial System Pressure
- ▲ 7.5 in. Dia. Cylinders (Hemi. Ends), 2 psig.
  Initial System Pressure
- ■ 7.5 in. Dia. Cylinders (Hemi. Ends) 5 psig.
  Initial System Pressure
- ○ 0% Foam Wall Void Configuration
  (Base Line)
  (25 ppi Foam)

P_c/P_1 - psi

% Void - Total

GP71 0937 39

50
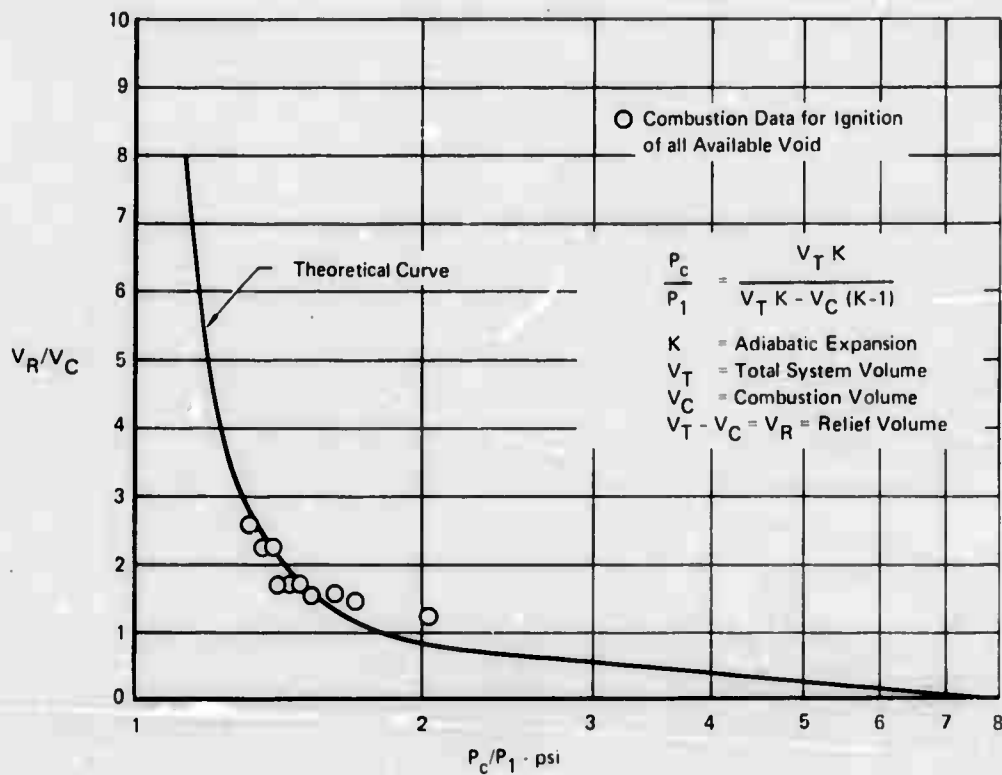
**FIGURE 24 PRESSURE RATIO vs RELIEF TO
COMBUSTION VOLUME RATIO-LINED WALL
FUSELAGE TANK**

GP71 0937 40

51
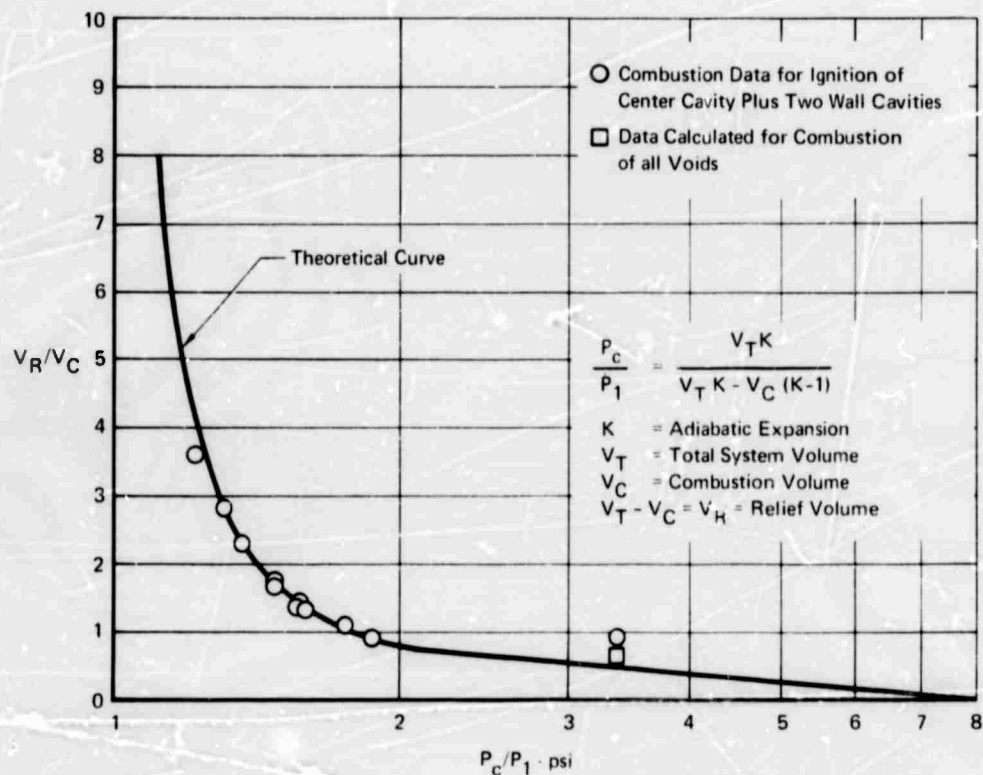
FIGURE 25 PRESSURE RATIO vs RELIEF TO COMBUSTION VOLUME RATIO
10 PERCENT VOIDED LINED WALL

FUSELAGE TANK

GP71-0937-41

52
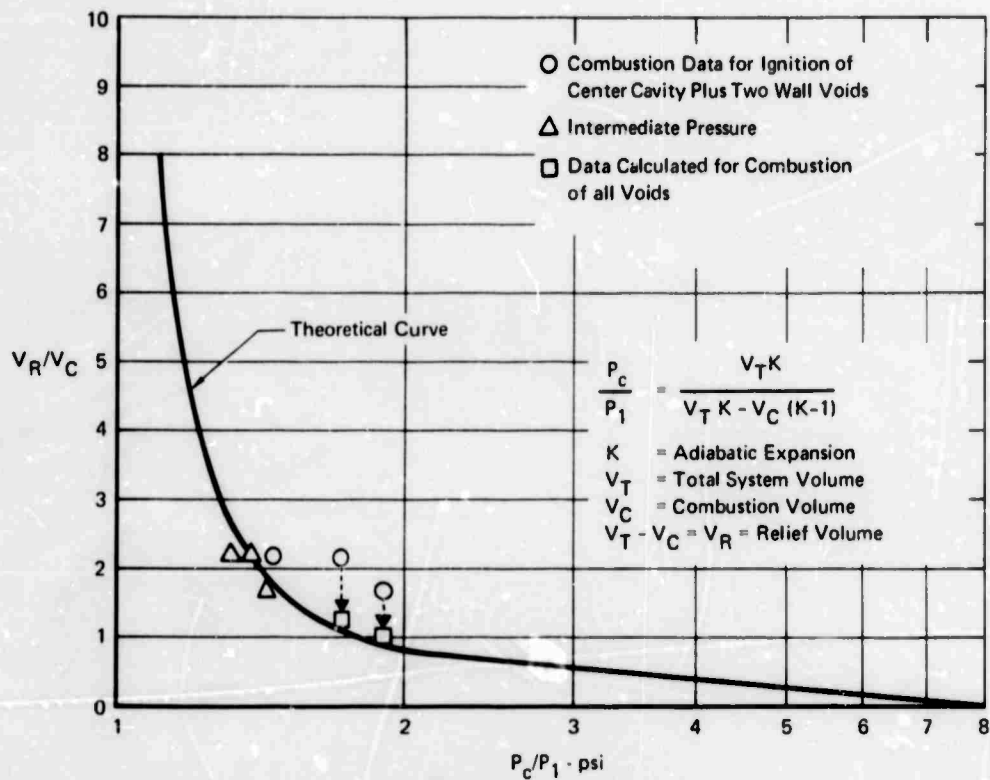
FIGURE 26 PRESSURE RATIO vs RELIEF TO COMBUSTION VOLUME RATIO
15 PERCENT VOIDED LINED WALL

FUSELAGE TANK

GP71-0937-42

53
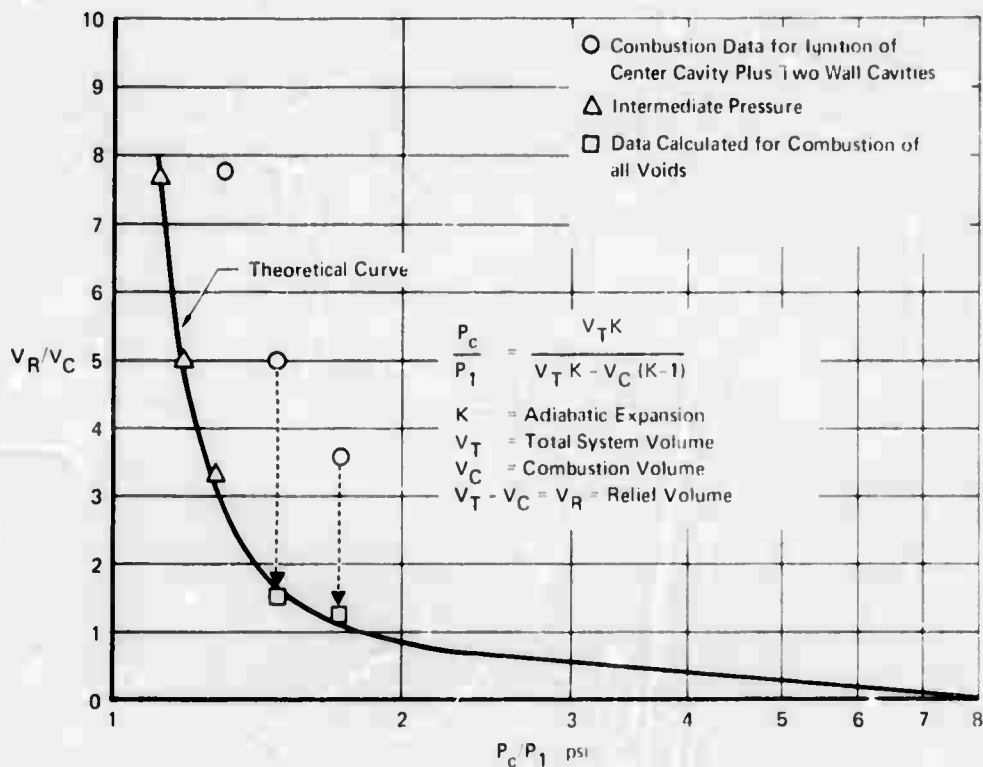
**FIGURE 27 PRESSURE RATIO vs RELIEF TO COMBUSTION VOLUME RATIO
25 PERCENT VOIDED LINED WALL**

FUSELAGE TANK

GP71 0937 43

54

Combustion Data for Ignition of External Void Plus Internal Void of Two Cylinders

Data Calculated for Combustion of all Voids

Theoretical Curve

V_R/V_C

$$\frac{P_c}{P_1} = \frac{V_T K}{V_T K - V_C (K-1)}$$

K = Adiabatic Expansion
V_T = Total System Volume
V_C = Combustion Volume
$V_T - V_C = V_R$ = Relief Volume

P_c/P_1 psi

FIGURE 28 PRESSURE RATIO vs RELIEF TO COMBUSTION VOLUME RATIO
15 INCH DIAMETER VOIDED CYLINDER
FUSELAGE TANK

GP71 0937 44

55

○ Max Pressure
△ Intermediate Pressure
□ Data Calculated for Combustion of all Voids

Theoretical Curve

V_R/V_C

$$\frac{P_C}{P_1} = \frac{V_T K}{V_T K - V_C (K-1)}$$

K = Adiabatic Expansion
V_T = Total System Volume
V_C = Combustion Volume
$V_T - V_C = V_R$ = Relief Volume

P_C/P_1 · psi
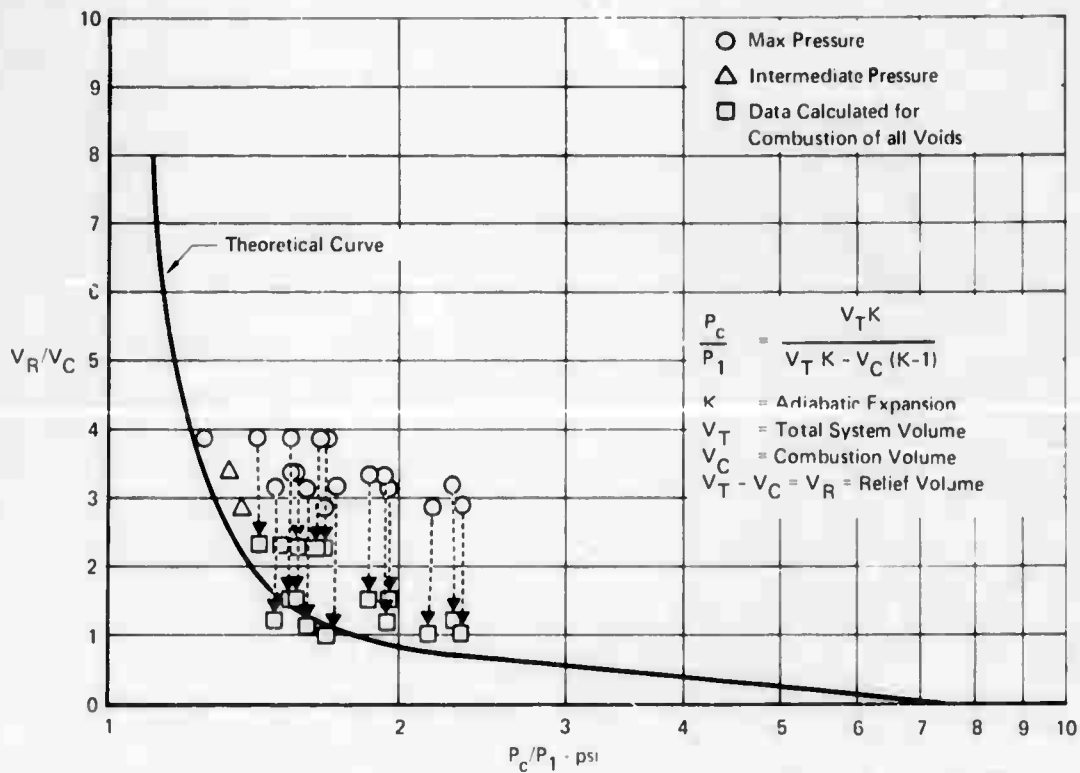
FIGURE 29 PRESSURE RATIO vs RELIEF TO COMBUSTION VOLUME RATIO
7.5 INCH DIAMETER CYLINDER FLAT ENDS

FUSELAGE TANK
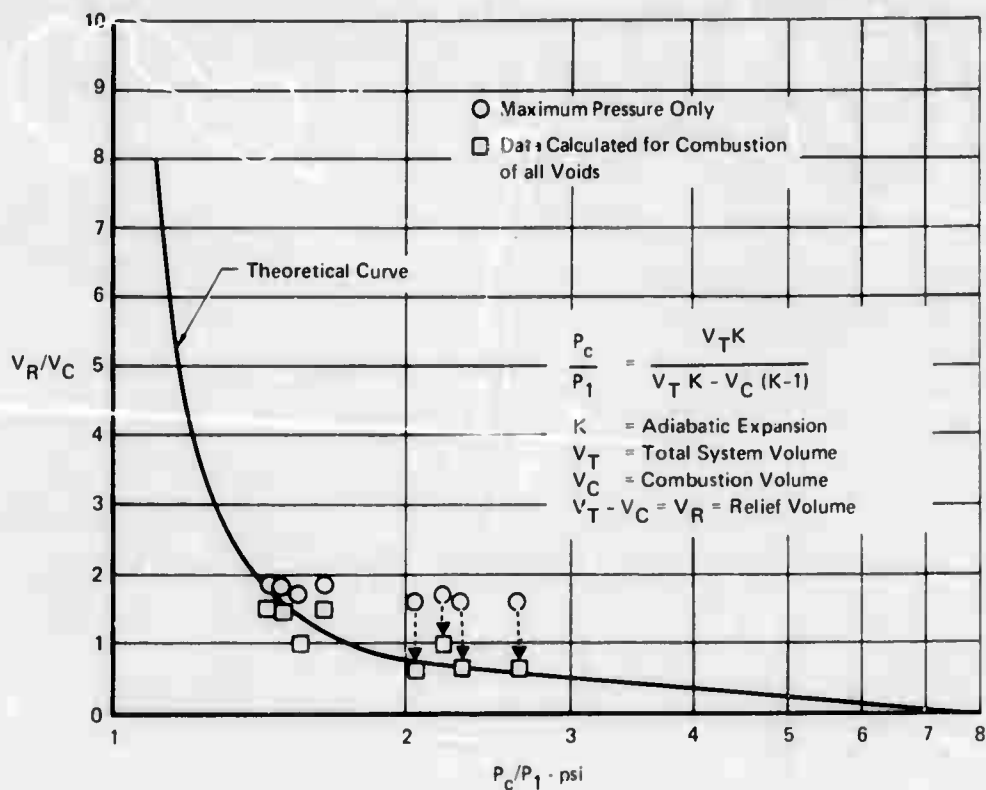
FIGURE 30 PRESSURE RATIO vs RELIEF TO COMBUSTION VOLUME RATIO
7.5 INCH CYLINDER - HEMI ENDS

FUSELAGE TANK
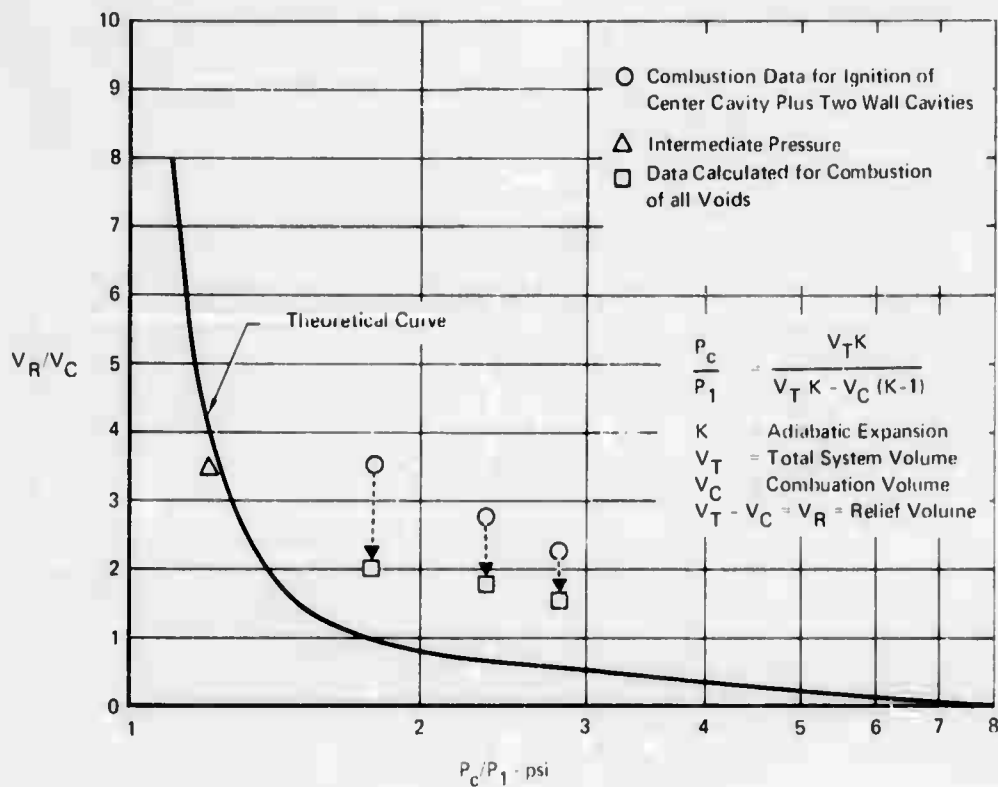
**FIGURE 31 PRESSURE RATIO vs RELIEF TO COMBUSTION VOLUME RATIO
10 PERCENT VOIDED LINED WALL**
FUSELAGE TANK 15 PPI FOAM

GP71 0937 47
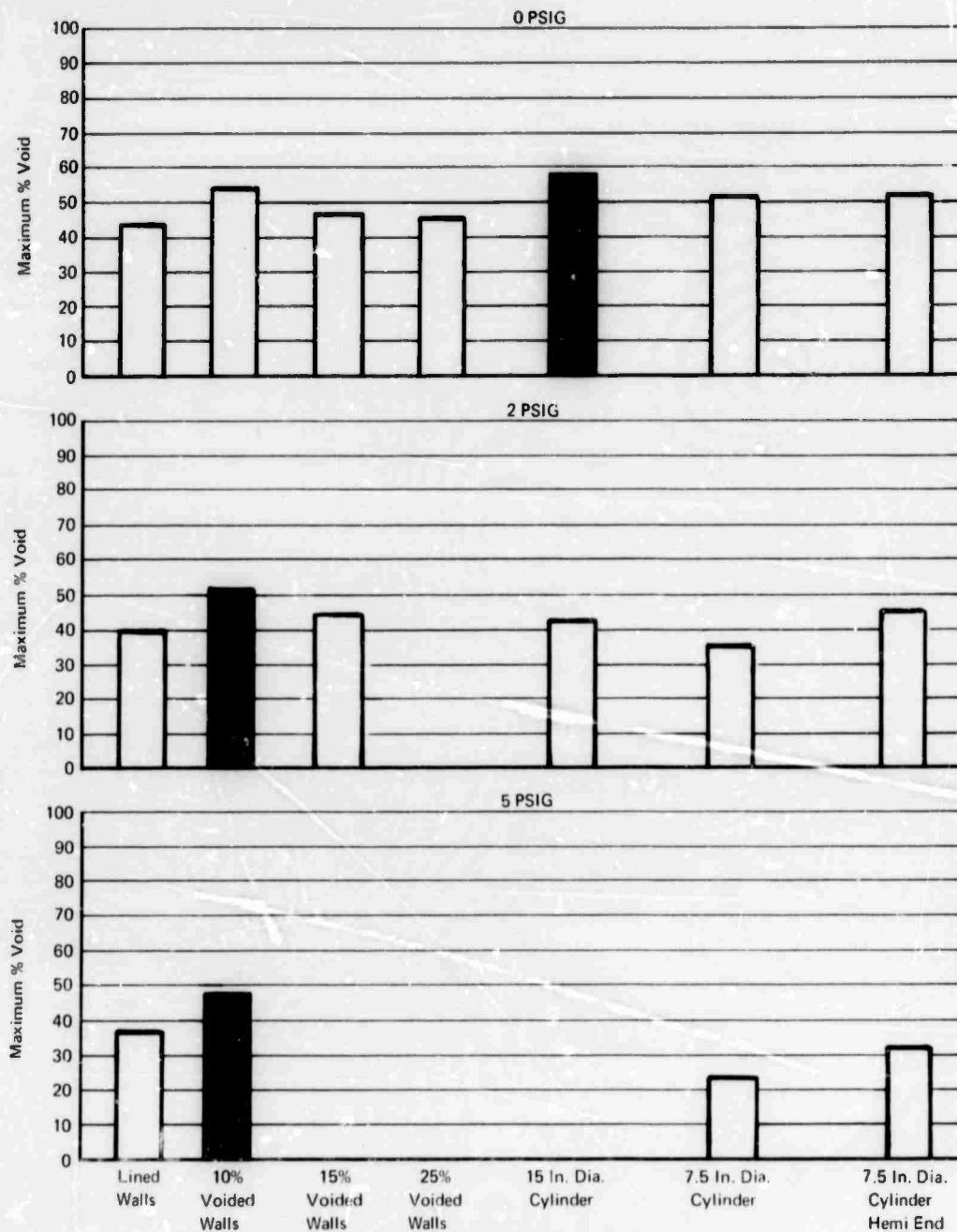
FIGURE 32 FUSELAGE TANK RESULTS

GP71 0937-48

TABLE IX

SMALL WING TANK TEST DATA

LINED WALLS

Test	Config.	Description	Foam Pore Size (ppi)	Foam Density (lb/ft³)	Propane/Air Vol (%)	Total Void (%)	Amb. Pressure (psia)	Initial System Pressure (psia)	Bomb Sample Ignition Pressure Rise (psig)	Fuel Tank Ignition Pressure (psig)					
										ΔP_1	ΔP_2	ΔP_3	ΔP_4	ΔP_5	ΔP_6
1	A	Lined walls	25	1.36	4.8	80	14.4	14.4	98.0	2.9	2.7	2.5	2.4	2.5	2.4
2	A	Lined walls	25	1.36	4.8	80	14.4	16.4	114.0	4.0	3.2	2.7	2.8	2.8	2.7
3	A	Lined walls	25	1.36	4.8	80	14.4	19.4	134.8	5.4	4.7	3.3	3.4	3.4	3.3

60

TABLE X

SMALL WING TANK TEST DATA

Test	Config.	Description	Foam Pore Size (ppi)	Foam Density (lb/ft3)	Propane/Air Vol (%)	Total Void (%)	Amb. Pressure (psia)	Initial System Pressure (psia)	Bomb Sample Ignition Pressure Rise (psig)	Fuel Tank Ignition Pressure (psig)					
										ΔP_1	ΔP_2	ΔP_3	ΔP_4	ΔP_5	ΔP_6
1	B	Egg Crate	25	1.36	4.8	60	14.35	14.35	98.2	.10	.10	.10	.10	.10	.10
2	B	Egg Crate	25	1.36	4.8	60	14.35	16.35	111.1	.10	.10	.10	.10	.10	.10
3	B	Egg Crate	25	1.36	4.8	60	14.35	19.35	128.2	3.60	3.80	3.60	3.70	3.70	3.60
4	B	Egg Crate	25	1.36	4.8	70	14.50	14.50	97.2	3.60	3.80	3.40	3.50	3.50	3.40
5	B	Egg Crate	25	1.36	4.8	70	14.36	14.36	98.0	.10	.10	.10	.10	.10	.10
6	B	Egg Crate	25	1.36	4.8	70	14.36	16.36	109.0	12.00	12.60	14.40	12.80	17.30	17.00
7	B	Egg Crate	25	1.36	4.8	70	14.46	16.46	101.0	13.00	13.50	12.90	13.50	15.20	14.80
8	B	Egg Crate	25	1.36	4.8	70	14.46	14.46	100.8	.30	.30	.30	.30	.30	.30
9	B	Egg Crate	25	1.36	4.8	70	14.46	16.46	112.8	.30	.30	.30	.30	.30	.30
10	B	Egg Crate	25	1.36	4.8	70	14.46	19.46	-	1.94	1.87	1.85	1.94	1.76	1.89
11	B	Egg Crate	25	1.36	4.8	70	14.48	19.48	130.0	2.42	2.47	2.43	2.42	2.45	2.38
12	B	Egg Crate	25	1.36	4.8	80	14.36	14.36	99.8	2.18	2.25	2.21	2.23	2.23	2.22
13	B	Egg Crate	25	1.36	4.8	80	14.36	16.36	113.3	2.65	2.64	2.61	2.62	2.53	2.50
14	B	Egg Crate	25	1.36	4.8	80	14.42	19.42	138.0	17.90	18.80	18.60	19.40	39.00	40.20
15	B	Egg Crate	25	1.36	4.8	90	14.44	14.44	94.5	7.00	7.20	7.00	7.00	7.00	-
16	B	Egg Crate	25	1.36	4.8	90	14.48	16.48	111.0	20.20	20.70	20.50	20.80	20.50	-

61

TABLE XI

SMALL WING TANK TEST DATA

Test	Config.	Description	Foam Pore Size (ppi)	Foam Density (lb/ft³)	Propane/Air Vol (%)	Total Void (%)	Amb. Pressure (psia)	Initial System Pressure (psia)	Bomb Sample Ignition Pressure Rise (psig)	Fuel Tank Ignition Pressure (psig)					
										ΔP_1	ΔP_2	ΔP_3	ΔP_4	ΔP_5	ΔP_6
1	C	Cylinders (15 in. dia. 12 in. long 2.4 in. wall 2.4 in. ends)	25	1.36	4.78	40	14.44	14.44	90.5	4.52	4.61	4.51	4.77	4.88	4.32
2	C	Cylinders (15 in. dia. 12 in. long 2.4 in. wall 2.4 in. ends)	25	1.36	4.78	40	14.44	16.44	111.8	12.90	12.60	12.70	13.00	13.90	13.20
3	C	Cylinders (15 in. dia. 12 in. long 2.4 in. wall 2.4 in. ends)	25	1.36	4.78	40	14.44	19.44	133.3	16.80	16.60	18.00	16.70	24.20	24.60
4	C	Cylinders (15 in. dia. 12 in. long 2.4 in. wall 2.4 in. ends)	25	1.36	4.788	40	14.48	14.48	101.2	14.50	15.80	13.50	13.60	11.90	11.00
5	C	Cylinders (15 in. dia. 12 in. long 1.38 in. wall 1.38 in. ends)	25	1.36	4.78	60	14.44	16.44		-	16.80	16.30	16.30	16.40	15.40

TABLE XII

6 CELL WING TANK TEST DATA

Test	Config.	Description	Foam Pore Size (ppi)	Foam Density (lb/ft3)	Propane/ Air Vol (%)	Total Void (%)	Amb. Pressure (psia)	Initial System Pressure (psia)	Bomb Sample Ignition Pressure Rise (psig)	Fuel Tank Ignition Pressure (psig)					
										ΔP_1	ΔP_2	ΔP_3	ΔP_4	ΔP_5	ΔP_6
1	D	Cylinders (7.5 in. dia. 12 in. long 2.45 in. wall 2.45 in. ends)	25	1.36	4.78	40	14.46	14.46	98.0	-	-	4.72	5.36	5.66	5.01
2	D	Cylinders (7.5 in. dia. 12 in. long 2.45 in. wall 2.45 in. ends)	25	1.36	4.78	40	14.46	16.46	110.5	-	9.60	9.34	9.95	14.65	14.25
3	D	Cylinders (7.5 in. dia. 12 in. long 2.45 in. wall 2.45 in. ends)	25	1.36	4.78	40	14.38	19.38	136.5	15.40	16.40	15.20	15.70	23.30	23.40
4	D	Cylinders (7.5 in. dia. 12 in. long 1.25 in. wall 1.25 in. ends)	25	1.36	4.78	60	14.36	14.36	101.2	7.70	8.10	7.90	8.30	8.30	7.90
5	D	Cylinders (7.5 in. dia. 12 in. long 1.25 in. wall 1.25 in. ends)	25	1.36	4.78	60	14.44	16.44	117.0	11.80	12.10	11.30	11.90	19.10	19.80
6	D	Cylinders (7.5 in. dia. 12 in. long 1.25 in. wall 1.25 in. ends)	25	1.36	4.78	60	14.44	19.44		18.70	20.00	18.70	19.00	30.00	27.40

63
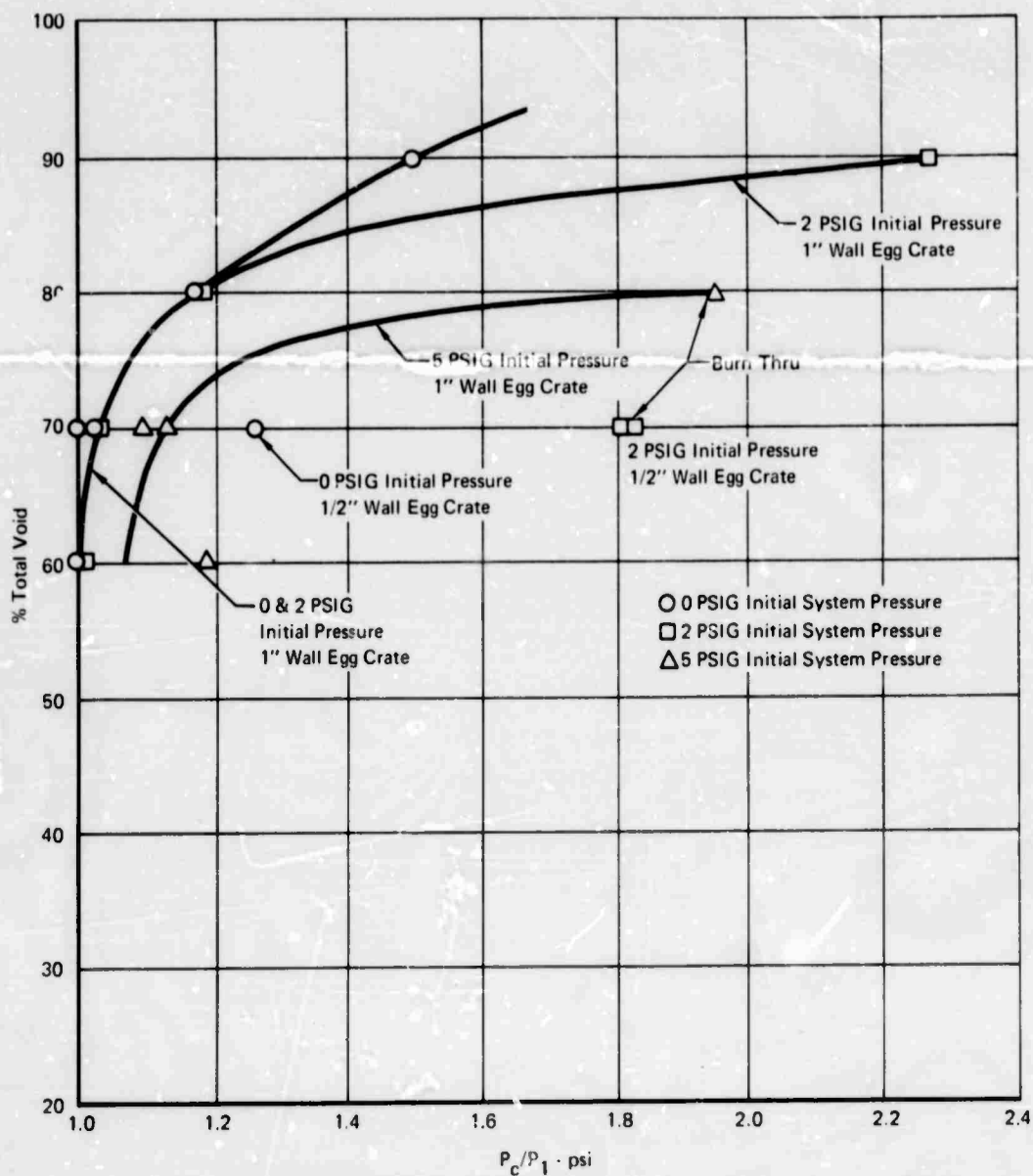
FIGURE 33 SIX CELL WING TANK EGG CRATE TESTS

GP71-0397-16

64
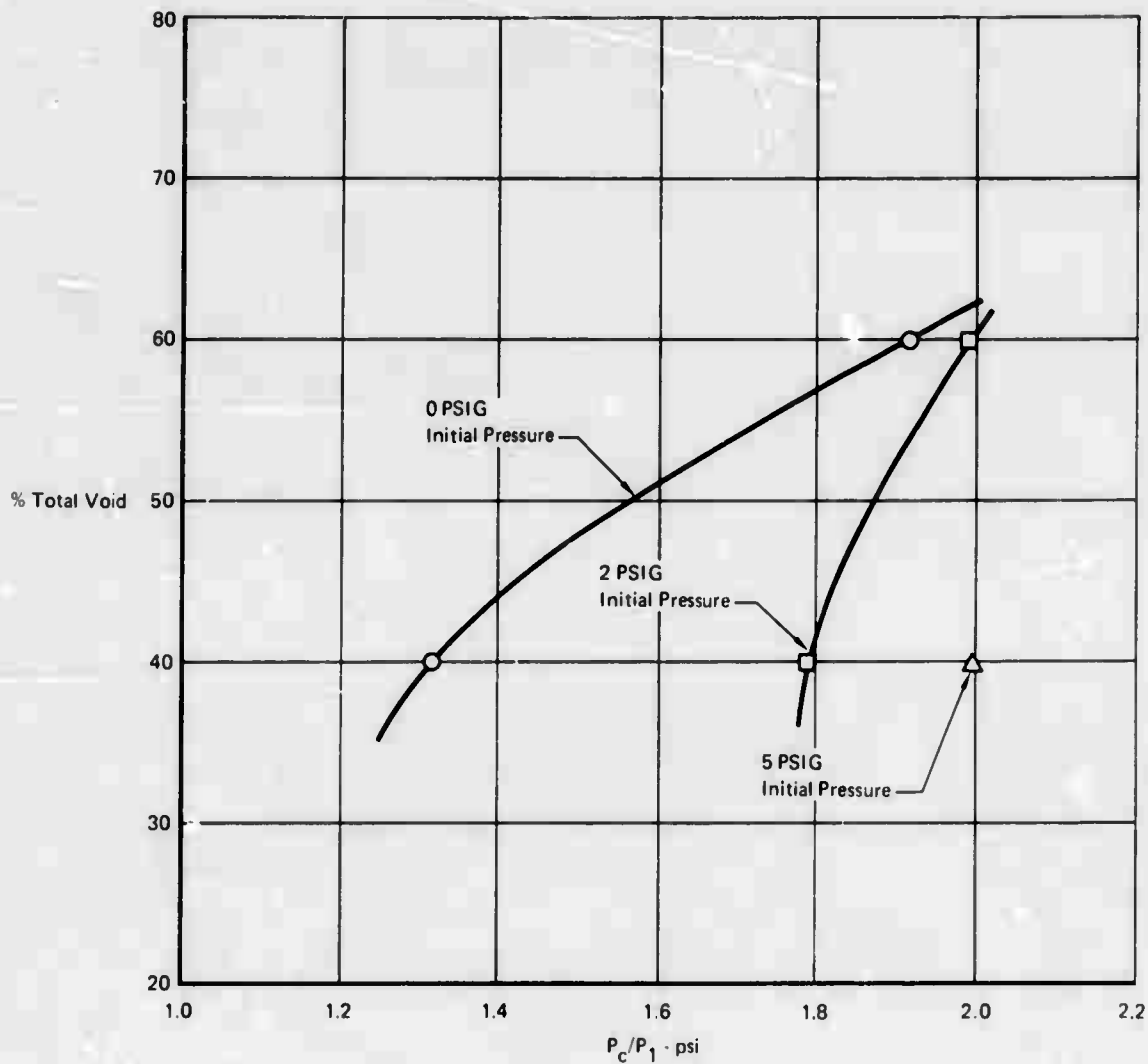
FIGURE 34 SIX CELL WING TANK CYLINDER TESTS
15 INCH DIAMETER

GP71 0937-17

65
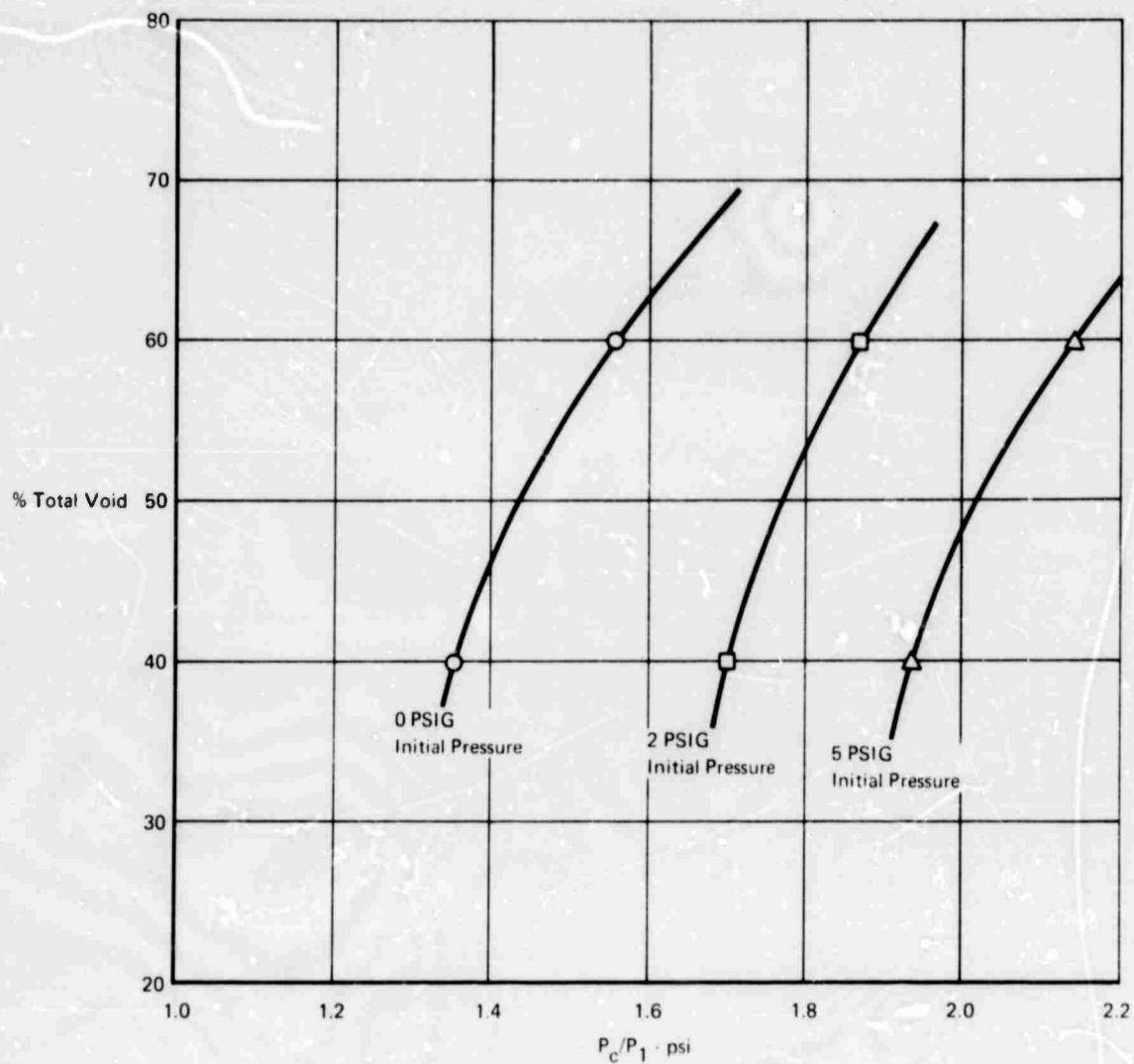
FIGURE 35 SIX CELL WING TANK CYLINDER TESTS
7.5 INCH DIAMETER HEMI ENDS
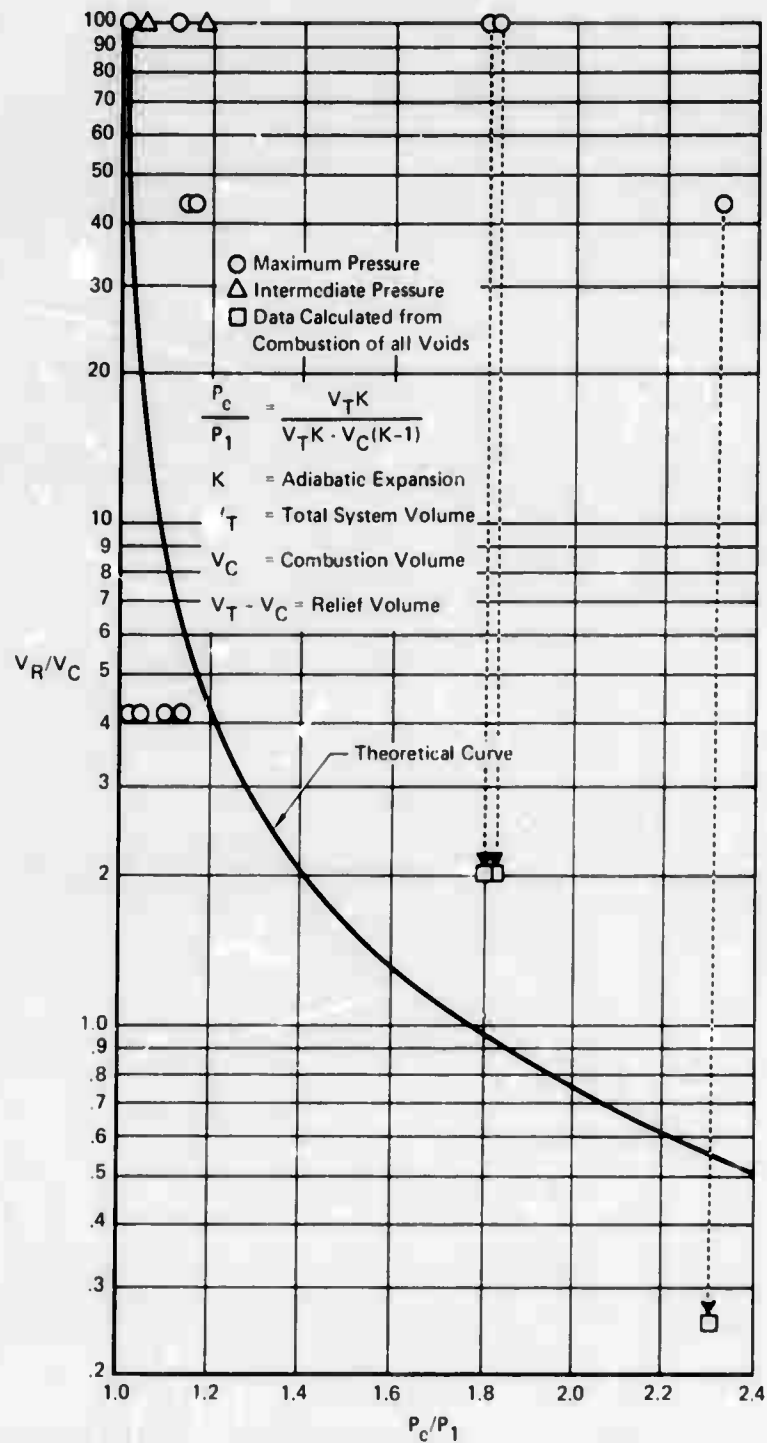
FIGURE 36 PRESSURE RATIO vs RELIEF TO COMBUSTION VOLUME RATIO - EGG CRATE
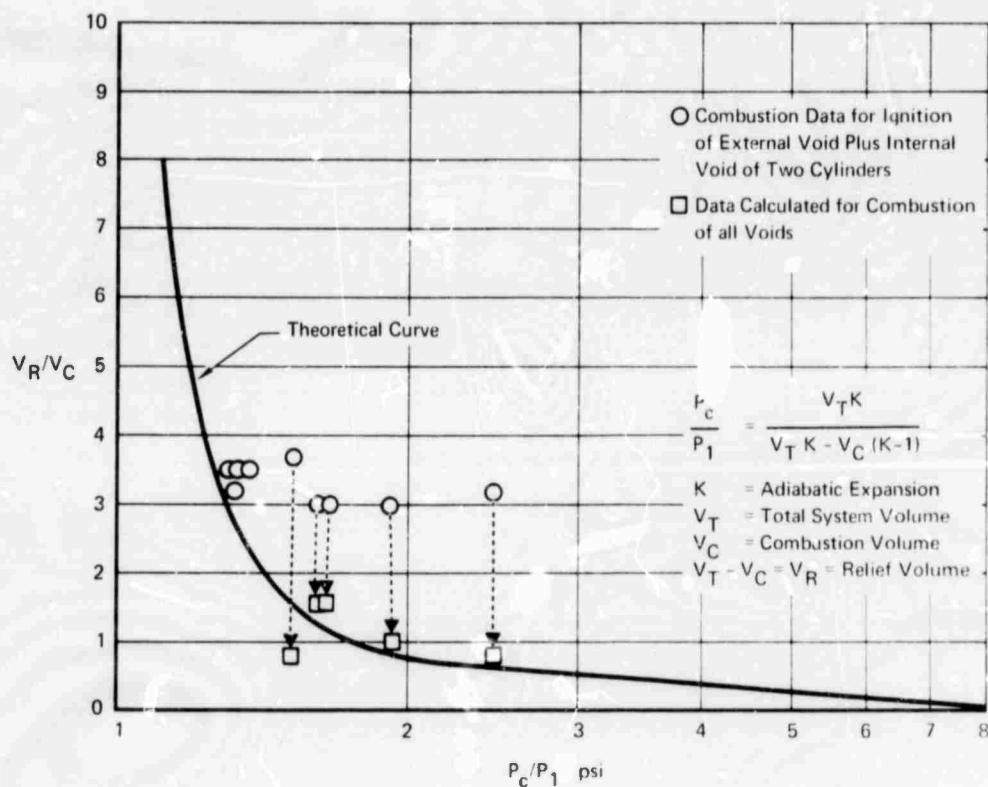SIX CELL WING TANK

GP71 0937 19

67
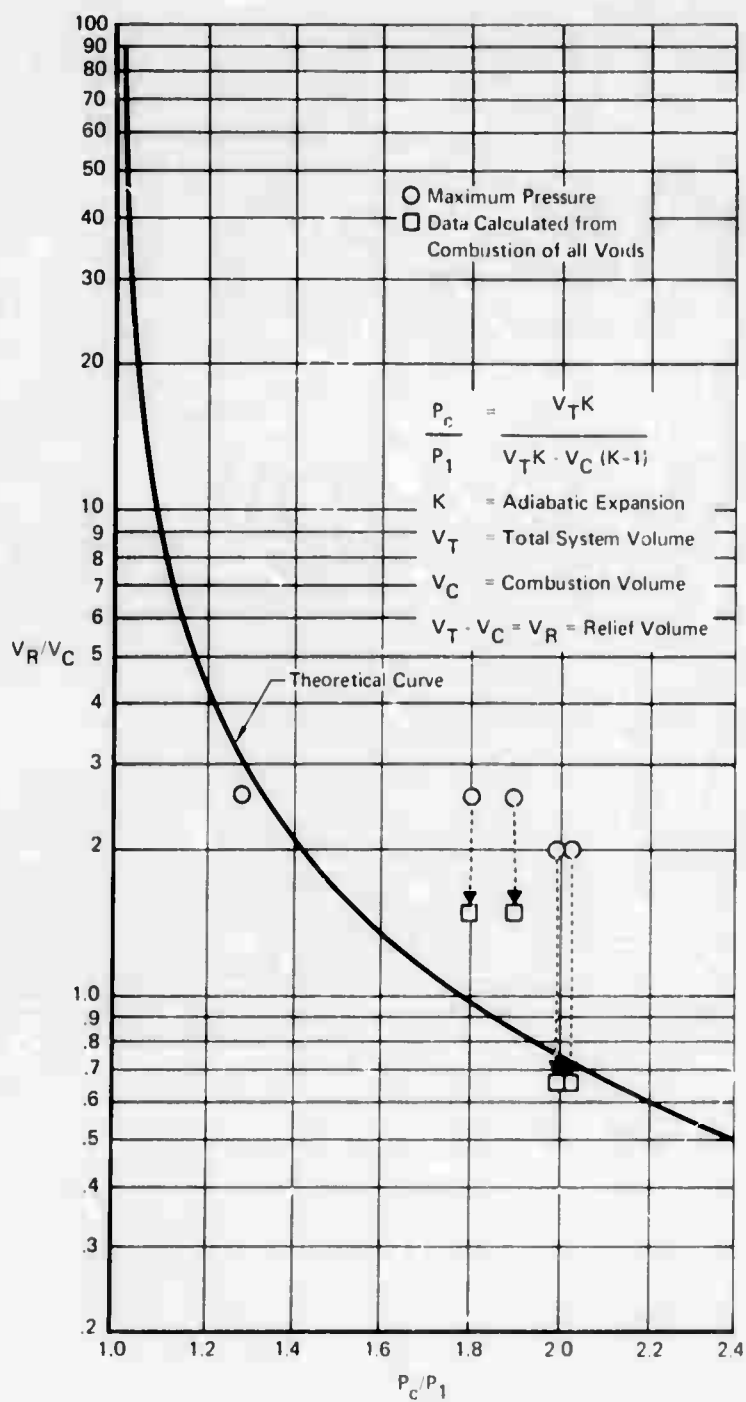
FIGURE 37 PRESSURE RATIO vs RELIEF TO COMBUSTION VOLUME RATIO -
15 INCH DIAMETER CYLINDER SIX CELL WING TANK

GP71 0937 21
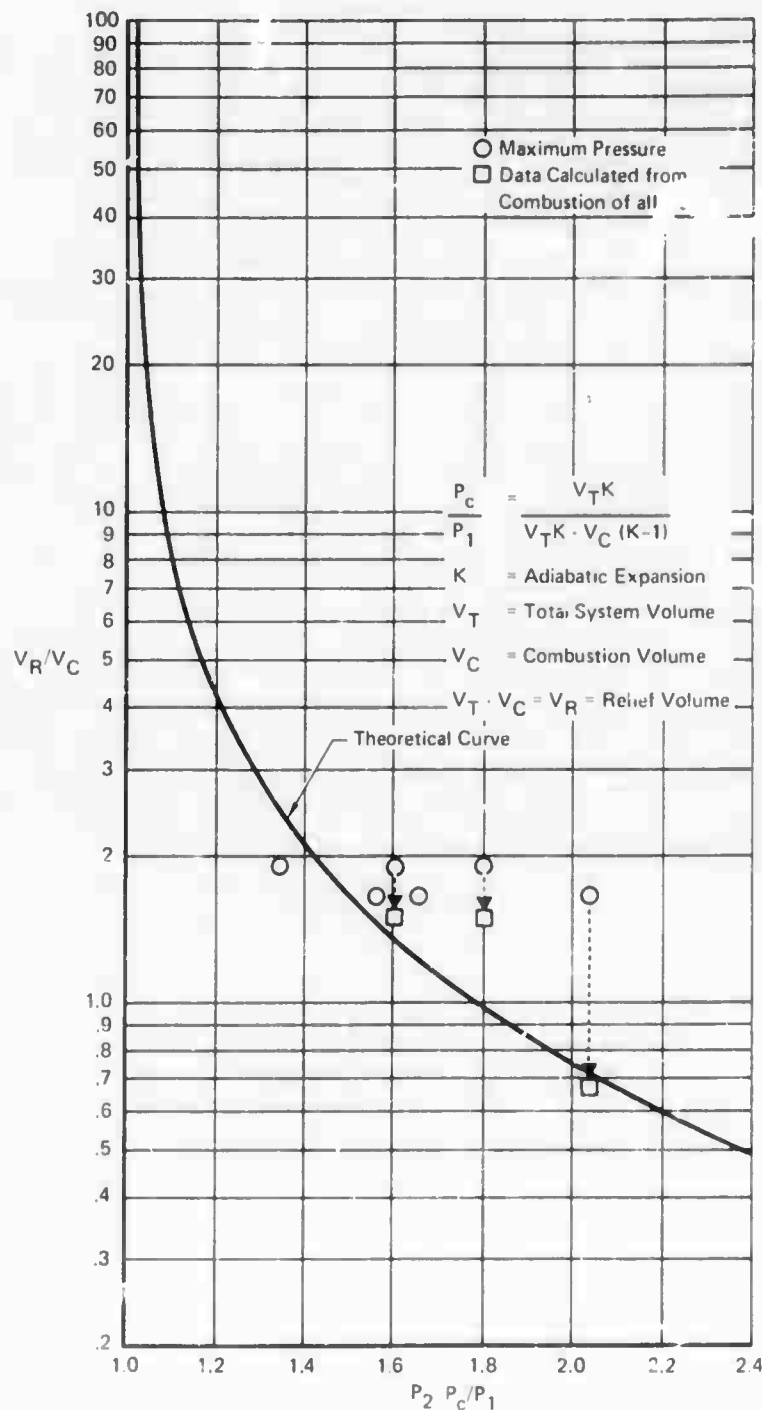
FIGURE 38 PRESSURE RATIO vs RELIEF TO COMBUSTION VOLUME RATIO -
7.5 INCH DIA. CYLINDERS
SIX CELL WING TANK

GP71 09: 7 20

69
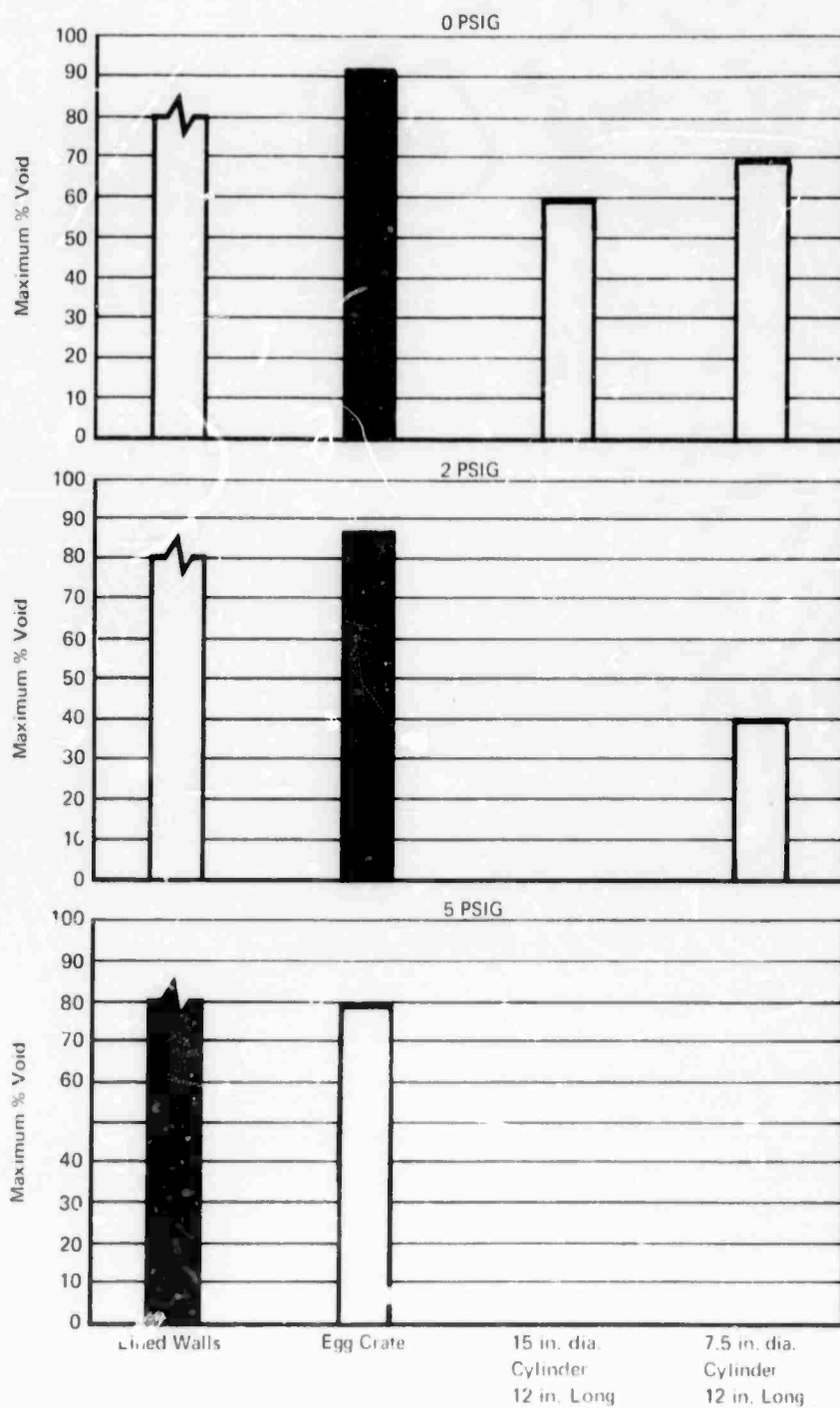
FIGURE 39 SIX CELL WING TANK RESULTS

GP71 0937 52

TABLE XIII

THREE CELL WING TANK

LINED WALLS

Test	Config.	Description	Foam Pore Size (ppi)	Foam Density (lb/ft³)	Propane/Air Vol (%)	Total Void (%)	Amb. Pressure (psia)	Initial System Pressure (psia)	Bomb Sample Ignition Pressure Rise (psig)	Fuel Tank Ignition Pressure (psig)		
										ΔP1	ΔP2	ΔP3
1	A	Lined Walls	25	1.35	4.8	80	14.35	14.35	91.0	18.6	20.2	24.3
2	A	Lined Walls	25	1.35	4.8	65	14.35	14.35	91.0	12.7	13.6	17.0
3	A	Lined Walls	25	1.35	4.8	55	14.30	14.30	—	11.2	12.0	14.5
4	A	Lined Walls	25	1.35	4.8	30	14.32	14.32	94.6	6.5	7.0	9.0

TABLE XIV

THREE CELL WING TANK TEST DATA

EGG CRATE

Test	Config.	Description	Foam Pore Size (ppi)	Foam Density (lb/ft³)	Propane/Air Vol (%)	Total Void (%)	Amb. Pressure (psia)	Initial System Pressure (psia)	Bomb Sample Ignition Pressure Rise (psig)	Fuel Tank Ignition Pressure (psig)		
										ΔP_1	ΔP_2	ΔP_3
1	B	Egg Crate	25	1.36	4.8	80	14.33	14.33	92.8	21.90	23.50	29.00
2	B	Egg Crate	25	1.36	4.8	40	14.40	14.40	93.2	1.03	1.09	1.21
3	B	Egg Crate	25	1.36	4.8	30	14.40	16.40	104.0	9.50	10.20	12.90
4	B	Egg Crate	25	1.36	4.8	50	14.38	19.38	-	7.50	8.30	9.80
5	B	Egg Crate	25	1.36	4.8	40	14.38	14.38	91.0	11.20	12.00	15.20
6	B	Egg Crate	25	1.36	4.8	30	14.38	16.38	98.0	9.50	10.50	13.20

72
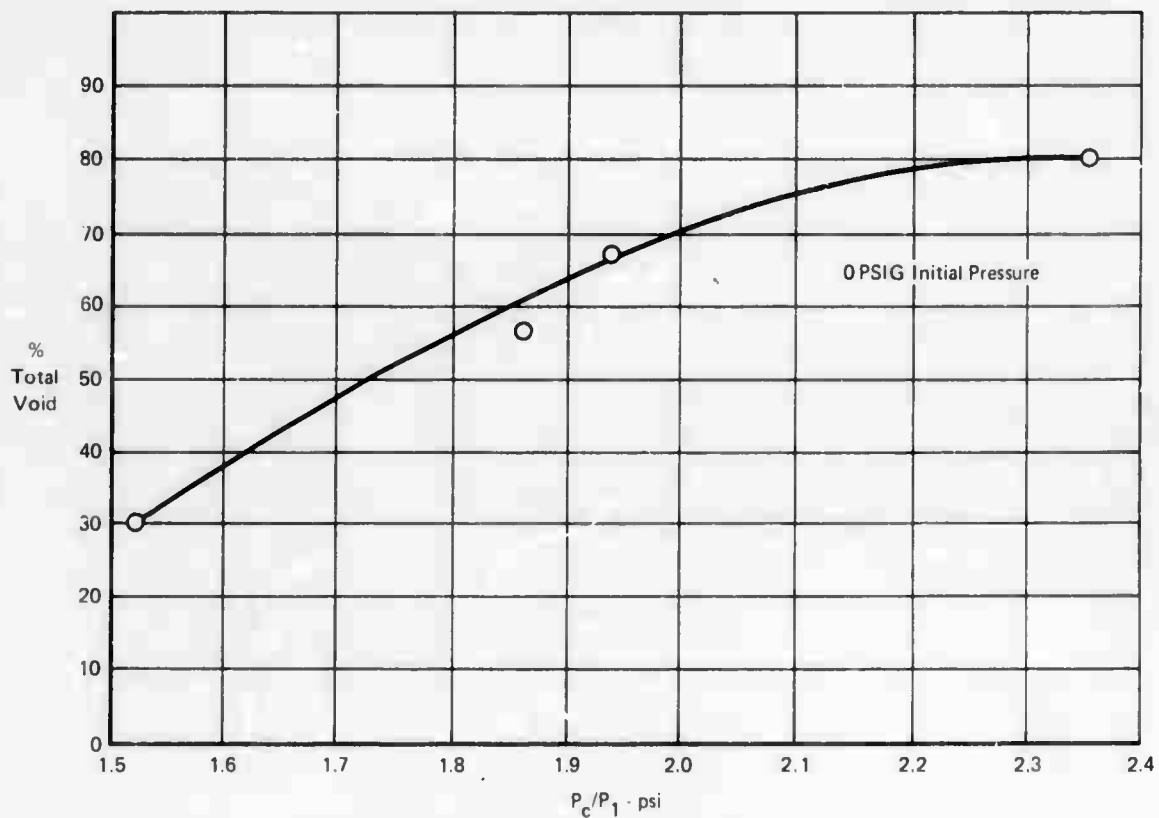
FIGURE 40 THREE CELL WING TANKS TESTS
LINED WALLS

GP71 0-037 23

73
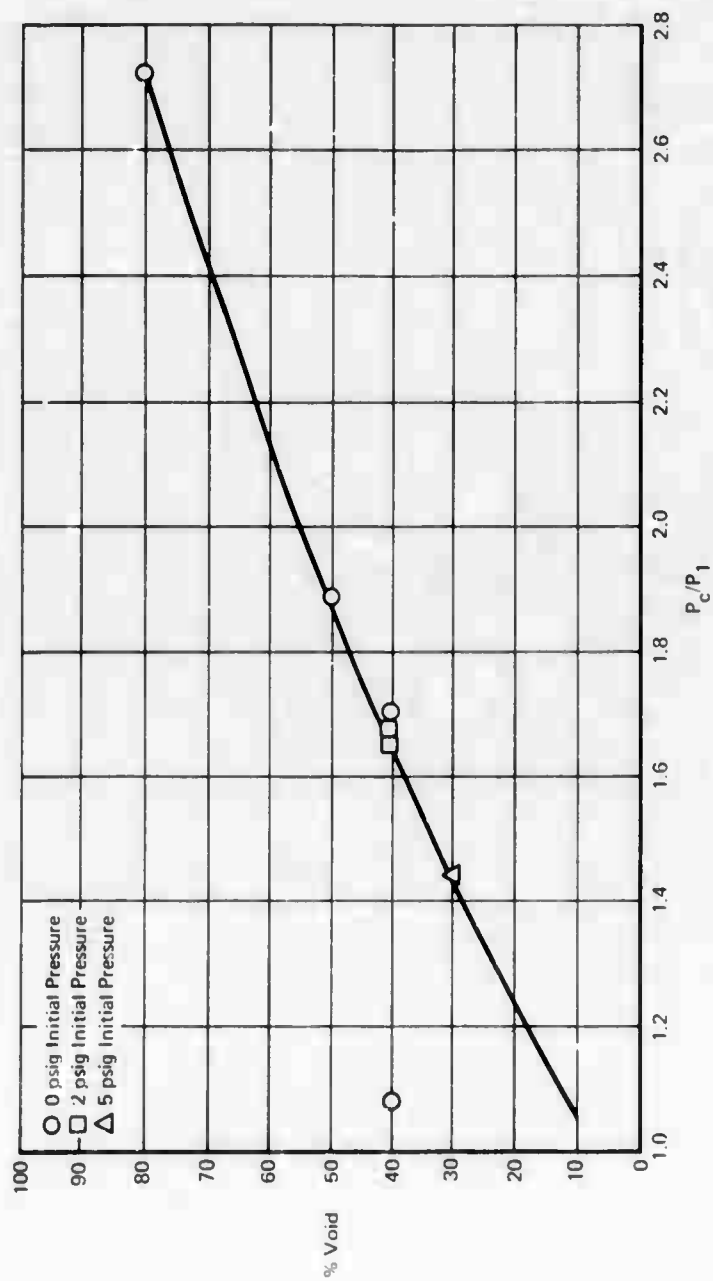
FIGURE 41   THREE CELL WING TANK EGG CRATE TESTS

GP71 0937 54

74
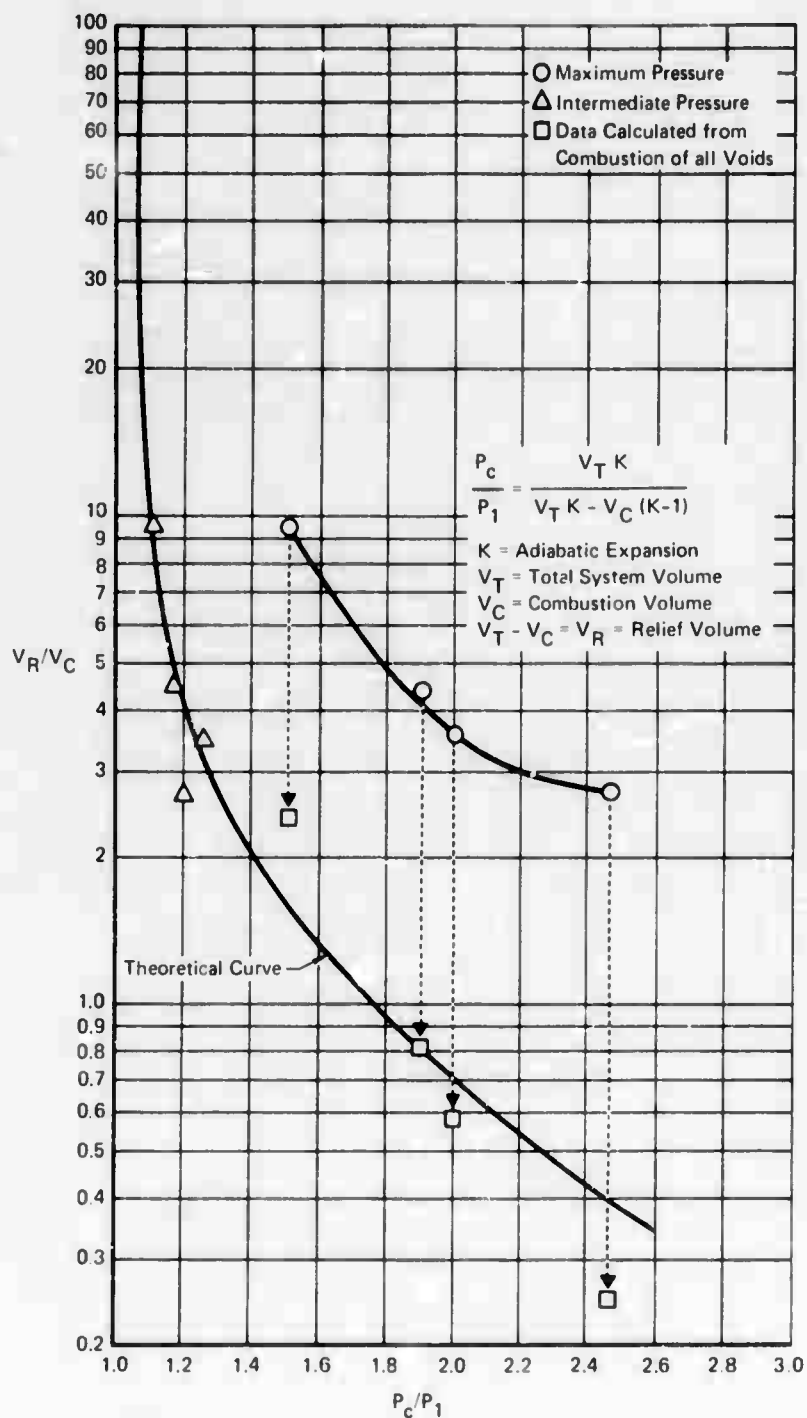
FIGURE 42   PRESSURE RATIOS vs RELIEF TO COMBUSTION VOLUME RATIO -
LINED WALL

THREE CELL WING TANK

GP71 0937 56

75
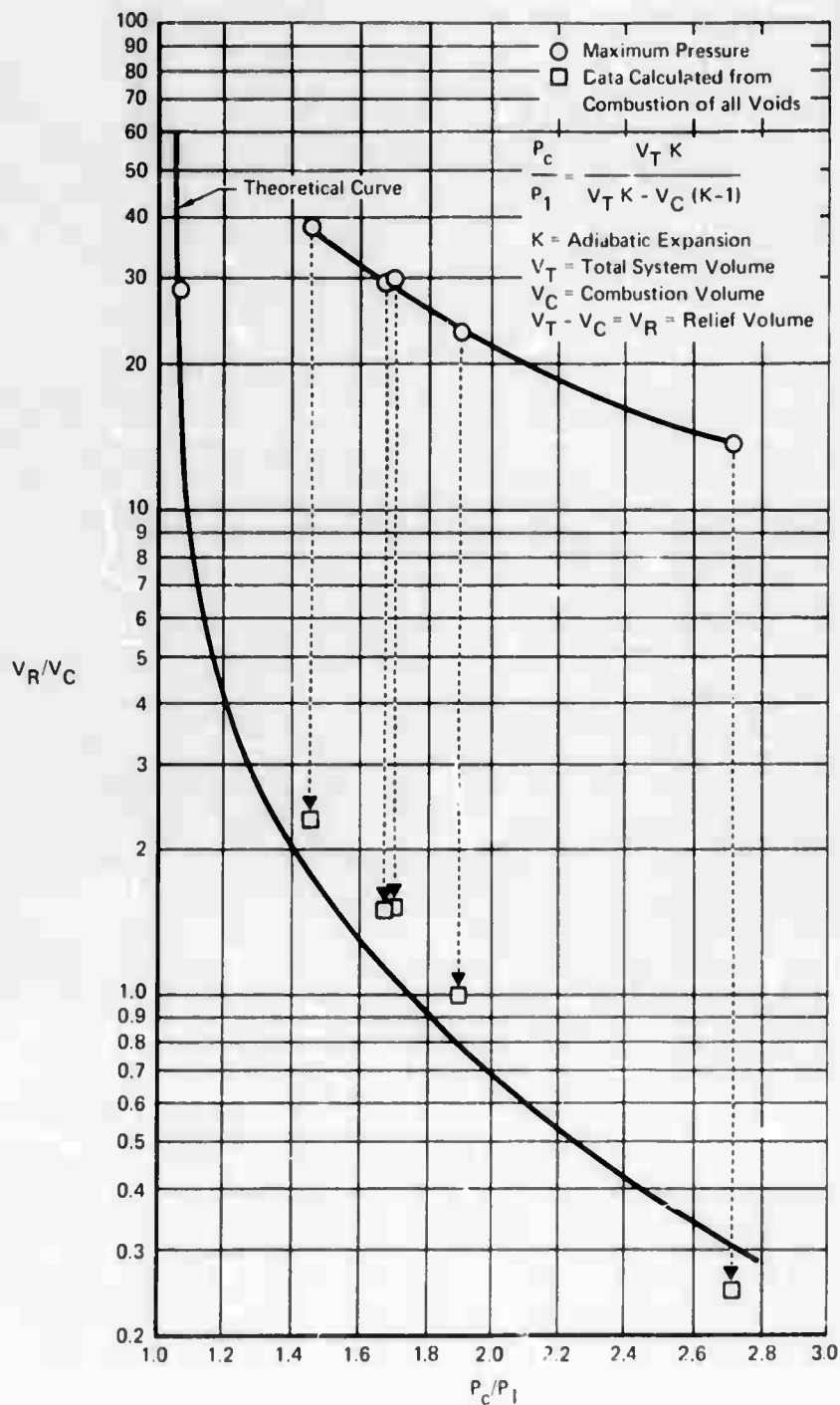
FIGURE 43 PRESSURE RATIOS vs RELIEF TO COMBUSTION VOLUME RATIO - EGG CRATE
THREE CELL WING TANK

GP71 0937 57

76
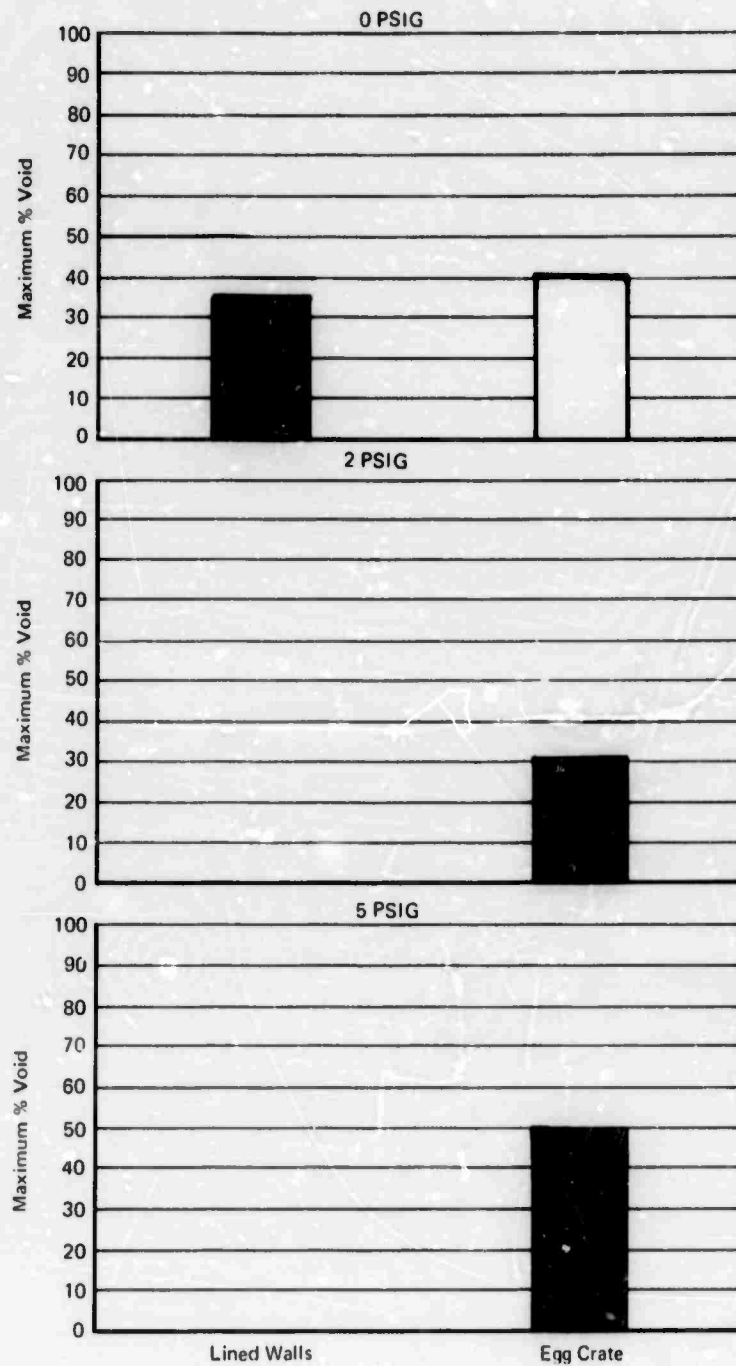
FIGURE 44 THREE CELL WING TANK RESULTS

GP71-0337-58

SECTION IV

PHASE II TEST PROGRAM

1.0 TEST SET-UP

1.1 Combustion Set-Up

The Phase II test set-up for evaluating arrestor effectiveness characteristics consisted of two 30-inch long 8-inch diameter 3/8" wall thickness plexiglass tubes, joined with a divider plate containing 50% open area. The tube set-up was designed to withstand the full combustion over-pressures generated by either a stoichiometric JP-4/air or propane/air mixture. Combustion volume to relief volume ratios of 1 to 1, 1 to 5 and 1 to 10 were provided by using predetermined lengths of plexiglass tubing for the combustion side of the system.

1.2 Instrumentation

Instrumentation consisted of strain gauge type pressure transducers located in each end of the plexiglass tube arrangement and a 40-gauge cromel-alumel thermocouple placed in the combustion side of the system. Pressure, temperature and ignition time data were recorded at 1000 cycles/second system response on oscillograph traces at 15 inches per second. The temperature data was used as a fire verification only. The combustion side of the tube was calibrated with spaced tape strips along its length and high speed movies (1000 frames/second) were taken to obtain flame speeds.

1.3 Explosive Mixture

The explosive mixture used for the combustion tests was the same as described for the Phase I effort, basically stoichiometric propane/air mixture. A chemical analysis of the commercial propane used in the program is included in Appendix I.

1.4 Ignition System

The power supply for the ignition system for the Phase II combustion tests is described in the Phase I test program. Ignition was accomplished by a point source ignitor with a 1/4-inch spark gap. Spark ignition was initiated at the mid-point of the combustion side of the tube set-up.

1.5 Fuel Flow Pressure Drop Set-Up

Fuel flow pressure drop tests were conducted using the 8-inch plexiglass tube set-up described in Paragraph 1.1. The two-inch thick test specimens were bonded to the divider plate containing a hole which was 50% of the cross sectional area. A flow straightener consisting of a 2-inch thick piece of aluminum honeycomb was installed in the flow tube inlet section. Fluid pumping rates were varied from 50 to 150 gallons per minute using JP-4 at ambient temperatures as the flow media.

Preceding page blank

1.5.1 Fuel Flow Test Instrumentation

Data instrumentation consisted of a turbine type flowmeter connected to a frequency counter to measure fuel flow, a U-tube manometer for measuring test specimen differential pressure and a pressure gauge to measure fuel inlet pressure. Flow measurements were taken from a digital read-out type Beckman counter. System accuracy for the flow instrumentation was $\pm$ 2 percent.

1.6 Thermophysical Properties Test Set-Up

1.6.1 Thermal Conductivity

A guarded hotplate apparatus with $\pm$ 2% accuracy within a mean temperature range of 150 to 800°F was used to generate the thermal conductivity data. Measurements were taken, with the material in a vacuum, in increments of 100°F over a mean temperature range of 150 to 400°F.

1.6.2 Specific Heat

Data for the specific heats of selected materials was taken with a Thermophysics Model AC-100 adiabatic calorimeter. Temperature increments of 100°F over a range of 0 to 400°F were used for specific heat data points with an accuracy of $\pm$2%.

1.6.3 Differential Thermal Analyzer

The Robert L. Stone Model KA-2HD differential thermal analyzer was used to determine material melting points, latent heats and heats of reaction. This technique measures the differential temperature between an inert reference and the sample material due to chemical reactions as a function of temperature. Data is recorded on thermograms which are shown in Figures 45 through 53.

1.6.4 Surface Area

Surface area measurements were made by the American Instrument Co. using a Numinico Model AFA 4. This device measures surface area by the low temperature gas absorption technique where the quantity of gas necessary to form a monolayer of gas molecules on the surface of the material is measured and recorded as surface area per unit material weight.

2.0 MATERIAL TEST CONFIGURATIONS

2.1 General

All material specimens for this phase of the program were tested in 2-inch thicknesses, cylindrically-cut to fit inside the plexiglass test set-up.

2.2 Material Configurations

Sixteen basic materials and configurations were tested to demonstrate their arrestor effectiveness. In addition, eleven coatings were applied to these various materials and configurations varying their chemical and thermophysical properties to determine any relationships applicable to their arrestor effectiveness. The material configurations and coatings tested are presented in Table 15. Table 16 describes these materials and their respective properties.

3.0 TEST PROCEDURE

3.1 Combustion Tests

In order to evaluate the many material configurations with a minimum number of tests, a test procedure was set up so as to test materials at the least severe test conditions first where failure would eliminate further testing of that material. This was accomplished by arranging the test set-up with a combustion volume to relief volume ratio of 1 to 10, initial system pressure of 0 psig and the material wetted with JP-5. Specimens that failed to show flame arrestor capabilities within the defined success criteria at these conditions were eliminated from further testing.

Ignition test procedures were the same for each specimen and test parameter. The sample was bonded to the plexiglass tube divider plate and weighed. The specimen was then wetted when applicable, allowed to drain for five minutes and again weighed. The divider plate and attached specimen were installed in the set-up and the pressure in the plexiglass tube reduced to 0.5 PSIA by a water eductor system. A pre-mixed stoichiometric propane/air mixture was introduced into both ends of the test fixture to a positive pressure, which was then vented through the bomb-sampler. When the desired test pressure was established, the vent was closed and the mixing tank and bomb-sampler isolated by closing the necessary valves. The bomb sample mixture was ignited and the pressure monitored to verify the stoichiometric mixture of the propane/air media. The mixture in the test article was then ignited and pressure and temperature measurements recorded on an oscillograph trace.

After the system was purged, the test plate was again weighed (Table 17). If the tested specimen was effective in limiting the system over-pressure to within the defined success criteria, the test was repeated at 2 and subsequently 5 psig initial system pressure. This procedure was repeated with combustion to relief volume ratios of 1 to 5 and 1 to 1.

Coatings as listed in Table 15 were applied to materials that showed a measure of success including all the honeycomb configurations in spite of their poor performance. Tests on these coated materials followed the same sequence as described in the previous paragraph.

Both wet and dry sample tests were conducted. Wetting agents included JP-5 and water.

3.2 Fuel Flow Tests

Fuel flow pressure-drop tests were conducted on candidate materials using JP-4 as the fluid media. The specimen was bonded to the plexiglass tube divider plate and installed in the test set-up. Pressure-drop readings were taken while increasing and decreasing flow rates from 50 to 150 and back to 50 gpm. Data for these are shown in Table 18 and Figures 54 through 59.

81

3.3 Thermophysical Properties Tests

Thermophysical properties tests were conducted on candidate materials as listed in Table 19. Thermal conductivity measurements within $\pm$ 2% were made in increments of 100°F over a mean temperature range of 150 to 400°F. Each of the test samples was sandwiched between the heater plate and a water-cooled heat sink. The heat through each test sample (one-half of the total electrical power supplied to the central heater) was manually adjusted by rheostates. Rheostates were also used to manually match the temperature of the guarded heater to the temperature of the central heater, thus ensuring a unidirectional heat flux through the test samples. By measuring the electrical power supplied to the central heater, the temperature drop across each test sample, and the thickness of each test sample, the thermal conductivity of the test material was calculated at steady-state by means of the one-dimensional form of Fourier's law of heat conduction. Data for these tests are shown in Figure 60.

Specific heats of the materials were measured in increments of 100°F over the range of 0 to 400°F. The sample was installed in the small flat box calorimeter which was lowered into the adiabatic guard chamber. A radiation shield was folded around the guard chamber and a vacuum bell-jar placed over the entire assembly. After evacuation f the enclosure, liquid nitrogen flowed through the cooling coil which was an integral part of the adiabatic guard chamber, thus lowering the chamber and calorimeter to their initial starting temperature. Upon reaching the desired low temperature, the heater on the calorimeter was turned on and a regulated preset D.C. power, was supplied to the calorimeter and contained sample. The energy supplied to the calorimeter serves only to raise the temperature of the calorimeter plus the enclosed sample. The heat supplied per degree rise in temperature represents the heat capacity of the two. Subtracting the predetermined heat capacity of the calorimeter from the total yields the heat capacity of the sample. The specific heat of the sample was obtained by dividing the sample heat capacity by the mass of the sample. Data for these tests are shown in Figure 61.

Melting point, latent heat and heats of reaction were determined by differential thermal analysis. The specimen was placed in contact with one junction of a differential thermocouple while the other junction was placed in contact with an amount of high purity alumina having the same thermal mass as that of the specimen. Temperature was then increased at a programmed rate in a controlled atmosphere. When the specimen undergoes an exothermic or endothermic reaction, the junctions of the differential thermocouple become unbalanced and an emf is generated and recorded. See Figure 45 through 53.

Specimen displacement volumes were obtained by submerging a weighed sample in a graduated cylinder partially filled with a known fluid. The displacement volume, V_t in percent of total bulk volume is given by:

$$\%V_t = Pb/Pt \ (100)$$

$$P_t = \text{true density}$$

$$P_b = \text{bulk density}$$

Fuel retention of the three successful combustion candidate materials was determined by submerging a weighed test sample in a room temperature fuel bath. The sample was then drained and re-weighed.

Surface area was measured by a low temperature gas absorption technique which measures the quantity of gas necessary to form a monolayer of gas molecules on the surface of a weighed sample.

4.0 RESULTS AND DISCUSSION OF RESULTS

4.1 Combustion Tests

Data for the combustion tests of the Phase II effort are presented in tabular and graphical form, Table 20 and Figures 62 through 65. The tables represent the raw data and reflect pressure increases from combustion for both the ignition and receiver sides of the test article. Testing of each specimen was initiated at the least severe system parameters of combustion to relief volume ratio of 1 to 10 and a JP-5 wetted specimen. Where material flame arrestor effectiveness at this condition did not meet the defined success criteria as previously discussed, no further combustion testing was performed with that specimen. It can be seen from Table 20, that considerable effort was saved using this method in that a great number of material configurations did not warrant further testing.

Graphs of the Phase II data are presented in the form of relief volume to combustion volume ratio versus the absolute final combustion pressure to initial system pressure ratio. Only 9 materials could be tested at a sufficient number of system parameters to successfully be graphed. These are shown in Figures 62 through 65 and give excellent correlation with the theoretical curve as previously established. Other material data points where obvious failure occurred correlate with this theoretical curve when the combustion volume is made equal to the total tube system volume minus the material volume. These were not plotted as the pressure rises and rise rates were too great to be useful as an aircraft fuel tank suppressant system. It can be seen that data correlation using this method is accomplished with the Phase I effort of the program. Of the nine configurations tested only three base materials produced results which warrant their consideration as effective flame arrestors. These were 25 ppi reticulated polyurethane foam, fire extinguishing foam and 3M Scotch Brite felt. Aluminum tube core and polyester screen produced erratic results and therefore their degree of success is questionable with respect to this testing.

The 25 ppi foam successfully suppressed the explosions for the following test conditions:

(1) V_r/V_c ratio of 10/1 at 0, 2 and 5 psig initial system pressures with wetted, water-wetted and dry materials.

(2) V_r/V_c ratio of 5/1 and 1/1 at 0 and 2 psig initial pressure with JP-5 and water-wetted material.

83

The fire extinguishing foam was effective for the following test condit'ons:

(1) Vr/Vc ratio of 10/1 and 5/1 at 0, 2 and 5 psig initial system pressure
          with JP-5 wetted, water-wetted and dry material.

(2) Vr/Vc ratio of 1/1 at 0 and 2 psig initial pressure with both wet
          and dry material.

Scotch Brite material was successful at all ratios of Vr/Vc tested for
0, 2 and 5 psig and wetted or dry material.

Coatings were applied to various materials as listed in Table 15 and in one
case showed marked improvement in the results. Aluminum tube core coated with
flourel in a Vr/Vc set-up of 10/1 at ambient initial pressure reduced the combustion
over-pressure from 17.5 psig to 1.5 psig. This only performed with such over-
whelming results in one case of several similarly coated materials, but indicates
that with the right combination of materials, configurations and coatings can
provide improved flame arrestors. Other coatings tested showed improvements also,
reducing combustion over-pressures by from 12 to 24%. Polysulfide-coated 1/8-inch
perforated aluminum honeycomb showing a 12% reduction in over-pressures and glass
resin-coated fiberglass providing the 24% change. Results of other material and
coating combinations ranged between this minimum and maximum percent improvement
as can be seen in Table 20. Coated foams showed little if any improvement over
the base material results and in the case of the KBr and KI coatings, higher com-
bustion over-pressures were obtained. Copper-coated foam has a greater flame
arresting effectiveness than nickel-coated foam or the base polyurethane foam
materials from an over-pressure standpoint.

Water and JP-5 wetted arrestor material performed better than dry materials
with respect to limiting pressure rise and flame propagation. The water wetted
samples performed only slightly better than the JP-5 wetted and dry specimen at
large Vr/Vc ratios in spite of the overwhelming thermal sink. This would indicate
that the action was more physical or chemical than thermal. At low Vr/Vc ratios;
i.e., 1:1 only the wetted material was successful in eliminating flame propation.
Here again the water wetted samples only slightly out performed the JP-5 wetted
materials indicating strong chemical effects.

Flame speeds for the combustion tests conducted at 0 psig initial pressure
with a stoichiometric propane air mixture were measured by high speed motion
pictures (1000 frames/sec). The number of frames that were spent showing the
propagation of the ignition kernal in the calibrated tube were counted and the
flame speed calculated. The average flame speed for these tests was 19 ft/sec.

4.2 Flow Test Results

Results of these tests are given in Table 18 and shown in Figures 54 through
59. Of the three most successful arrestor test materials, the 25 ppi foam
resulted in the lowest pressure drop. As can be seen from the tabulated data,
pressure drop reading for the foam and felt materials do not repeat as the flow
is cycled from 50 to 150 to 50 gpm rates. This is due to the collapsing of
the material as the flow is increased and the failure of the material to regain

84

its original shape as the flow is decreased. After a period of time, the material does return to its original shape and the tests results were repeatable. Materials felt to have promising flame arresting capabilities in addition to the three discussed above, were also flow tested for data correlation purposes and system analysis.

4.3 Thermophysical Properties Test

Thermophysical properties measurements, included thermal conductivity, specific heat, surface area, bulk density, specific fuel retention, melting temperature and heat of reaction of selected materials. Configurations that showed little or no potential flame arresting capabilities were not carried through the complete thermophysical properties testing in that no benefit could be realized toward the comparison of materials without successful combustion test data. Table 19 shows the data applicable to the various materials. Figures 60 and 61 represent the thermal conductivity and specific heats at various test temperatures. Figures 45 through 53 show the traces from the DTA measurements. Thermal conductivity and specific heat data have been included as a variable in the regression analysis of Phase III of the program and are given in Section VI of this report.

CONCLUSIONS AND RECOMMENDATIONS

5.0 Conclusions

Phase II of the program has shown that other materials and configurations can be effectively employed as fire and explosion attenuators in aircraft fuel tanks. Although the number of material configurations that performed within the test article was not representative of an actual aircraft fuel system.

o The most efficient flame arrestor materials tested for all combustion parameters considered were the 3M polyester felt, (Scotch Brite) followed by fire extinguishing and 25 ppi Scott reticulated polyurethane foam.

o The proper combination of material configurations and coatings can be effective flame arrestors. Felts and foams appear to be the most promising configurations.

o Large pore diameter materials are not effective flame arrestor configurations.

o Wetting the material affected system performance from an over-pressure standpoint and showed a greater flame arresting effectiveness where the Vr/Vc ratios were small.

o More material damage resulted in tests with dry specimens.

o The combination of fiberglass honeycomb coated with glass resin produced the greatest improvement in arrestor effectiveness due to coating addition.

o JP-4 fluid pressure drop is lower for the 25 ppi reticulated polyurethane than other equally effective foam and felt materials.

o The material thermophysical properties of thermal conductivity and specific heat have a small effect on the explosion attenuating effectiveness.

6.0 RECOMMENDATIONS

It is recommended that further testing of arrestor materials be conducted where specimen thickness to combustion volume can be varied and the L/D ratios for effective flame arresting can be determined. It is also recommended that these tests concentrate on foam and felt materials. Ignition energy also needs to be investigated as a variable for this type system.

Preceding page blank

Heat of Fusion = 134 cal/gr
Heat of Reaction = 3080 cal/gr
cp = 0.64 Btu/# – °F
Temp of Fusion = 200°C
Temp of Reaction = 288°C

500°C (932°F)

400°C (752°F)

300°C (572°F)

Melting Point

200°C (392°F)

Exothermic — Endothermic
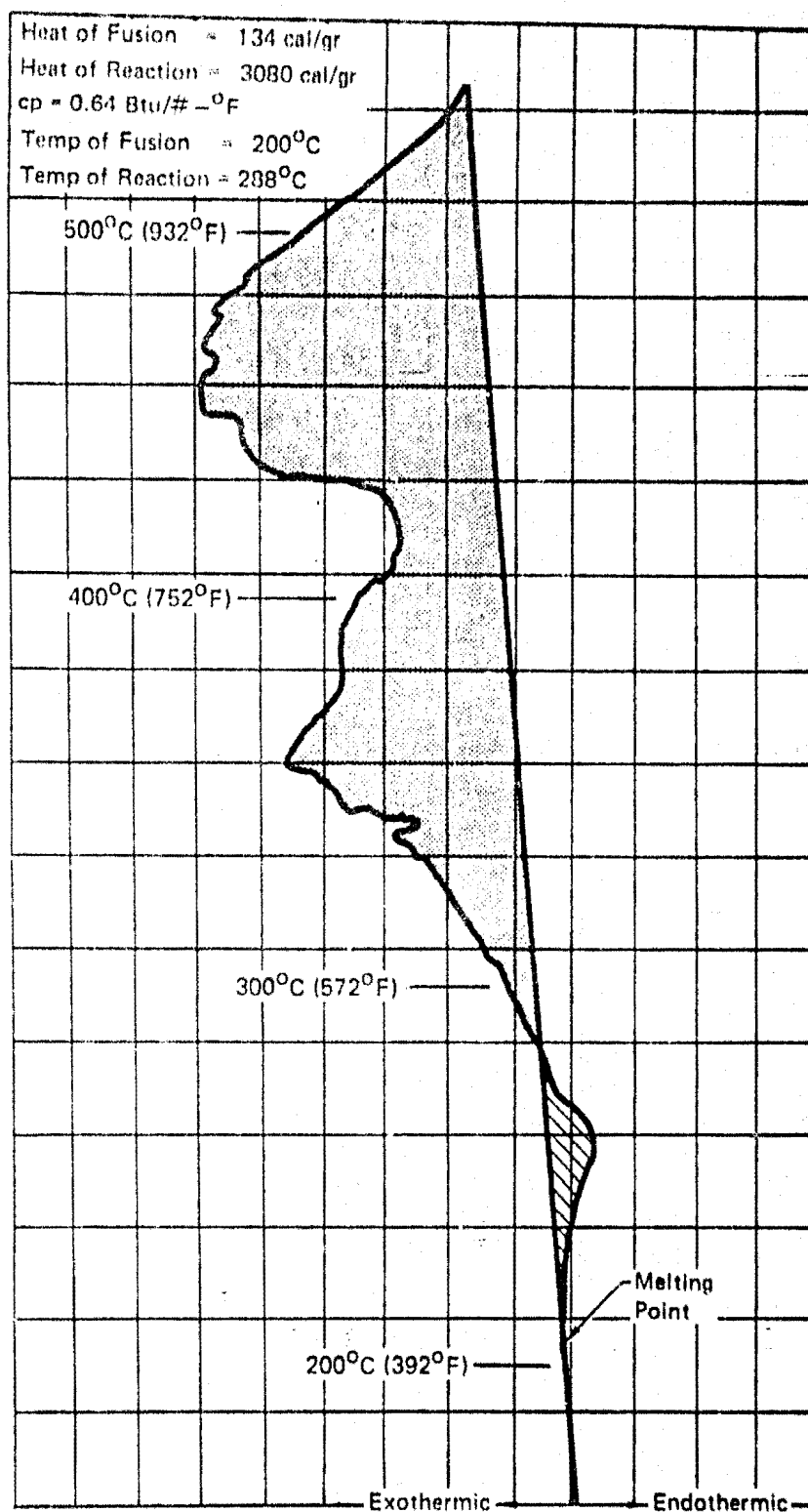
FIGURE 45 DTA TRACE

25 PPI FOAM

150 µV 2.239 mg Sample

GP71-1605-9

88

Heat of Fusion = 17.6 cal/gr
Heat of Reaction = 2530 cal/gr
cp = 0.48 Btu/# –°F
Temp of Fusion = 210°C
Temp of Reaction = 227°C

500°C (932°F)

400°C (752°F)

300°C (572°F)

Melting Point

200°C (392°F)

Exothermic — — Endothermic —
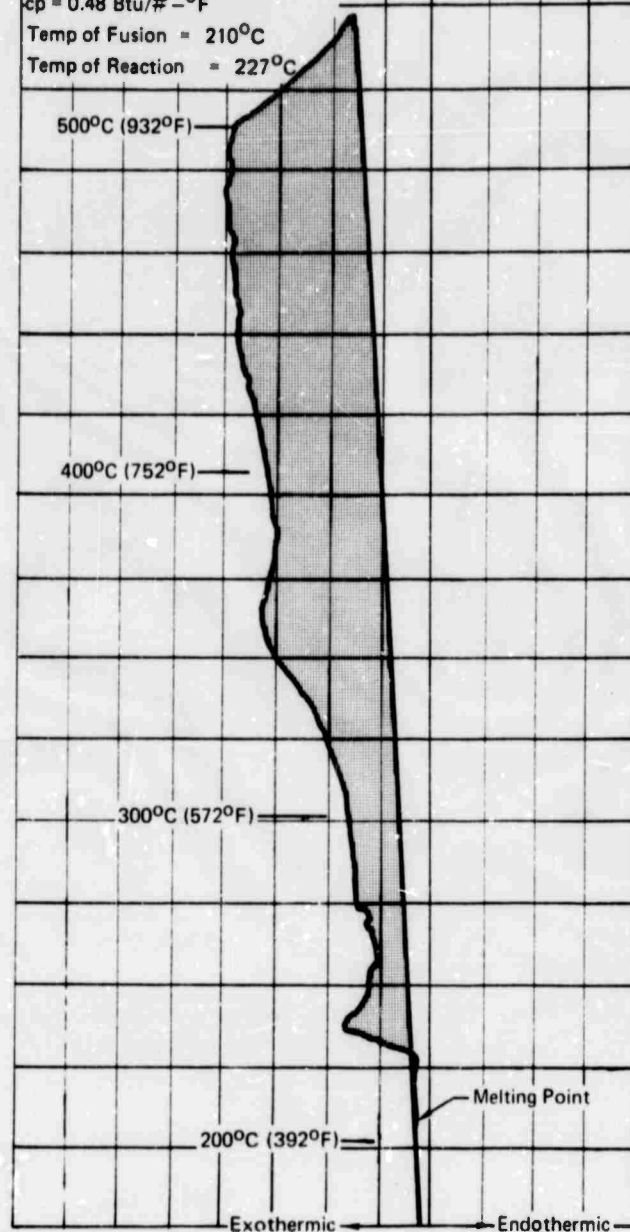
FIGURE 46 DTA TRACE

FIRE EXTINGUISHER FOAM   150 μV   2.451 mg Sample

GP71-1605-11

89

Heat of Fusion = 5.4 cal/gr
Heat of Reaction = 2530 cal/gr
cp = 0.53 Btu/# °F
Temp of Fusion = 215°C
Temp of Reaction = 281°C

(932°F) 500°C

(752°F) 400°C

(572°F) 300°C

Melting Point

(392°F) 200°C

Exothermic — — Endothermic
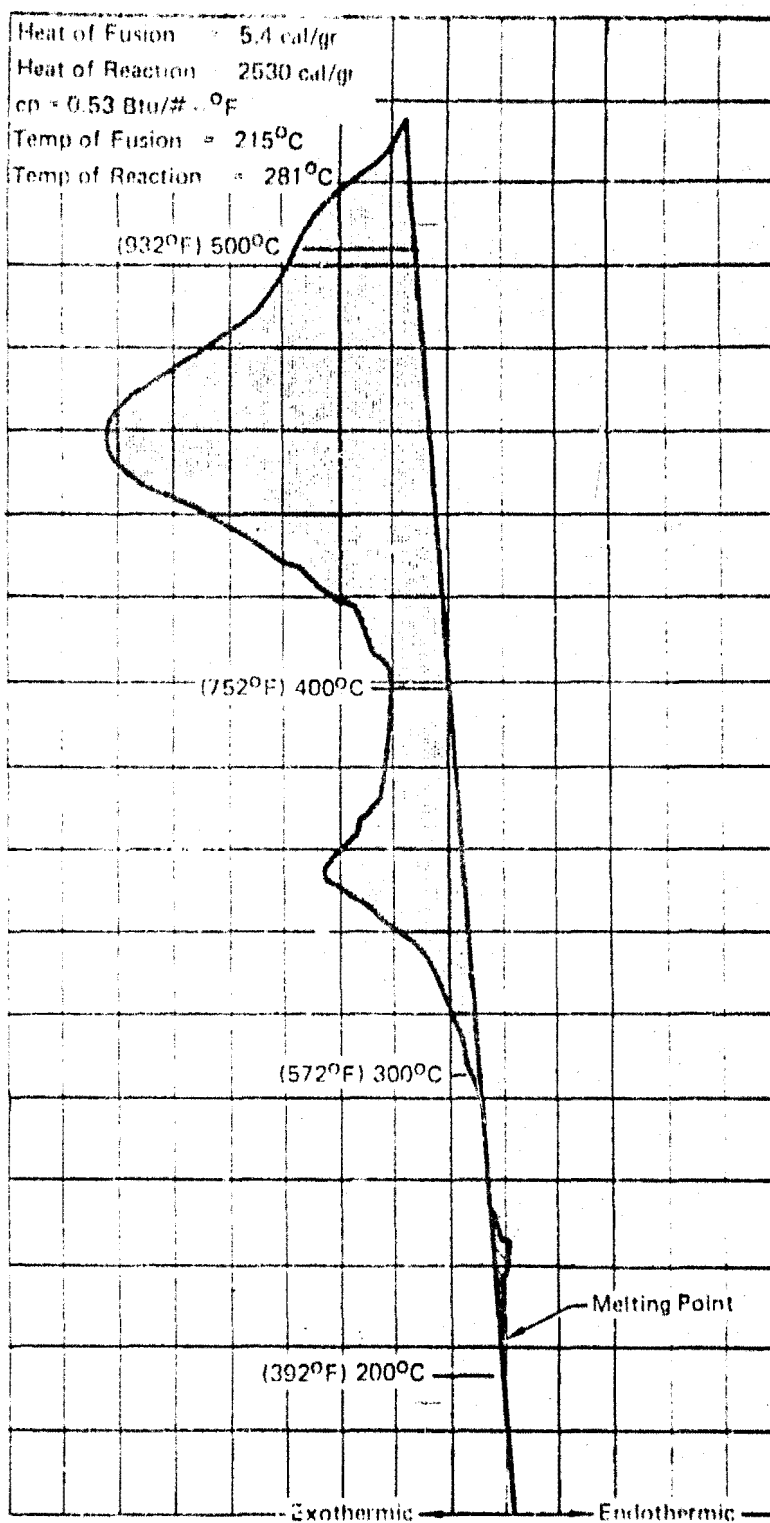
FIGURE 47 DTA TRACE

3M SCOTCH BRITE   150 µV   2.647 mg Sample

GP21-1005-12

90
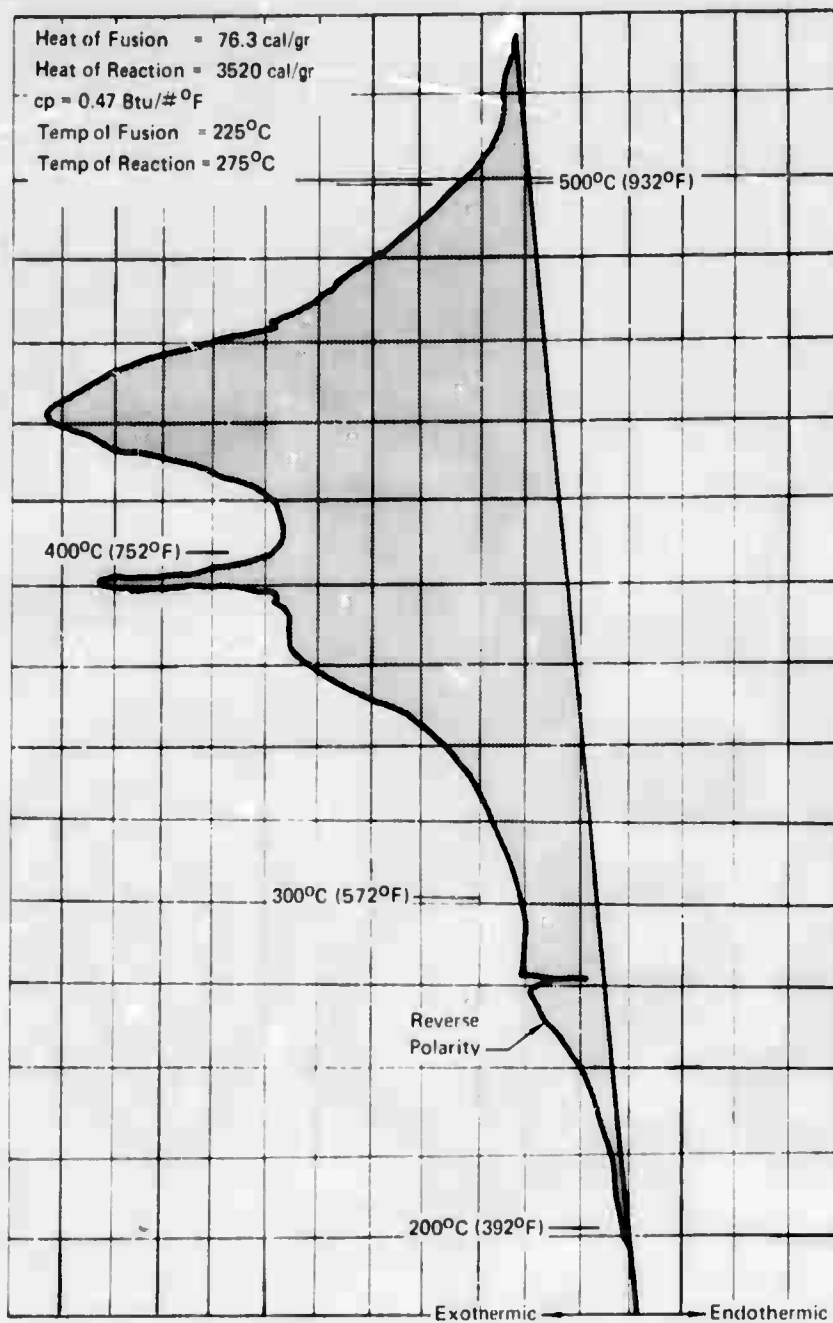
FIGURE 48 DTA TRACE

25 PPI FOAM COATED WITH POLYSULFIDE   150 μV   3.581 mg Sample

GP71 1605 14

91

Heat of Fusion = 70.0 cal/gr
Heat of Reaction = 2760 cal/gr
c_p = 0.59 Btu/# $-^{o}$F
Temp of Fusion = 230°C
Temp of Reaction = 292°C

500°C (932°F)

400°C (752°F)

300°C (572°F)

Melting
Point

Exothermic   Endothermic

200°C (392°F)
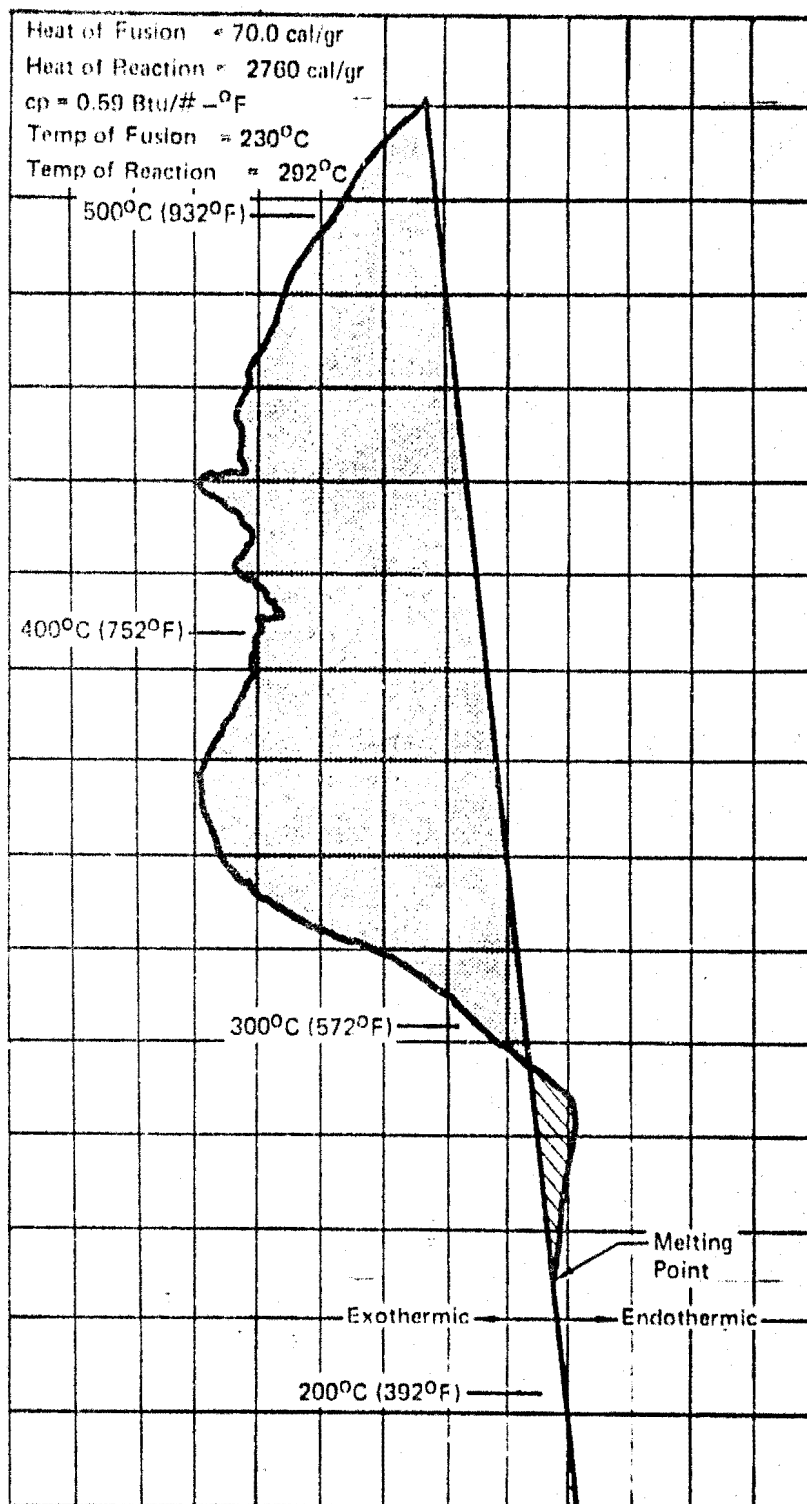
FIGURE 49   DTA TRACE

25 PPI FOAM COATED WITH GLASS RESIN   150 μV   3.300 mg Sample

QP71 1605 10

92
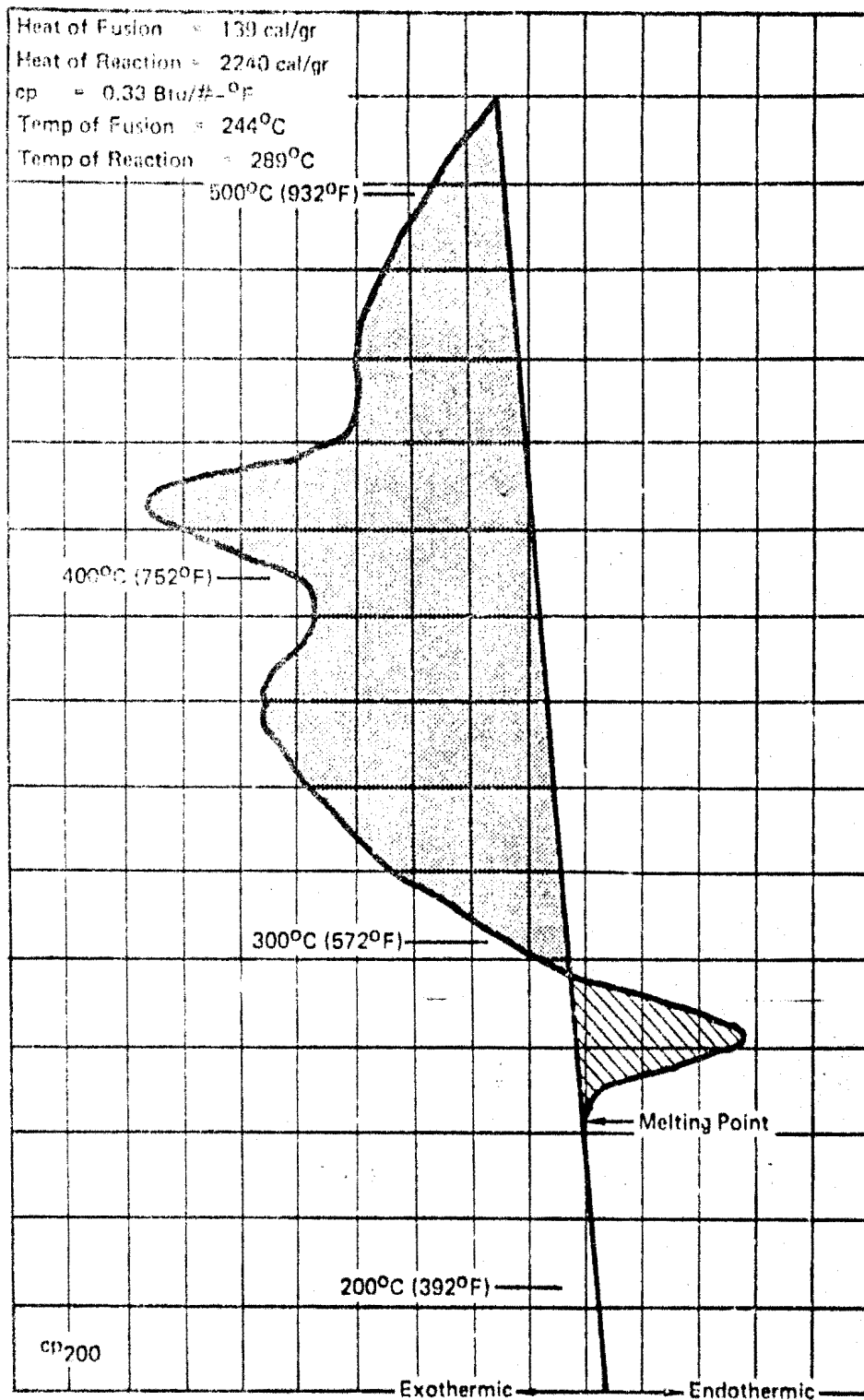
FIGURE 50 DTA TRACE

25 PPI FOAM COATED WITH REDAR VITON   150 μV   4.137 mg Sample

Heat of Fusion = 37.8 cal/gr
Heat of Reaction = 3320 cal/gr
cp = 0.41 Btu/# – $^{\circ}$F
Temp of Fusion = 225°C
Temp of Reaction = 287°C

500°C (932°F)

400°C (752°F)

300°C (572°F)

Melting Point

200°C (392°F)

Exothermic — Endothermic
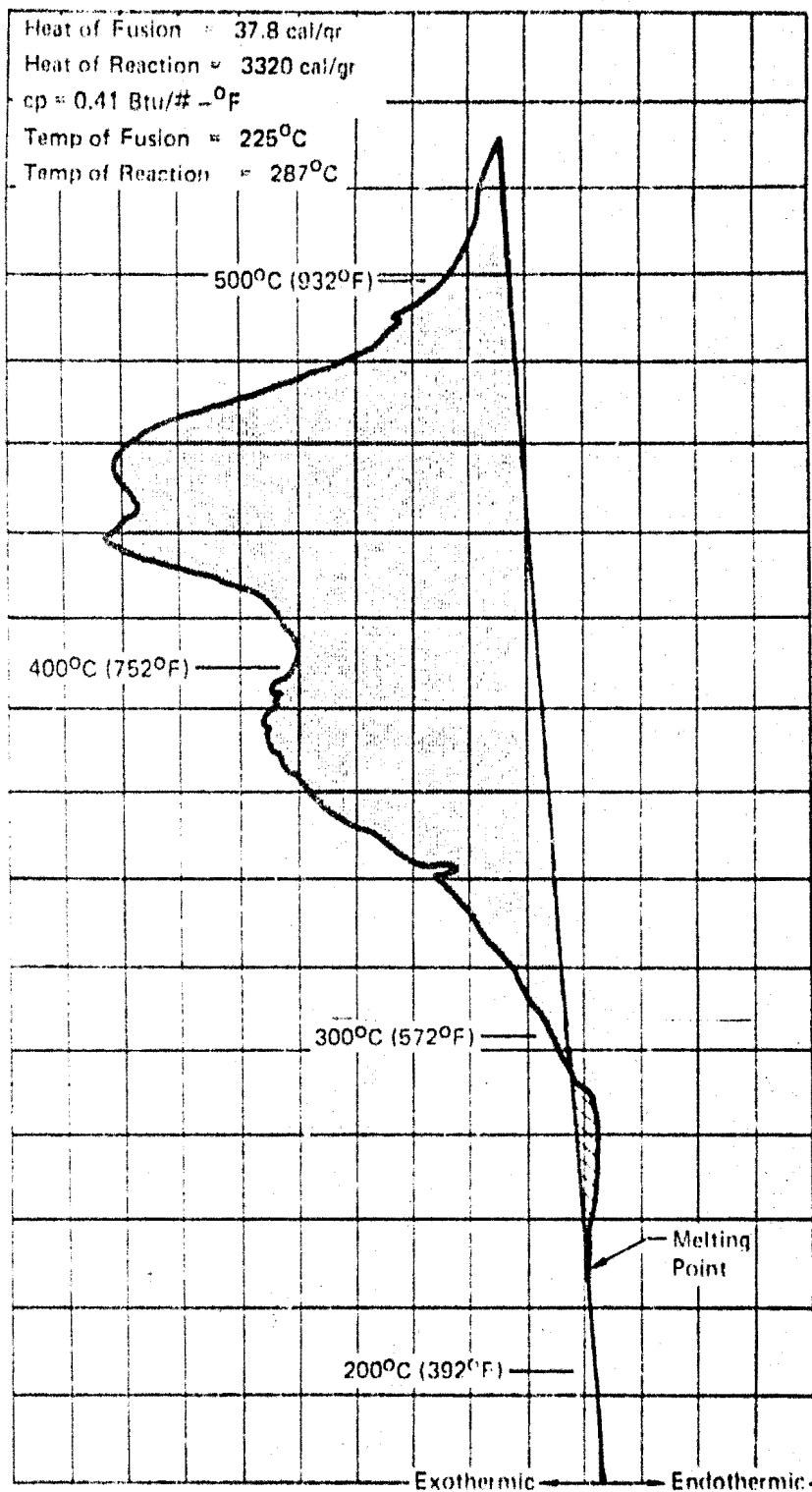
FIGURE 51 DTA TRACE

25 PPI FOAM COATED WITH KEL-F   150 µV   3.057 mg Sample

QP71 1606 B

94
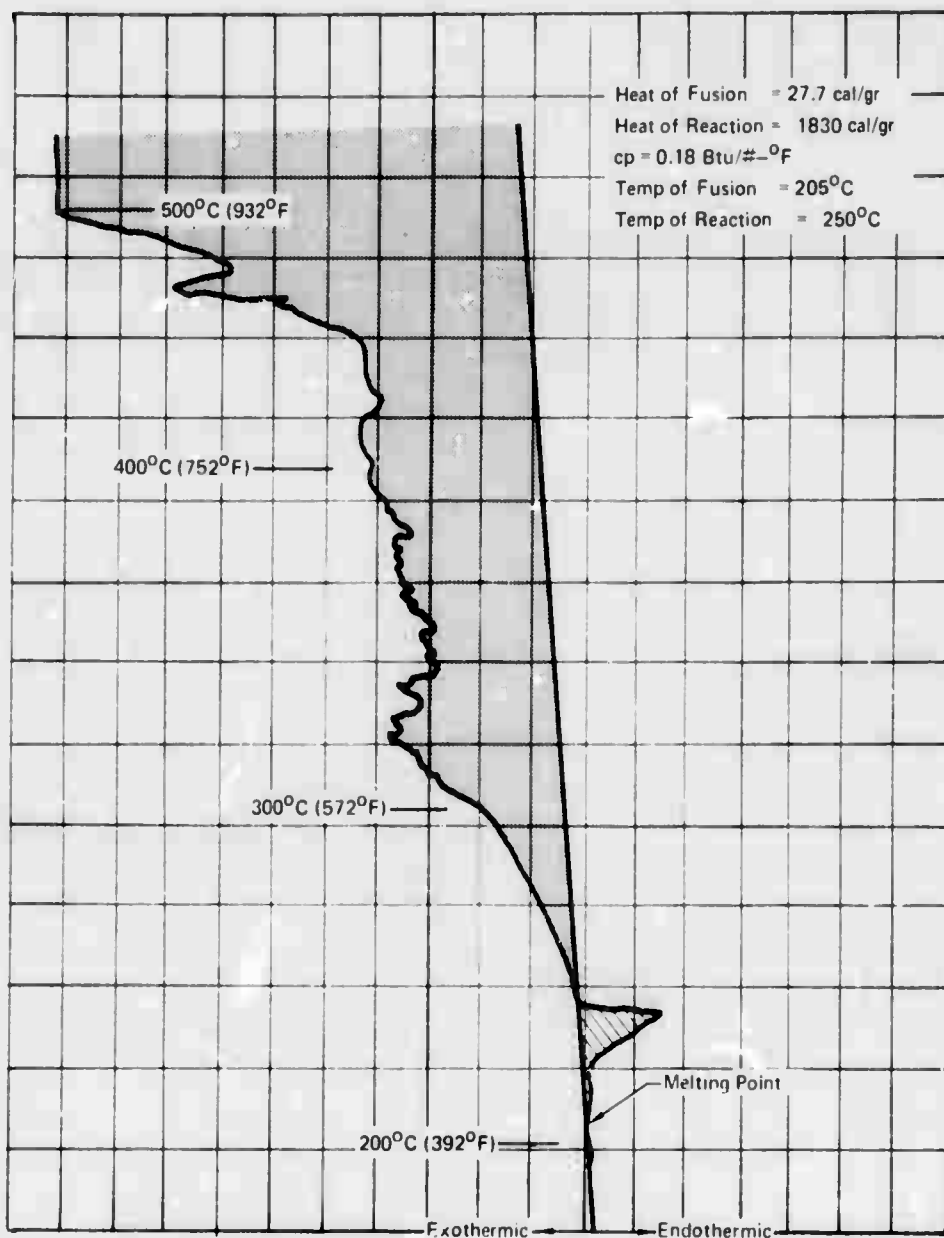
FIGURE 52 DTA TRACE

POLYESTER SCREEN   150 μV   6.285 mg Sample

95
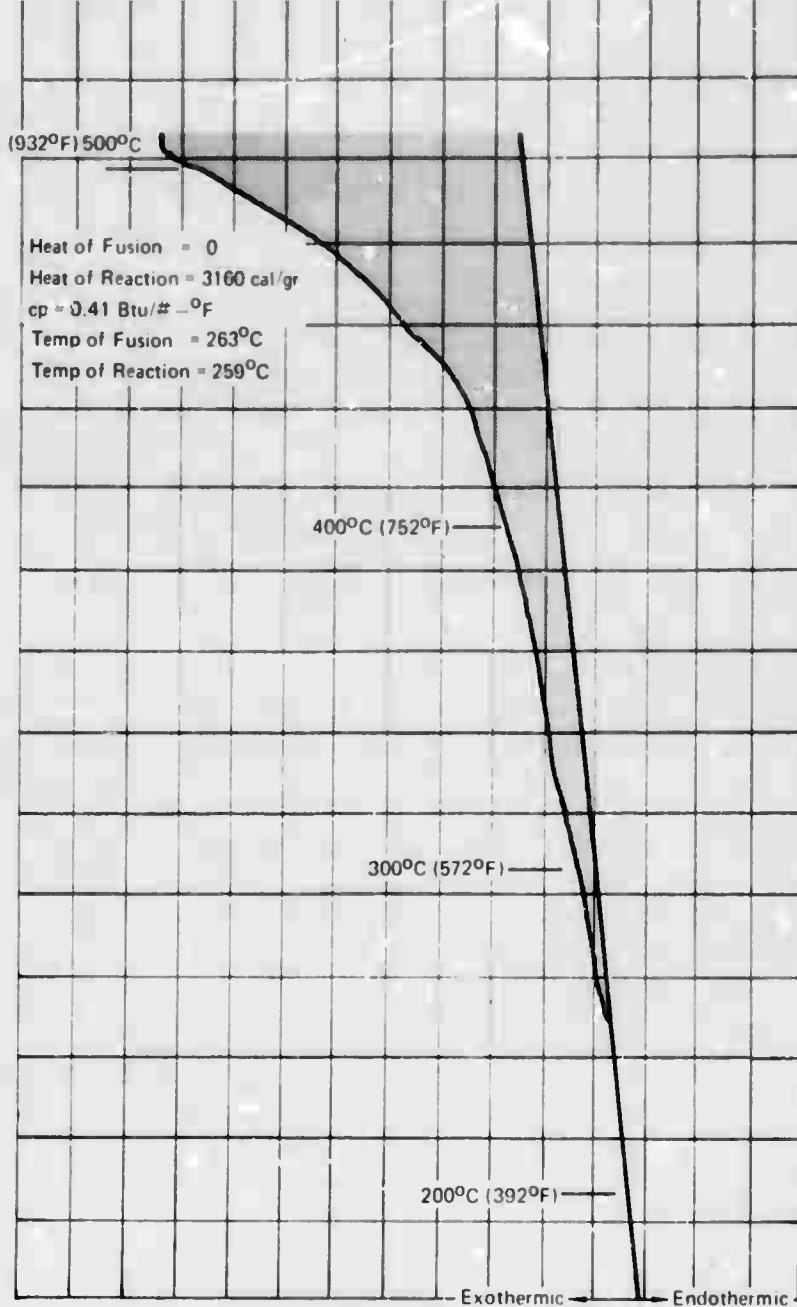
FIGURE 53 DTA TRACE

NOMEX HONEYCOMB   150 μV   3.581 mg Sample

TABLE XX

MATERIAL CONFIGURATIONS

Materials / Coating	Kel-F	Flourel	Polysulfide	Glass Resin	Radar Viton	Polyurethane	Nickel	Copper	Fuel	Water
Foam 25 ppi	X		X	X	X				X	X
Foam 15 ppi	X		X	X	X		X	X	X	
Fire Extinguishing Foam	X		X	X	X				X	X
3M Scotch Brite									X	X
Aluminum Honeycomb	X	X	X	X	X	X			X	X
Aluminum 1/8" Hexagon Honeycomb	X	X	X	X	X				X	
Perforated Aluminum Honeycomb	X	X	X	X	X	X			X	
Aluminum Tube Core (Dimpled)	X	X	X	X	X	X			X	X
Fiberglass Round Honeycomb (Tubes)	X	X	X	X	X				X	
Fiberglass Sine Wave Honeycomb (Corregation)	X		X							
Nomex Round Honeycomb	X		X						X	
Nomex Sine Wave Honeycomb (Corregation)	X		X		X	X				
Stainless Steel Tubes 3/16 Diameter 0.049 Wall									X	
Viton Tubes									X	
Polyester Screen (Rolled)									X	
Stainless Steel Screen (Chevron)						X			X	
Copper Plated 25 ppi Foam									X	X
Nickel Plated 25 ppi Foam									X	X

97

TABLE XVI
MATERIAL PROPERTIES

	Configuration & Designation	Material	Cell Size (Inch)	Foil Thickness (Inch)	Cell Walls	Cell Shape	Density #/Ft³
1.	Honeycomb AL-1/8-5052-.001K-4.5	Aluminum Alloy 5052 H39	1/8	.001	Non-Perforated	Hexagonal	4.5
2.	Honeycomb AL-F/30-5052-.0013N-4.3	Aluminum Alloy 5052 H39		.0013	Non-Perforated	Flex-Core	4.3
3.	Honeycomb AL-1/8-5052-.005-12.1	Aluminum Alloy 5052 H39	1/8	.003	Perforated	Hexagonal	12.1
4.	Honeycomb AL-1/8-5052-.0013N	Aluminum Alloy 5052 H39	1/8	.0013		Tube Core	
5.	Honeycomb HRH-10-1/8-3.0	DuPont Nomex Nylon Paper	1/8		Non-Perforated	Hexagonal	3.0
6.	Honeycomb HRH-10-F/50-3.5	DuPont Nomex Nylon Paper			Non-Perforated	Flex-Core	3.5
7.	Honeycomb HRP-3/16-4.0	Glass Fabric Reinforced Plastic	3/16		Non-Perforated	Hexagonal	4.0
8.	Honeycomb HRP-F/50-3.5	Glass Fabric Reinforced Plastic	.1375	.0490	Non-Perforated	Flex-Core	3.5
9.	Metal Tubes	Aluminum ID = .0395"					

Configuration & Designation	Material	Cell Size (Inch)	Wall Thickness (Inch)	Cell Walls	Cell Shape	Density #/Ft.3
10. Viton Tube (OD = 1/8")	Viton Sponge Rod					
11. Screen Cloth (69% open area)	Polyester	1800	500			
12. Screen Cloth (59.3% open area)	Steel	16 opening/linear inch	Wire dia. = .023			
13. Reticulated Foam	Polyurethane	25 ppi				1.36
14. Reticulated Foam	Polyurethane	15 ppi				1.36
15. Reticulated Foam	Polyurethane with fire retardant chemicals	35 ppi				
16. Felt (Scotch Brite)	Polyester					
17. PC 1981, 3M Company	Kel-F					
18. R/M L-3203-6, Raybestos/Manhattan	Flourel					
19.	Polysulfide					
20. Type 650 Glass Resin, Owens-Illinois	Glass Resin					
21. Redar-RP-902-01, R.Z. Darling Company	Redar Viton					

TABLE XVI (CONT'D)
MATERIAL PROPERTIES

Configuration & Designation	Material	Cell Size (Inch)	Wall Thickness (Inch)	Cell Walls	Cell Shape	Density #/Ft.³
22. Vibrathane A-761, Uniroyal Chemical	Polyurethane					
23. Reticulated Foam	Ni Plating Solution					
24. Reticulated Foam	Cu Plating Solution					
25. Teflon-S 958-207 Green, Dupont	Teflon					

Test No.	Material	Before Firing			After Firing		(A)-(B) (Oz)	Wetting Agent
		Plate Weight (Oz)	Material Weight (Oz)	Sample + Wetting Agent (Oz) (A)	Sample Weight (Oz) (B)	Dry Sample Weight (Oz)		
1	Foam 25 ppi	49	.5	52.0	50.5	49.0	1.5	JP-5
2	Foam 25 ppi	49	1.0	52.0	51.5	50.0	.5	JP-5
3	3M Scotch-Brite	49	2.0	52.0	52.0	—	0	JP-5
4	Foam 15 ppi	48	1.5	52.5	50.0	—	2.5	JP-5
5	Foam 25 ppi	48	2.0	53.0	52.0	—	1.0	JP-5
6	3M Scotch-Brite	48	1.5	51.0	50.5		.5	JP-5
7	3M Scotch-Brite	49	1.5	52.0	52.0		0	JP-5
8	3M Scotch-Brite			51.5	51.0	50.0	.5	H2O
9	3M Scotch-Brite			52.5	52.0	51.0	.5	H2O
10	3M Scotch-Brite			52.5	52.0	51.0	.5	H2O
11	Fire Extinguishing Foam			52.0	51.5	51.0	.5	JP-5
12	Fire Extinguishing Foam			53.0	52.5	52.0	.5	JP-5
13	Fire Extinguishing Foam			53.0	52.5	52.5	.5	JP-5
14	Foam 25 ppi			54.0	51.5	50.5	1.0	H2O

Test No.	Material	Before Firing			After Firing		(A)-(B) (Oz)	Wetting Agent
		Plate Weight (Oz)	Material Weight (Oz)	Sample + Wetting Agent (Oz) (A)	Sample Weight (Oz) (B)	Dry Sample Weight (Oz)		
15	Foam 25 ppi				54.0	51.0		H2O
16	Foam 25 ppi			55.0	54.0	52.0	1.0	H2O
17	Fire Extinguishing Foam			56.0	54.0	52.0	2.0	H2O
18	Fire Extinguishing Foam			56.0	54.0	53.5	2.0	H2O
19	Fire Extinguishing Foam			57.0	57.0	55.0	0	H2O
20	Foam 25 ppi	48	1.5	52.5	51.0			JP-5
21	Foam 25 FFi	48	2.5	52.0	52.0		.5	JP-5
22	Foam 25 ppi	48	2.5	52.0	50.5	50.5	1.5	JP-5
23	Foam 25 ppi	48	1.5	54.5	53.5		1.0	H2O
24	Foam 25 ppi	48	2.0	55.0	52.0		3.0	H2O
25	Foam 25 FFi	48	2.0	54.5	53.5		1.0	H2O
26	Fire Extinguishing Foam	48	3.0	54.5	52.0	51.0	2.5	JP-5
27	Fire Extinguishing Foam	48	4.5	58.0	55.0	52.0	3.0	JP-5
28	Scotch-Brite	48	3.0	55.0	53.0		2.0	JP-5
29	Scotch-Brite	48		56.0	51	51.0	2.5	JP-5

TABLE XVII (Cont'd)

| Test No. | Material | Before Firing | | | After Firing | | (A)-(B) (Oz) | Wetting Agent |
		Plate Weight (Oz)	Material Weight (Oz)	Sample + Wetting Agent (Oz) (A)	Sample Weight (Oz) (B)	Dry Sample Weight (Oz)		
30	Scotch-Brite	48	3.0		50.5			Dry
31	Fire Extinguishing Foam	48	3.0		51.0			Dry
32	Foam 25 ppi	48	1.5		49.0			Dry
33	Foam 25 ppi	48	2.0		50.0			Dry
34	Foam 25 ppi	48	1.5		48.5			Dry
35	Foam 25 ppi	48	1.5		48.5			Dry
36	Foam 25 ppi	48	1.5		49.5			Dry
37	Scotch-Brite	48	2.0		50.0			Dry
38	Fire Extinguishing Foam	48	4.0		52.0			Dry
39	Foam 25 ppi	48	2.0	55.0	52.0	50.0	3.0	H2O
40	Foam 25 ppi	48	2.0	52.0	50.5	50.0	1.5	JP-5
41	Foam 25 ppi	48	1.0		48.5			Dry
42	Fire Extinguishing Foam	48	2.5	56.0	54.0	50.5	2.0	JP-5
43	Fire Extinguishing Foam	48	3.5	59.0	54.0	51.0	5.0	H2O
44	Fire Extinguishing Foam	48	2.0		50.0			Dry

103

Test No.	Material	Before Firing			After Firing		(A)–(B) (Oz)	Wetting Agent
		Plate Weight (Oz)	Material Weight (Oz)	Sample + Wetting Agent (Oz) (A)	Sample Weight (Oz) (B)	Dry Sample Weight (Oz)		
45	Fire Extinguishing Foam	48	3.5		50.0			Dry
46	Scotch Brite	48	3.5	55.0	53.0	—	2.0	H$_2$O
47	Scotch Brite	48	2.0	53.0	52.0	—	1.0	JP-5
48	Scotch Brite	48	3.0		51.0	—		Dry
49	Scotch Brite Foam 25 ppi	48.0	3.0		51.0	—		Dry
50	Pink Foam	48	2.0		49.5	—		Dry
83	Al-1/8" Hexagnol Honeycomb Kel-F Coating	48	4.5	54.1	53.8		.3	JP-5
84	Al-Tube Core Kel-F Coating	48	7.5	59.5	57.9		1.6	JP-5
85	Al-1/8" Hexagnol Honeycomb Kel-F Coating	48	3.9	59.0	55.0		4.0	JP-5
86	Fiberglass 1/8" Round Round Honeycomb Kel-F Coating	48	2.9	52.0	51.5		.5	JP-5
87	Al-1/8" Perforated Honeycomb Kel-F Coating	48	9.3	58.7	58.4		.3	JP-5
88	Nomex 1/8" Sine Wave Honeycomb Kel-F Coating	48	3.4	52.5	52.0		.5	JP-5

TABLE XVIII (Cont'd)

Test No.	Material	Before Firing			After Firing		(A)-(B) (Oz)	Wetting Agent
		Plate Weight (Oz)	Material Weight (Oz)	Sample + Wetting Agent (Oz) (A)	Sample Weight (Oz) (B)	Dry Sample Weight (Oz)		
89	Nomex 3/16" Round Honeycomb Kel-F Coating	48	3.4	52.2	51.2	—	1.0	JP-5
90	Fiberglass 1/8" Sine Wave Honeycomb Kel-F Coating	48	3.0	52.0	51.5	—	.5	JP-5
92	Al-1/8" Perforated Honeycomb Glass Resin	48	9.0	57.7	57.0	—	.7	JP-5
93	Al-1/8" Hexagnol Honeycomb Glass Resin	48	4.1	53.6	53.1	—	.5	JP-5
94	Al-1/8" Hexagnol Honeycomb Glass Resin	48	4.5	54.2	53.9	—	.3	JP-5
95	Fiberglass 1/8" Round Honeycomb Glass Resin	48	3.4	53.9	53.0	—	.9	JP-5
96	Al-Tube Core Glass Resin	48	7.8	58.4	58.2	—	.2	JP-5
97	Al-1/8" Perforated Honeycomb Radar Viton Coating	48	9.1	58.7	58.7	—	0	JP-5
98	Al-1/8" Hexagnol Honeycomb Viton Coating	48	4.5	54.4	54.1	—	.3	JP-5

TABLE XVIII (Cont'd)

Test No.	Material	Before Firing			After Firing			Wetting Agent
		Plate Weight (Oz)	Material Weight (Oz)	Sample + Wetting Agent (Oz) (A)	Sample Weight (Oz) (B)	Dry Sample Weight (Oz)	(A)-(B) (Oz)	
99	Al-1/8" Hexagnol Honeycomb Viton Coating	48	5.4	54.0	54.7		.2	JP-5
100	1/8" Fiberglass Round Honeycomb Viton Coating	48	3.2	52.8	52.5		.3	JP-5
101	Fiberglass 1/8" Sine Wave Honeycomb Viton Coating	48	4.2	53.4	52.8		.6	JP-5
102	Al-Tube Core Viton Coating	48	9.0	59.7	58.9		.8	JP-5
103	Fiberglass 1/8" Round Honeycomb Polysulfide Coating	48	6.2	53.3	56.0			JP-5
104	Nomex 3/16" Round Honeycomb Polysulfide Coating	48	6.7	56.0	55.4		.5	JP-5
105	Nomex 1/8" Sine Wave Honeycomb Polysulfide Coating	48	5.9	54.7	54.4		.3	JP-5
106	Fiberglass 1/8" Sine Wave Honeycomb Polysulfide Coating	48	8.3	57.1	57.0		.1	JP-5
107	Al-1/8" Hexagnol Honeycomb Polysulfide Coating	48	8.8	58.7	58.4		.3	JP-5

| Test No. | Material | Before Firing | | | After Firing | | (A)−(B) (Oz) | Wetting Agent |
		Plate Weight (Oz)	Material Weight (Oz)	Sample + Wetting Agent (Oz) (A)	Sample Weight (Oz) (B)	Dry Sample Weight (Oz)		
108	Al-1/8" Hexagnol Honeycomb Polysulfide Coating	48	7.4	57.0	56.8		.2	JP-5
109	Al-1/8" Perforated Honeycomb Polysulfide Coating	48	13.0	63.4	62.9		.5	JP-5
110	Polyester Roll	48	18.0	68.5				JP-5
111	Al-Tube Core	48	14.0	63.5	63.0		.5	JP-5
112	25 ppi - Foam Glass Resin	48	1.9	63.4	52.6	49.9	10.5	JP-5
113	25 ppi - Foam Ni Coating	48	3.5	63.9	52.0	50.6	11.9	JP-5
114	25 ppi - Foam Kel-F Coating	48	2.6	53.6	48.0	50.6	5.6	JP-5
115	25 ppi - Foam Glass Resin	48	2.6	54.7	53.3	50.6	1.4	JP-5
116	25 ppi - Foam Viton Coating	48	2.6	55.7	52.5		3.2	JP-5
117	25 ppi - Foam Polysulfide Coating	48	4.2	56.2	54.0		2.2	JP-5
118	Al-Tube Core Flourel Coating	48	8.8	59.0	58.7		.3	JP-5
119	Polyester Roll	48	3.4	20.0				JP-5
121	25 ppi - Foam Viton Coating	48	2.4	55.2	54.4		.3	JP-5

Test No.	Material	Before Firing		After Firing				
		Plate Weight (Oz)	Material Weight (Oz)	Sample + Wetting Agent (Oz) (A)	Sample Weight (Oz) (B)	Dry Sample Weight (Oz)	(A-B) (Oz)	Wetting Agent
122	25 ppi – Foam Polysulfide Coating	48	5.0	56.2	54.2	53.0	2.0	JP-5
123	25 ppi – Foam Glass Resin	48	2.6	53.1	51.8	50.6	1.3	JP-5
124	25 ppi – Foam Kel-F Coating	48	2.6	53.1	52.5	50.6	.6	JP-5

TABLE XVIII

MATERIALS FUEL FLOW PRESSURE DROP DATA

Material	Fuel Flow Rate (GPM)	Pressure Drop (In. Fuel)
25 ppi Foam	52.0	1.6
	103.0	6.2
	148.0	12.6
	103.0	6.8
	49.0	1.6
	52.0	1.7
	103.0	6.4
	150.0	17.6
	102.0	7.5
	57.0	2.0
	59.0	1.8
	103.0	5.3
	150.3	12.0
	105.0	7.0
Fire Extinguishing Foam	49.0	12.1
	106.0	15.4
	140.0	28.8
	102.0	16.3
	51.0	15.2
	49.0	13.9
	102.0	16.1
	140.0	30.3
	102.0	16.7
	53.0	15.2
3M Scotch Brite	55.4	6.1
	100.6	17.0
	156.0	39.4
	104.0	19.1
	56.5	6.7
	102.0	18.2
	153.0	41.0
	102.0	19.5
	57.7	5.3
	104.0	15.3
	152.0	32.5
	60.0	5.8
Al-1/8" Honeycomb 2" Thick 4.5 lb/ft^2	63.0	0.4
	105.0	1.0
	150.0	2.0
	106.0	1.1
	54.0	0.2
	63.5	0.4
	105.0	1.0
	150.0	2.0
	106.0	1.1
	54.4	0.2

TABLE XVIII (CONT'D)

Material	Fuel Flow Rate (GPM)	Pressure Drop (In. Fuel)
Al-1/8" Perforated 2" Thick Honeycomb 12.1 lb/ft^2	56.5 103.0 155.0 104.0 55.5	0.6 1.4 3.0 1.5 0.5
Al-1/8" Hexagnol 2" Thick Honeycomb 4.3 lb/ft^2	52.0 104.C 150.0 102.0 51.0	0.4 1.3 2.3 1.3 0.4
Al Tube Core	59.0 103.0 151.0	0.8 1.7 3.5
Fiberglass 1/8" Round 2" Thick Honeycomb 3.0 lb/ft^2	57.5 104.0 150.0 103.0 65.5	0.3 1.0 2.0 0.9 0.5
Fiberglass 1/8" Sine 2" Thick Wave Honeycomb 3.5 lb/ft^2	54.4 102.0 146.0 100.0 56.5	0.2 0.8 1.7 0.8 0.2
25 ppi Foam Copper Plated	54.0 105.0 150.0 102.0 53.0	4.3 5.5 11.1 5.6 5.1
25 ppi Foam Polysulfide Coated	53.0 104.0 141.0 103.0 50.0 51.0 103.0 143.0 104.0 53.0	2.0 7.9 20.8 10.1 1.9 1.8 8.2 22.4 10.8 2.1

FIGURE 54   FLOW vs PRESSURE DROP OF 25 PPI POLYURETHANE FOAM - UNCOATED AND COATED WITH POLYSULFIDE

GP71-1372-4

111
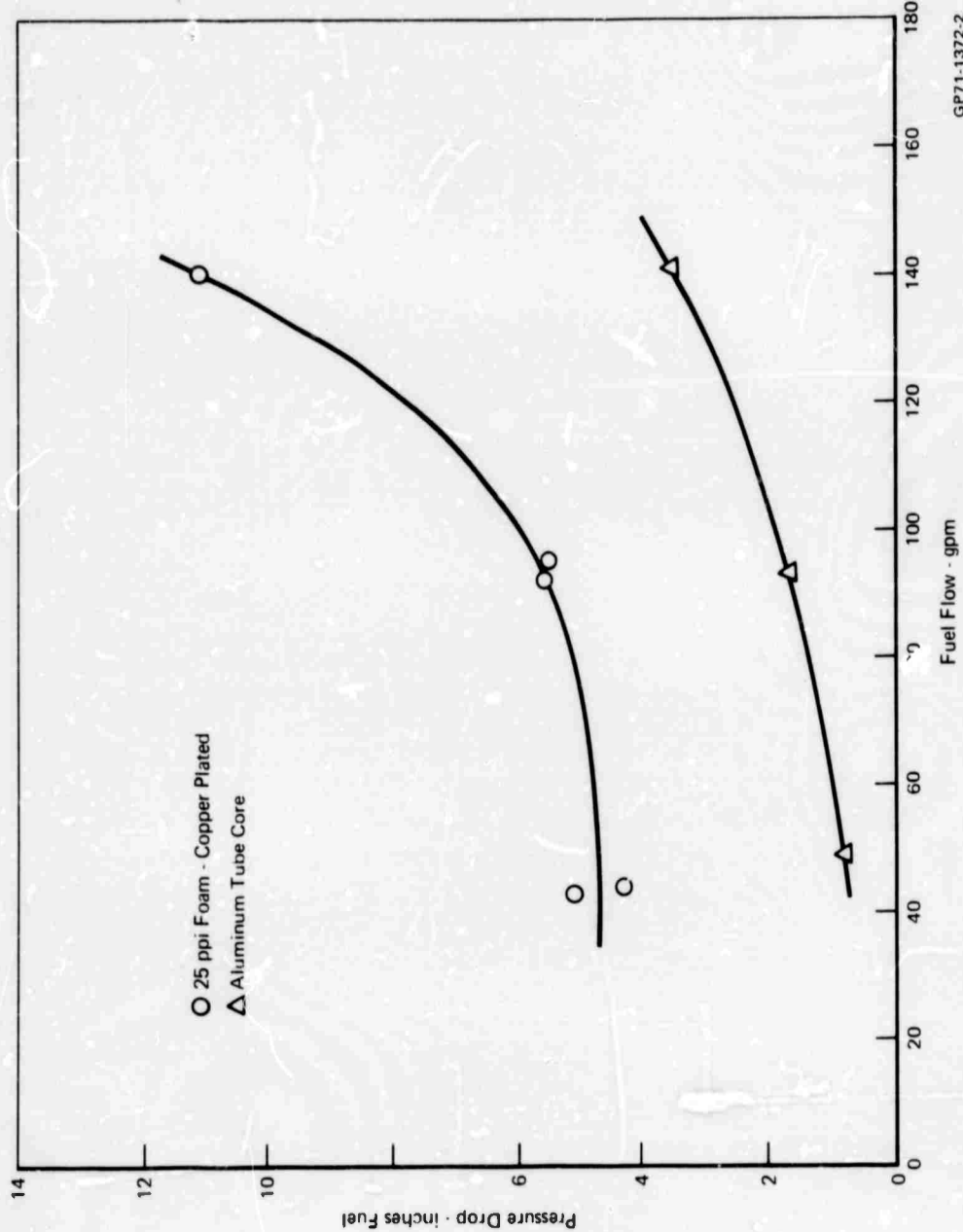
FIGURE 55 FLOW vs PRESSURE DROP - 25 PPI POLYURETHANE FOAM PLATED WITH COPPER AND ALUMINUM TUBE CORE

GP71-1372-2

112
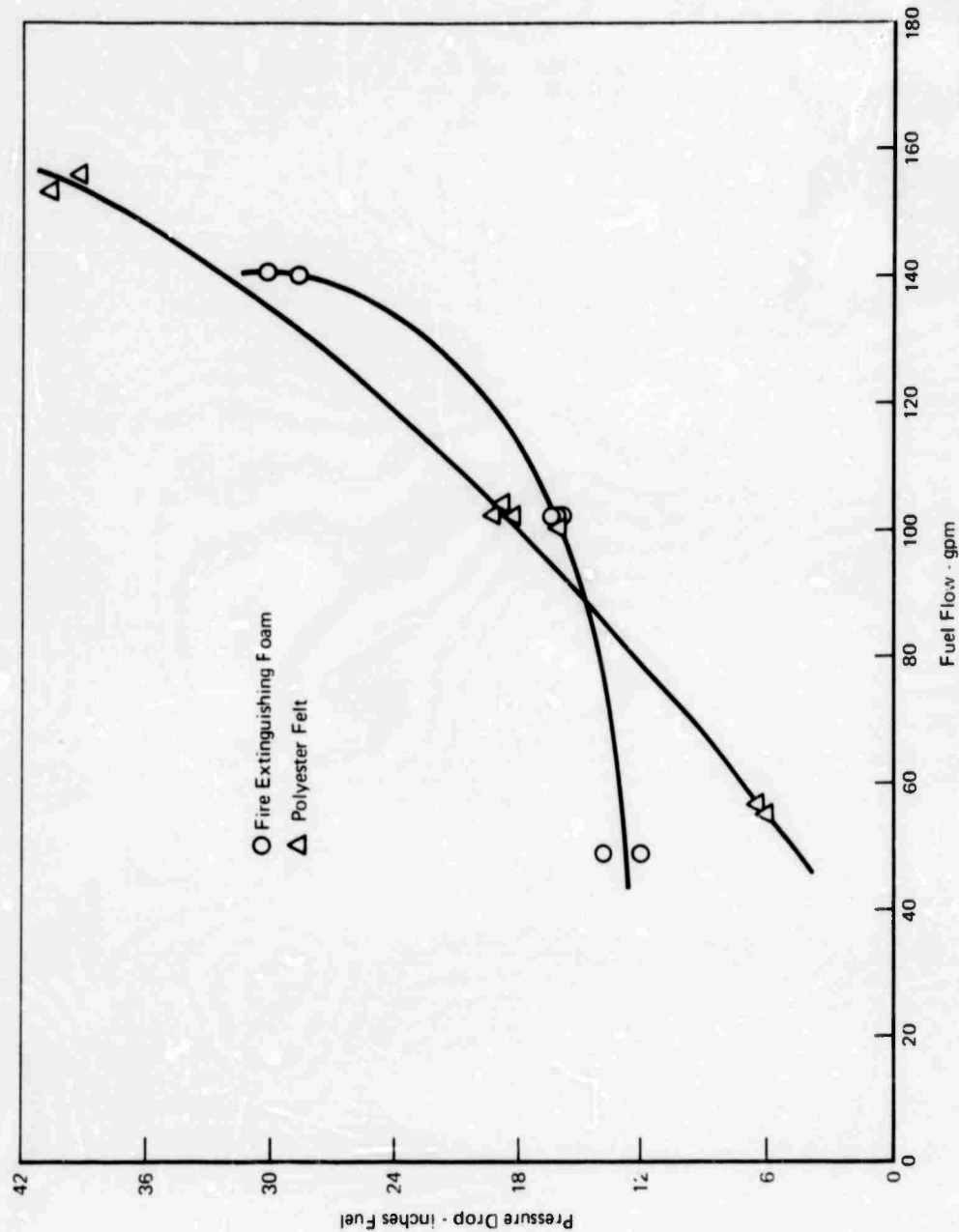
FIGURE 56   FLOW vs PRESSURE DROP -
FIRE EXTINGUISHING FOAM AND POLYESTER FELT

GP71 1372 3

113
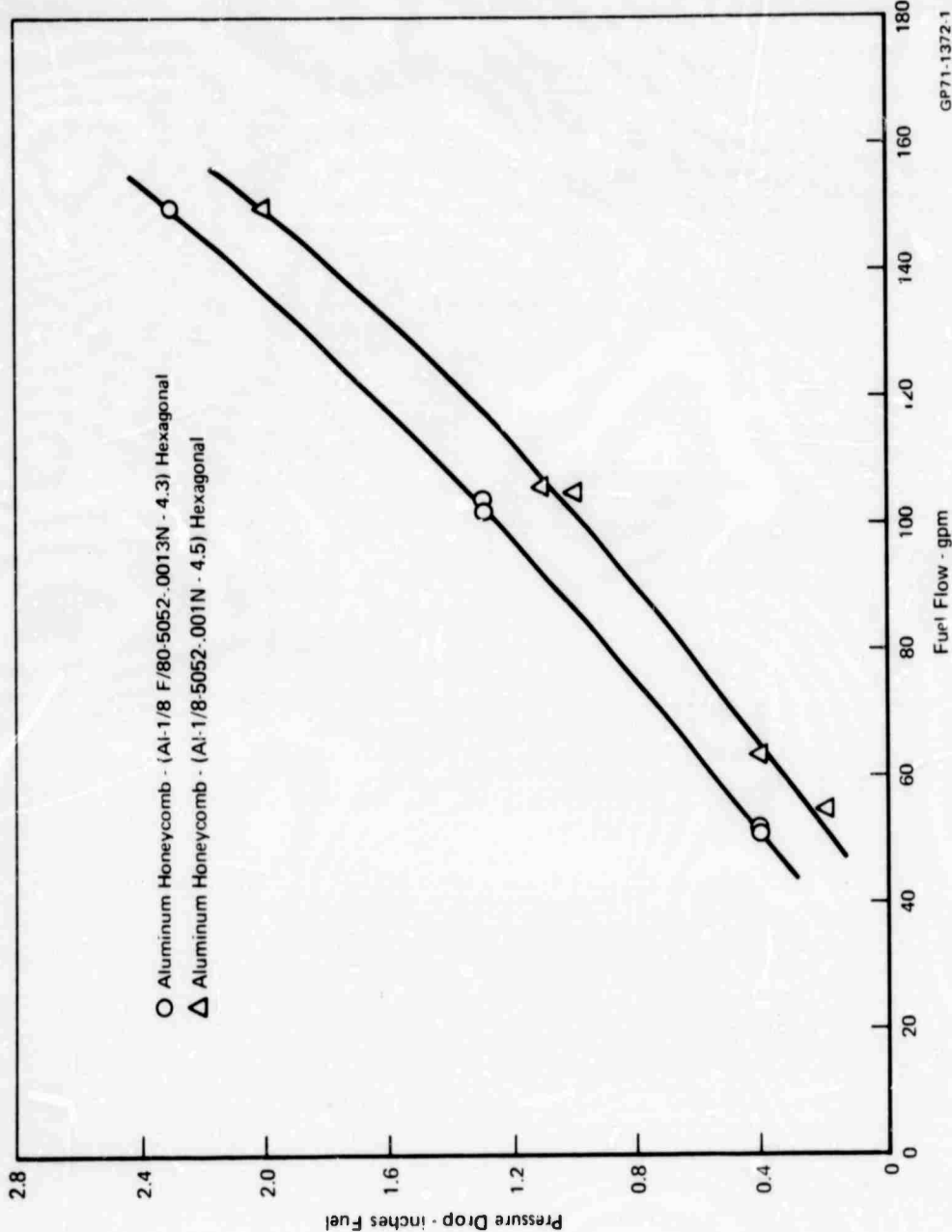
FIGURE 57   FLOW vs PRESSURE DROP - ALUMINUM HONEYCOMB

O Aluminum Honeycomb - (Al-1/8 F/80-5052-.0013N - 4.3) Hexagonal
△ Aluminum Honeycomb - (Al-1/8-5052-.001N - 4.5) Hexagonal

GP71-1372-1

114
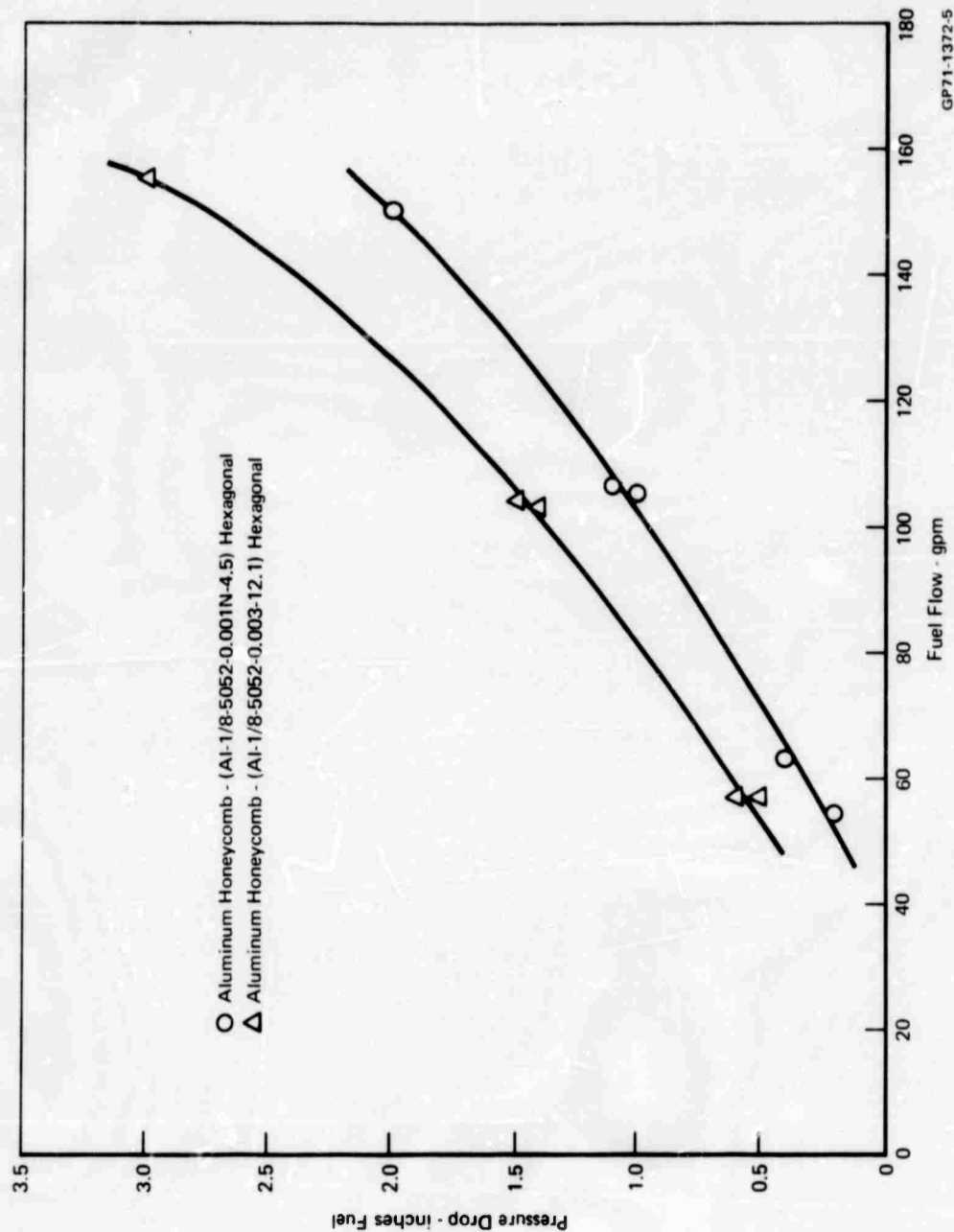
FIGURE 58 FLOW vs PRESSURE DROP - ALUMINUM HONEYCOMB

GP71-1372-5

115
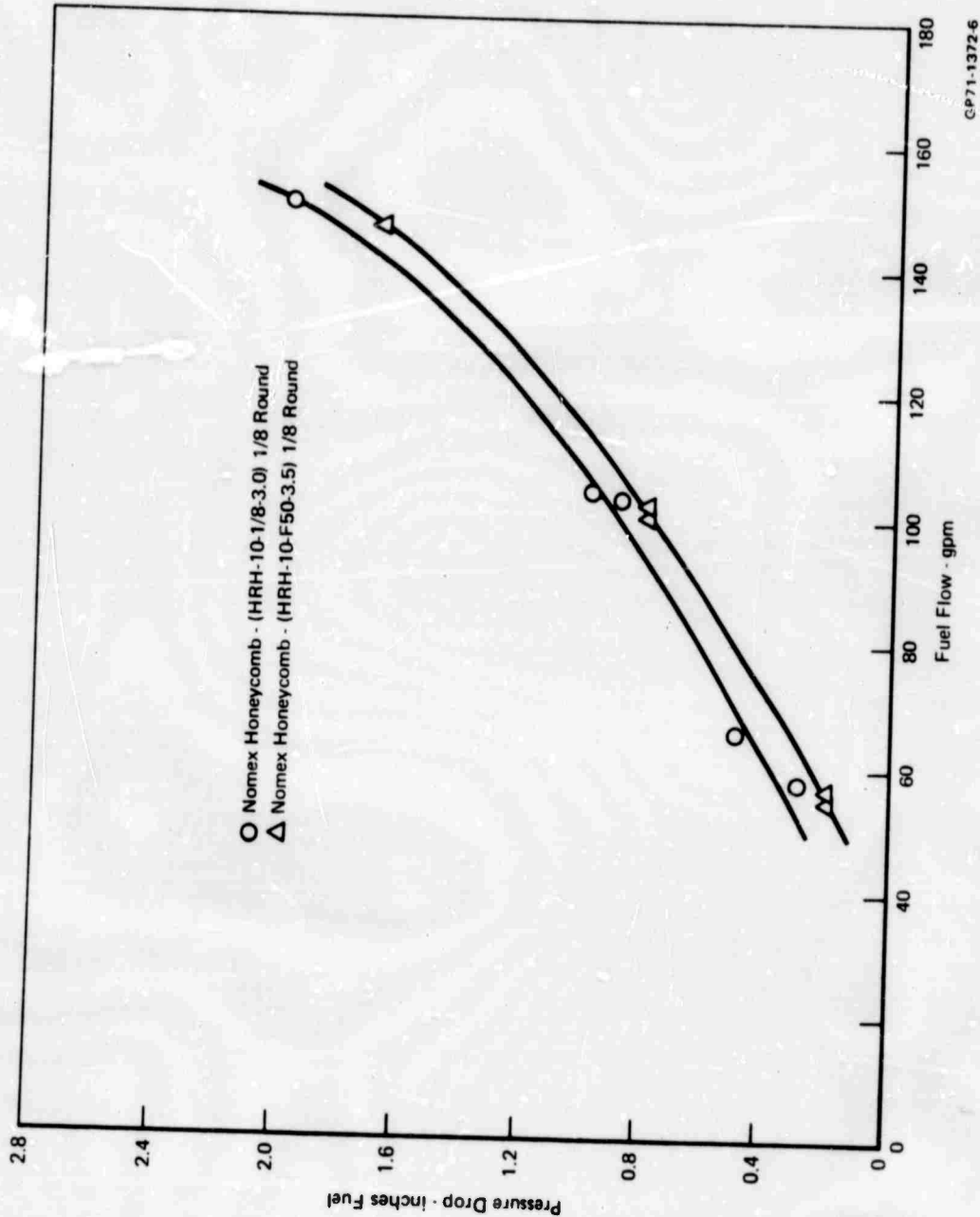
FIGURE 59 FLOW vs PRESSURE DROP - NOMEX HONEYCOMB

GP71-1372-6

116

TABLE XIX

MATERIAL THERMOPHYSICAL PROPERTIES

PROPERTIES MATERIAL	K BTU-IN/ HR-FT² F	Cp BTU/#-F	T MELT F	HEAT OF REACTION BTU/#	BULK DENSITY #/FT³	DISPLACEMENT %	SPECIFIC FUEL RETENTION #/FT³	SURFACE AREA FT²/#
FOAM 25 ppi	0.47	.63	392	5560	1.66	2.2	2.56 (5%)	4880
SCOTCH-BRITE	0.13	.53	419	4560	2.90	2.09	3.66(7.3%)	4400
FOAM-25 ppi KEL-F	0.32	.58	437	5990	-	-	-	6350
FOAM-POLYSULFIDE	0.33	.46	437	6350	-	-	-	3420
FOAM-GLASS RESIN	0.41	.59	416	4980	-	-	-	6850
FOAM-REDAR VITON	0.27	-	471	4040	-	-	-	4400
FOAM-K Br	0.30	.5	-	-	-	-	-	10750
FOAM-KI	0.32	.52	-	-	-	-	-	3420
FIRE EXTINGUISHING FOAM	0.24	.55	410	4560	3.77	4.4	7.30(14.6%)	1470
FOAM-N1 PLATED	0.39	-	-	-	-	-	-	2440
FOAM-Cu PLATED	1.52	-	-	-	-	-	-	1965
POLYESTER SCREEN	-	.18	401	3300	-	-	-	4400
NOMEX HONEYCOMB	†	.41	498	5700	-	-	-	-
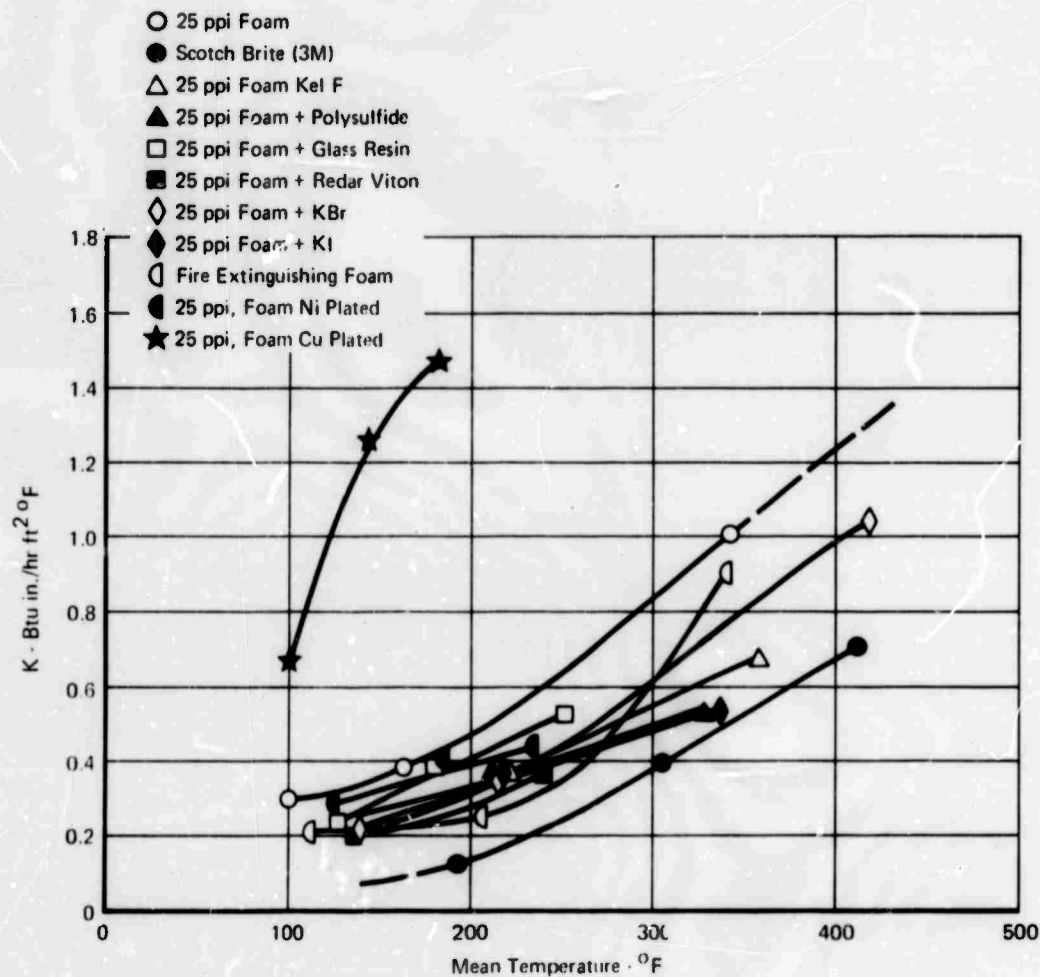
FIGURE 60 THERMAL CONDUCTIVITY OF FLAME ARRESTOR MATERIALS

GP71-1605-6

118
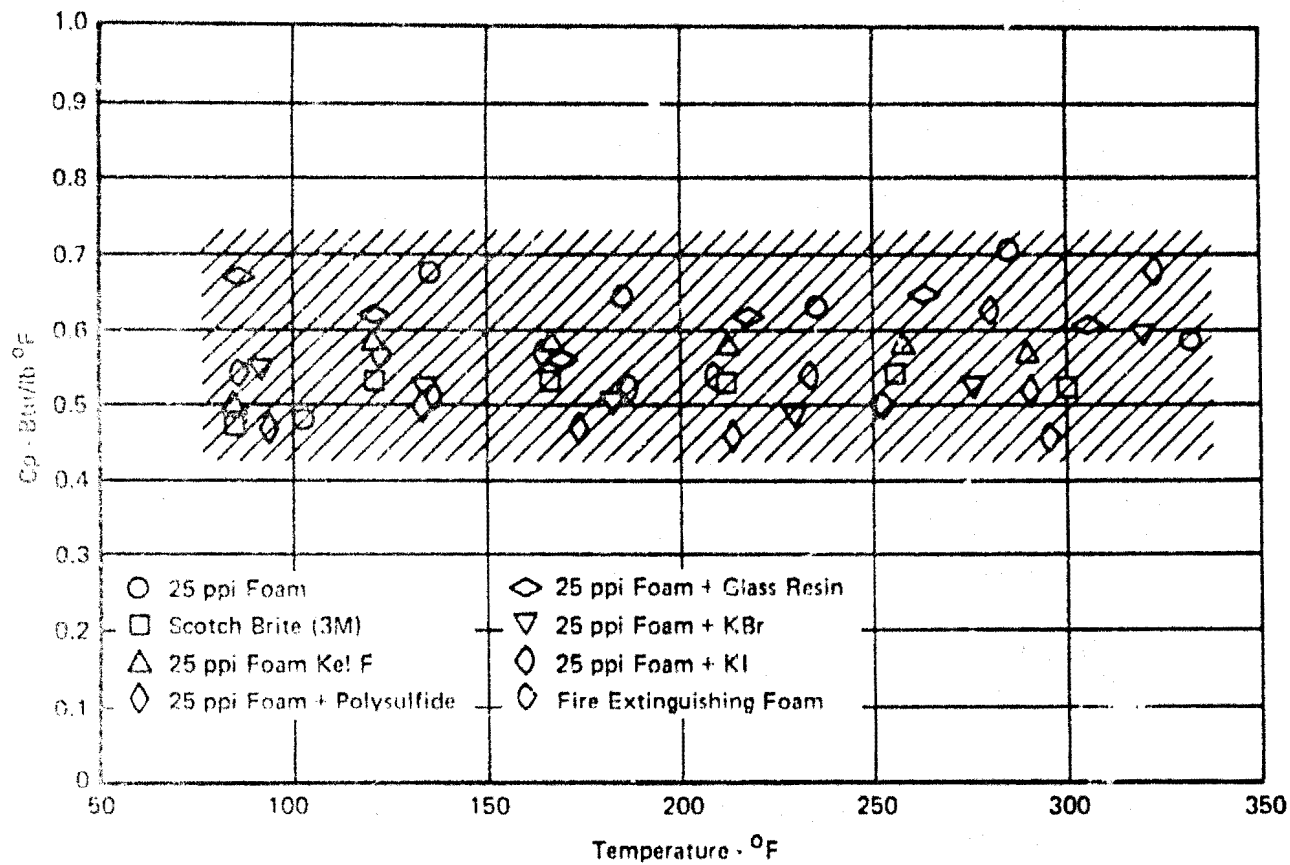
FIGURE 61 SPECIFIC HEAT OF FLAME ARRESTOR MATERIALS

GP71 1605 5

119

TABLE XX

MATERIAL COMBUSTION TESTS

Material	Ambient Pressure (psia)	Volume Ratio V_2/V_C	Tube Initial Pressure (psia)	ΔP Combustion Side (psig)	ΔP Receiver Side (psig)	Wetting Agent
Foam 25 ppi	14.50	10/1	14.50	2.0	2.1	JF5
Foam 25 ppi	14.44	10/1	14.44	1.7	1.8	H_2O
Foam 25 ppi	14.27	10/1	14.27	1.8	1.8	Dry
Foam 25 ppi	14.48	5/1	14.43	4.1	3.9	JF5
Foam 25 ppi	14.43	5/1	14.42	3.5	2.5	H_2O
Foam 25 ppi	14.31	5/1	14.31	3.8	3.7	Dry
Foam 25 ppi	14.5	1/1	14.5	17.0	14.5	JF5
Foam 25 ppi	14.5	1/1	14.5	17.0	14.5	JF5
Foam 25 ppi	14.41	1/1	14.41	62.9	62.6	Dry
Foam 25 ppi	14.23	10/1	16.23	2.4	2.4	JF5
Foam 25 ppi	14.48	10/1	16.48	2.0	2.1	H_2O
Foam 25 ppi	14.31	10/1	16.31	In excess of 35 psi		Dry
Foam 25 ppi	14.48	5/1	16.43	4.3	4.1	JF5
Foam 25 ppi	14.48	5/1	16.48	4.2	4.2	H_2O
Foam 25 ppi	14.31	5/1	16.31	1.9	1.9	Dry
Foam 25 ppi	14.38	5/1	16.33	4.5	4.4	Dry
Foam 25 ppi	14.41	1/1	16.41	15.0	14.8	JF5
Foam 25 ppi	14.37	1/1	15.37	14.9	14.4	H_2O

TABLE XX (Cont'd)

Material	Ambient Pressure (psia)	Volume Ratio V_R/V_C	Tube Initial Pressure (psia)	Δp Combustion Side (psia)	Δp Receiver Side (psia)	Wetting Agent
Foam 25 ppi	14.46	10/1	19.46	-	-	JF5
Foam 25 ppi	14.45	10/1	19.43	3.0	2.5	H_2O
Foam 25 ppi	14.31	10/1	19.31	79.5	-	Dry
Foam 25 ppi	14.43	5/1	19.48	In excess of 35 psi		JF5
Foam 25 ppi	14.43	5/1	19.48	In excess of 35 psi		H_2O

TABLE XX (Cont'd)

Material	Ambient Pressure (psia)	Volume Ratio V_R/V_C	Tube Initial Pressure (psig)	Δ Combustion Side (psig)	Δ Receiver Side (psig)	Wetting Agent
25 ppi Foam Polysulfide	14.4	10/1	14.4	2.5	2.2	JF5
25 ppi Foam Polysulfide Coating	14.7	5/1	14.7	4.4	4.1	JF5
25 ppi Foam Polysulfide Coating	14.5	1/1	14.5	-	-	JF5
25 ppi Foam Redar-Viton	14.4	10/1	16.4	2.5	2.3	JF5
25 ppi Foam Viton Coating	14.7	5/1	14.7	4.7	4.4	JF5
25 ppi Foam Viton Coating	14.5	1/1	14.5	58.8	58.6	JF5

122

TABLE ?? (Cont'd)

Material	Ambient Pressure (psia)	Volume Ratio V_2/V_1	Tube Initial Pressure (psia)	ΔP Combustion Side (psig)	ΔP Receiver Side (psig)	Wetting Agent
Fire Extinguishing Foam	14.60	10/1	14.60	1.7	1.7	JF5
Fire Extinguishing Foam	14.43	10/1	14.43	1.5	1.4	H$_2$O
Fire Extinguishing Foam	14.60	10/1	16.60	2.0	2.0	JF5
Fire Extinguishing Foam	14.43	10/1	16.43	1.9	1.7	H$_2$O
Fire Extinguishing Foam	14.42	1/1	16.42	15.6	15.2	Dry
Fire Extinguishing Foam	14.60	10/1	19.60	2.2	2.2	JF5
Fire Extinguishing Foam	14.43	10/1	19.43	2.1	2.1	H$_2$O
Fire Extinguishing Foam	14.43	10/1	19.43	2.4	2.3	Dry
Fire Extinguishing Foam	14.43	5/1	19.43	5.0	4.7	JF5
Fire Extinguishing Foam	14.43	5/1	19.43	4.5	4.4	H$_2$O
Fire Extinguishing Foam	14.31	5/1	19.31	4.5	4.5	Dry
Fire Extinguishing Foam	14.41	1/1	19.41	17.2	16.7	JF5
Fire Extinguishing Foam	14.41	1/1	19.41	16.5	16.0	H$_2$O
Fire Extinguishing Foam	14.42	1/1	19.42	93.5	-	Dry

TABLE XX (Cont'd)

Material	Ambient Pressure (psia)	Volume Ratio V_D/V_C	Tube Initial Pressure (psia)	ΔP Combustion Side (psig)	ΔP Receiver Side (psig)	Wetting Agent
3M Scotch-Brite	14.29	10/1	14.29	1.6	1.6	JP5
3M Scotch-Brite	14.62	10/1	14.62	1.7	1.7	H$_2$O
3M Scotch-Brite	14.40	10/1	16.40	2.0	2.0	JP5
3M Scotch-Brite	14.5?	10/1	16.5?	2.0	2.1	H$_2$O
3M Scotch-Brite	14.40	1/1	16.40	14.9	14.5	Dry
3M Scotch-Brite	14.40	10/1	19.40	2.1	2.4	JP5
3M Scotch-Brite	14.68	10/1	19.68	2.3	2.3	H$_2$O
3M Scotch-Brite	14.44	10/1	19.44	2.5	2.3	Dry
3M Scotch-Brite	14.44	5/1	19.44	4.9	4.9	JP5
3M Scotch-Brite	14.44	5/1	19.44	4.8	4.7	H$_2$O
3M Scotch-Brite	14.31	5/1	19.31	5.2	4.3	Dry
3M Scotch-Brite	14.40	1/1	19.40	17.7	17.3	JP5
3M Scotch-Brite	14.40	1/1	19.40	17.6	17.4	H$_2$O
3M Scotch-Brite	14.40	1/1	19.40	20.3	-	Dry

TABLE XX (Cont'd)

Material	Ambient Pressure (psia)	Volume Ratio V_V/V_C	Tube Initial Pressure (psig)	Δi Combustion Side (psig)	Δi Receiver Side (psig)	Wetting Agent
Al-Tube Core	14.7	10/1	14.7	59.0	57.2	JF5
Al-Tube Core	14.4	10/1	14.4	54.3	52.7	JF5
Al-Tube Core	14.5	10/1	14.5	17.4	17.5	JF5
Al-Tube Core	14.5	10/1	16.5	71.1	57.2	JF5
Al-Tube Core	14.43	10/1	14.43	27.4	24.3	H_2O
Al-Tube Core Flourel Coating	14.4	10/1	14.4	1.5	1.4	JF5
Al-Tube Core Flourel Coating	14.4	10/1	16.4	66.5	64.7	JF5
Al-Tube Core Flourel Coating	14.7	5/1	14.7	51.9	44.3	JF5
Al-Tube Core Glass Coating	14.7	10/1	14.7	15.0	15.0	JF5
Al-Tube Core Kel-F Coating	14.71	10/1	14.71	61.0	52.9	JF5
Al-Tube Core Viton Coating	14.7	10/1	14.7	51.3	50.0	JF5
Al-Tube Core Teflon Coating	14.5	10/1	14.5	51.3	55.2	JF5
Al-Tube Core Polyurethane Coating	14.5	10/1	14.5	51.4	55.1	JF5

TABLE XX (Cont'd)

Material	Ambient Pressure (psia)	Volume Ratio V_R/V_C	Tube Initial Pressure (psig)	ΔP Combustion Side (psig)	ΔP Receiver Side (psig)	Wetting Agent
15 PPI - Foam	14.39	10/1	14.39	-	-	JP5
25 PPI - CU Coated	14.35	1/1	14.35	Pressure In Excess of 35 psi		JP5
25 PPI - CU Coated	14.39	10/1	16.39	1.7	2.3	JP5
25 PPI - CU Coated	14.40	10/1	16.40	2.0	2.3	Dry
25 PPI - CU Coated	14.35	5/1	16.35	3.5	4.3	JP5
25 PPI - CU Coated	14.40	1/1	16.40	Pressure In Excess of 35 psi		JP5
25 PPI - CU Coated	14.39	10/1	19.39	2.9	-	JP5
25 PPI - CU Coated	14.40	10/1	19.40	Pressure In Excess of 35 psi		Dry
25 PPI - CU Coated	14.35	5/1	19.35	4.2	5.1	JP5

TABLE XX (Cont'd)

Material	Ambient Pressure (psia)	Volume Ratio V_R/V_C	Tube Initial Pressure (psig)	ΔP Combustion Side (psig)	ΔP Receiver Side (psig)	Wetting Agent
Polyester Roll	14.7	10/1	14.7	15.0	15.0	JP5
Polyester Roll	14.7	5/1	14.7	3.0	2.7	JP5
Polyester Roll	14.7	5/1	14.7	3.4	3.2	JP5
Polyester Roll	14.5	1/1	14.5	66.0	64.3	JP5
Stainless Steel Screen Wire	14.5	10/1	14.5	51.3	54.6	JP5
Viton Bronze Rod	14.5	10/1	14.5	25.0	5.1	JP5
Al-1/8-0.49 Wall Tube	14.4	10/1	14.4	51.3	50.8	JP5
Al-1/8" Hexagonal Honeycomb	14.4	10/1	14.4	70.0	58.2	JP5
Al-1/8" Hexagonal Honeycomb Flourel Coating	14.72	10/1	14.72	64.3	62.7	JP5
Al-1/8" Hexagonal Honeycomb Flourel Coating	14.72	10/1	14.72	59.3	58.0	JP5
Al-1/8" Hexagonal Honeycomb Glass Resin	14.7	10/1	14.7	57.5	55.8	JP5
Al-1/8" Hexagonal Honeycomb Glass Resin	14.7	10/1	14.7	55.3	53.2	JP5

TABLE XX (Cont'd)

Material	Ambient Pressure (psia)	Volume Ratio V_R/V_C	Tube Initial Pressure (psig)	ΔP Combustion Side (psig)	ΔP Receiver Side (psig)	Wetting Agent
Al-1/8" Hexagonal Honeycomb Kel-F Coating;	14.71	10/1	14.71	57.5	55.8	JP5
Al-1/8" Hexagonal Honeycomb Kel-F Coating;	14.71	10/1	14.71	64.3	62.8	JP5
Al-1/8" Hexagonal Honeycomb Polysulfide Coating;	14.7	10/1	14.7	53.7	52.7	JP5
Al-1/8" Hexagonal Honeycomb Polysulfide Coating;	14.7	10/1	14.7	59.5	58.2	JP5
Al-1/8" Hexagonal Honeycomb Viton Coating	14.7	10/1	14.7	64.4	61.7	JP5
Al-1/8" Hexagonal Honeycomb Viton Coating	14.7	10/1	14.7	59.5	58.0	JP5
Al-3/8" Hexagonal Honeycomb Teflon Coating	14.5	10/1	14.5	60.2	63.9	JP5
Al-1/8" Hexagonal Honeycomb Polyurethane Coating;	14.5	10/1	14.5	55.9	59.2	JP5
Al-1/8" Round Honeycomb Teflon Coating;	14.5	10/1	14.5	5?.8	61.7	JP5
Al-1/8" Round Honeycomb Polyurethane Coating;	14.5	10/1	14.5	57.2	62.0	JP5

TABLE XX (CONT'D)

Material	Ambient Pressure (psig)	Volume Ratio V_R/V_C	Tube Initial Pressure (psig)	ΔP Combustion Side (psig)	ΔP Receiver Side (psig)	Wetting Agent
Al-1/8" Perforated Honeycomb	14.4	10/1	14.4	68.8	55.5	JP5
Al-1/8" Perforated Honeycomb	14.7	10/1	14.7	59.7	58.0	JP5
Al-1/8" Perforated Honeycomb Kel-F Coating	14.7	10/1	14.7	63.8	62.0	JP5
Al-1/8" Perforated Honeycomb Polysulfide Coating	14.7	10/1	14.7	55.3	53.5	JP5
Al-1/8" Perforated Honeycomb Redar Viton Coating	14.7	10/1	14.7	59.7	57.5	JP5

TABLE XX (CONT'D)

Material	Ambient Pressure (psia)	Volume Ratio V_R/V_C	Tube Initial Pressure (psig)	ΔP Combustion Side (psig)	ΔP Receiver Side (psig)	Wetting Agent
Nomex 1/8" Sine Wave Honeycomb	14.5	10/1	14.5	74.5	59.8	JP5
Nomex 1/8" Sine Wave Honeycomb	14.5	10/1	14.5	74.2	59.2	JP5
Nomex 1/8" Sine Wave Honeycomb Kel-F Coating	14.7	10/1	14.7	64.5	62.8	JP5
Nomex 1/8" Sine Wave Honeycomb Polysulfide Coating	14.7	10/1	14.7	62.3	60.0	JP5
Nomex 3/16" Round Honeycomb Kel-F Coating	14.7	10/1	14.7	60.8	56.5	JP5
Nomex 3/16" Round Honeycomb Polysulfide Coating	14.7	10/1	14.7	56.5	55.5	JP5
75% Hole	14.7	10/1	14.7	70.0	68.7	Valve Open at Side

130

Material	Ambient Pressure (psia)	Volume Ratio V_R/V_C	Tube Initial Pressure (psig)	ΔP Combustion Side (psig)	ΔP Receiver Side (psig)	Wetting Agent
25 ppi Foam Potassium Iodide Coating	14.58	10/1	14.58	13.5	14.6	JP5
25 ppi Foam Potassium Iodide Coating	14.56	10/1	16.58	71.0	74.9	JP5
25 ppi Foam Potassium Bromide Coating	14.58	10/1	14.58	12.4	13.7	JP5
25 ppi Foam Potassium Bromide Coating	14.58	10/1	16.58	62.0	65.9	JP5
25 ppi Foam Glass Resin	14.7	10/1	14.7	2.5	2.2	JP5
25 ppi Foam Glass Resin	14.4	10/1	16.4	2.5	2.3	JP5
25 ppi Foam Glass Resin	14.7	5/1	14.7	4.5	4.8	JP5
25 ppi Foam Glass Resin	14.5	1/1	14.5	57.9	53.1	JP5
25 ppi Foam Kel-F Coating	14.7	5/1	14.7	4.4	4.2	JP5
25 ppi Foam Kel-F Coating	14.5	1/1	14.5	62.0	58.7	JP5

TABLE XX (CONT'd)

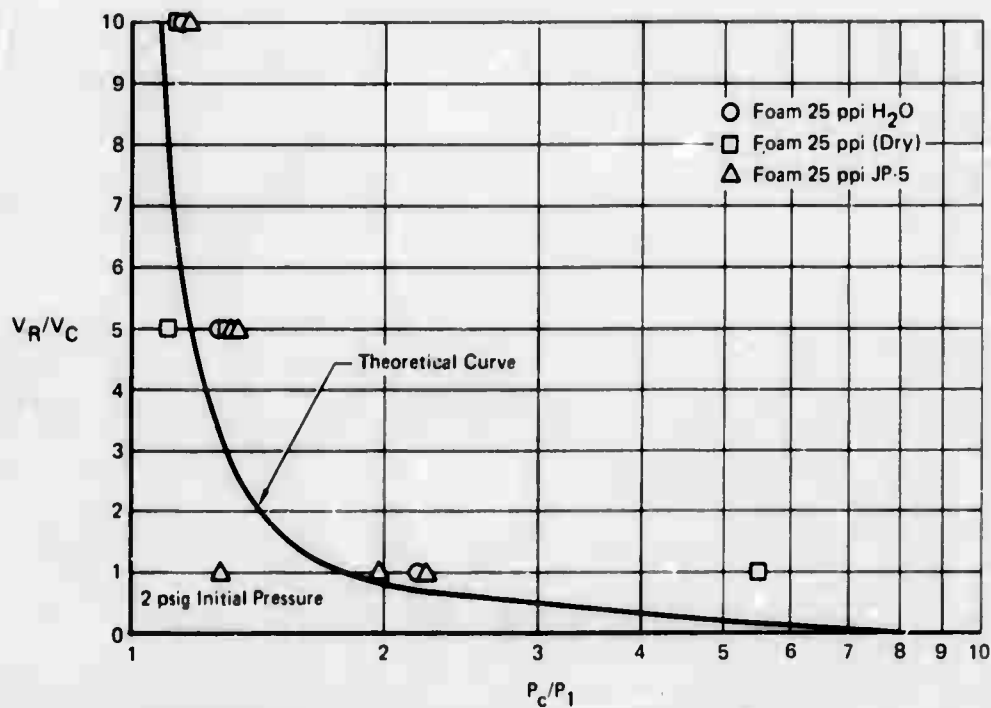| Material	Ambient Pressure (psia)	Volume Ratio V_R/V_C	Tube Initial Pressure (psig)	ΔP Combustion Side (psig)	ΔP Receiver Side (psig)	Wetting Agent
25 ppi - Foam Ni Coating	14.7	10/1	14.7	No Data - Burn Thru		JP5
25 ppi - Foam Ni Coated	14.44	10/1	16.44	Pressure in Excess of 35 psi		JP5
25 ppi - Foam Ni Coated	14.44	10/1	19.44	Pressure in Excess of 35 psi		JP5

FIGURE 62 PRESSURE RATIO vs RELIEF TO COMBUSTION VOLUME RATIO

PLEXIGLAS TUBE TESTS
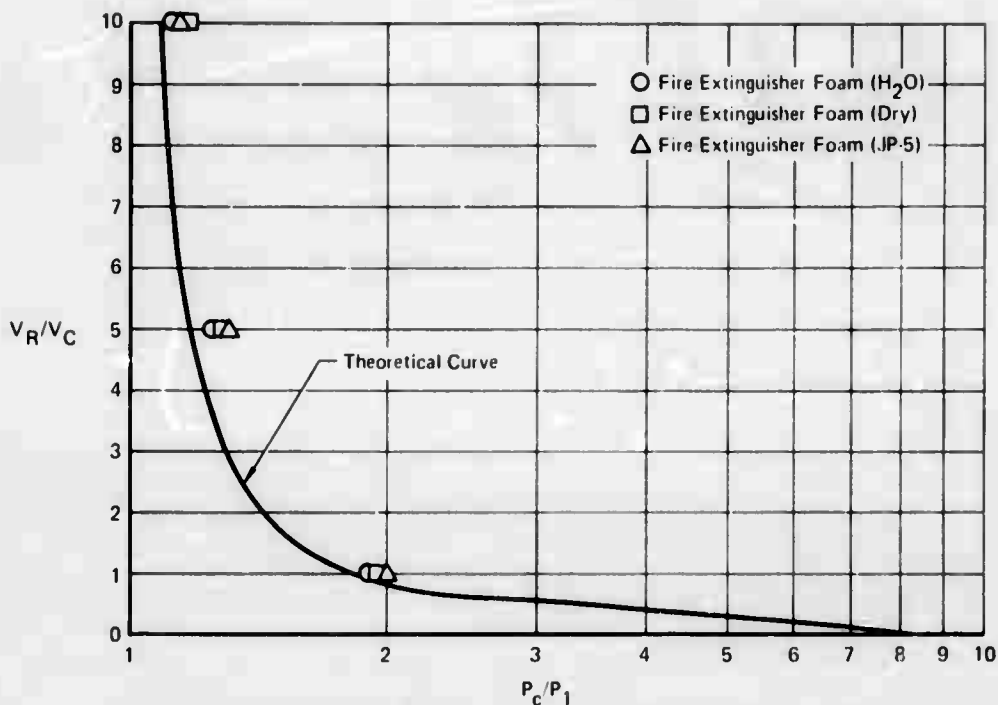
GP71-1605 4

133

FIGURE 63 PRESSURE RATIO vs RELIEF TO COMBUSTION VOLUME RATIO

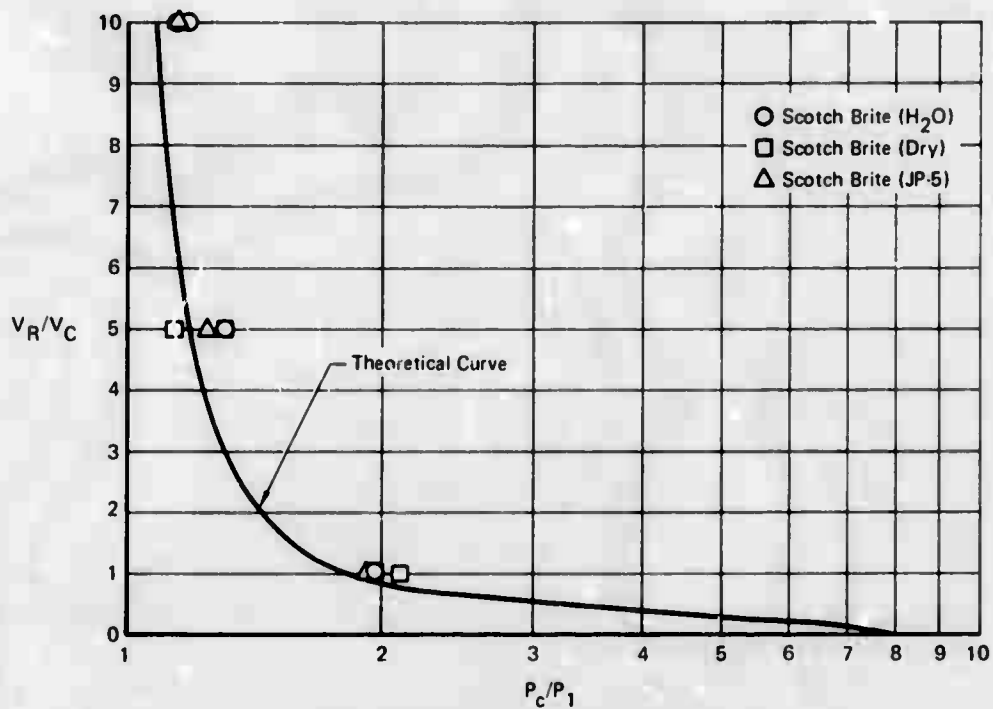PLEXIGLAS TUBE TESTS

GP71 1605 1

134

FIGURE 64   PRESSURE RATIO vs RELIEF TO COMBUSTION VOLUME RATIO
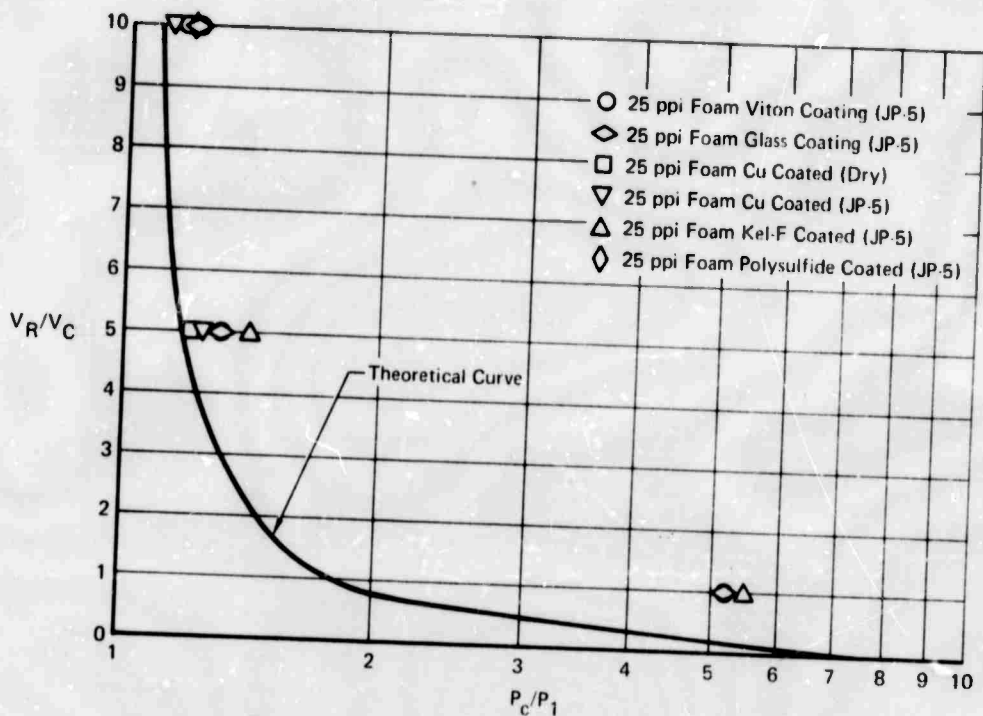
PLEXIGLAS TUBE TESTS

GP71 1605 3

135

FIGURE 65 PRESSURE RATIO vs RELIEF TO COMBUSTION VOLUME RATIO

PLEXIGLAS TUBE TESTS

GP71 1605 2

136

SECTION VI

PHASE III

1.0 ANALYSIS OF PROGRAM RESULTS

1.1 General

The object of Phase III of the program was defined as data analysis of Phases I and II results. The analysis was to lead to an engineering estimate of the future potential of the concepts and techniques developed and an evaluation of the materials investigated with respect to their flame arresting effectiveness. In order to accomplish this task, an analytical model of the explosion suppression system was established and a computer regression analysis of the data was conducted.

1.2 Explosion Suppression System Model

The simplest model of a relieved explosion which simulated the tests performed is a single-cell configuration as shown in Figure 66-A. In this model V_c is the combustion volume and V_f the arrestor volume. The relief volume in this case is supplied by the arrestor material only. If, however, the depth of the arrestor material is greater than that needed to eliminate flame propagation, then voiding behind the arrestor material is possible as shown in Figure 66-B. The relief volume now is V_r plus V_f with basically no change in the model parameters.
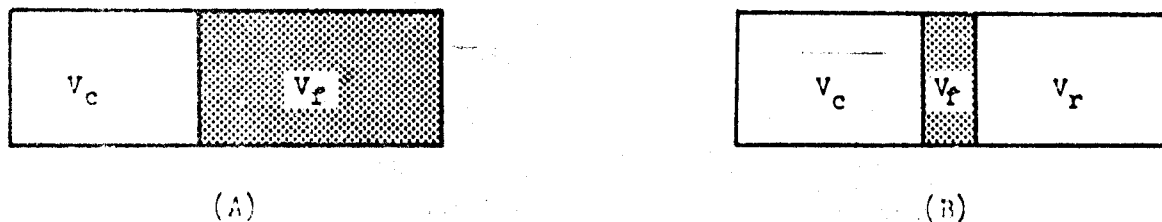

(A)   (B)

FIG. 66

SINGLE CELL MODEL

Further expansion of the complexity of the model to simulate a multicell wing tank, would be to place a wall behind the arrestor material which allows pressure communication, but with a variable degree of restriction as shown in Figure 67-A & B.

(A)   (B)

FIG. 67

MULTI CELL MODEL

This model configuration is essentially a two-cell model which can act as the single cell (Fig. 66 A & B) when the restriction is zero or infinity. The model can be further expanded to a multicell configuration by adding more units, simulating a wing tank with a number of cells formed by the perforated ribs and spars.

All four models can be analyzed by using the model in Figure 67-B within the stated limits since the other model configurations are simply special cases of Figure 67-B.

The analysis of the model uses the simple P, V, T, relationships before and after the combustion process while allowing free expansion to occur. Although static equilibrium conditions are assumed, the analysis is valid for the non-restricted configurations, and by introducing an experimentally determined average restriction factor, the maximum dynamic pressure in the combustion volume can be correlated.

Since in the combustion of hydrocarbons with air, little or no change occurs in the average molecular weight or total moles of gas present, the following relationship is assumed to be true.

$$P_1 V_1 / T_1 = P_2 V_2 / T_2 = nR = C.$$

Further, since the maximum ratio of (T_2/T_1) is eight for most hydrocarbon/air stoichiometric mixtures of interest and is independent of all other model parameters, it is considered a constant, K, the adiabatic expansion factor in the analysis. Thus the combustion process, can be written as

$$KT_1 V_1 = P_2 V_2 \quad \text{or} \quad P_2/P_1 = K \quad \text{where } V_1 = V_2 \tag{2}$$

The above equation is satisfactory for unrelieved explosions; however, when free expansion is allowed and flame propagation is limited to the available combustion volume, several attenuating effects take place. First some of the available unreacted and partially reacted (quenched) combustible gases are transported through the arrestor material into the relief volume. Consequently, not all of the originally available combustion volume is reacted. Concurrently, because of mass transfer into the relief volume, the corresponding relief pressure increases limiting subsequent mass transfer. The restriction plate behind the arrestor (foam) reinforces this latter effect resulting in higher effective relief pressures and thereby higher combustion chamber over-pressures.

Returning to the model and introducing V_x (Fig. 68) as that portion of the combustion volume actually reacted and which when fully expanded against the relief back-pressure expands just to the arrestor face, we obtain the following equation:

FIG. 68

MULTICELL MODEL

138

$$KP_1(V_x)^n = PC(V_c)^n \qquad (3)$$

where P_1 is the initial pressure, and n is the reversible polytropic exponent where PV^n = constant. Using the relationship $PV^n = C$ and summing the initial PV^n products to final equilibrium, results in the following relationships:

$$P_1KV_x{}^n + P_1V_c{}^n - P_1V_x{}^n + P_1V_f{}^n + P_1V_r{}^n = P_2V_t{}^n, \text{ and} \qquad (4)$$

$$P_cV_c{}^n + P_cV_f{}^n + P_rV_r{}^n = P_2V_t{}^n \qquad (5)$$

Equating Eqs. (4) and (5) and substituting Eq. (3) to eliminate V_x yields:

$$\frac{P_c}{P_1} = \frac{K(A^n + B^n + 1)\lambda}{(KA^n + KB^n + \lambda)} \qquad (6)$$

where $A = V_r/V_c$ and $B = V_f/V_c$. The λ term is the average restriction value defined as the ratio of P_c/P_r. It can be seen from Eq. (6) that as the relief volume goes to zero, A, goes to zero and the equation reduces to that of a single cell with no orifice restriction factor, and ($P_c = P_2$):

$$\frac{P_c}{P_1} = \frac{P_2}{P_1} = \frac{K(B^n + 1)}{(KB^n + 1)} \qquad (7)$$

Likewise, as B approaches zero the equation reduces to

$$\frac{P_c}{P_1} = \frac{P_2}{P_1} = K,$$

the maximum explosion over-pressure given in Eq. (2).

Since the process modeled is not constant pressure, volume or temperature the value of n varies. The value used in correlating the data herein was n = 1 (isothermal).

1.2.1 Phase I Data and Model Analysis

The Phase I data generally followed the model analysis. Divergence from the analytical model did occur with respect to initial pressure yielding a distinct curve for each initial pressure. This effect was more pronounced for the hollow body configurations. For this reason, the initial pressure was included in the computer analysis as one of the variables. It was also noticed that divergence from the model analysis occurred at Vr/Vc ratios below 1.5. The explanation of this divergence is felt to be the fact that higher pressures resulting from the combustion cause deeper penetration of the flame front into the foam thereby increasing the combustion volume.

139

Where progressive burning occurred which was only in the multicell or multi-void configurations strong deviation from the model analysis was indicated. It was found by study of the oscillograph traces however that the initial pressure peak correlated well with the model and that if the pressure at which the following peaks started was used as an initial pressure, this data, too, correlated well with the analytical model. Some small discrepancies with this procedure were noted in cases where the external volume around the hollow bodies was small. In this case, the squeegee effect of differential burning and thereby pressure pumping or circulation of the combustible mixture from within the hollow bodies was conjectured. Study of high-speed motion pictures of these configurations would indicate this possibility. When the external void is large and has good flame paths, then the external ignition is rapid and uniform, giving better results. This can be seen by comparing the seven and one-half inch diameter cylinder data. The shorter hemispherical head cylinders with the interconnected external voids out performed the long flat end cylinders which had a number of small independent external voids. The external ignition in the latter case lasted much longer allowing for greater circulation of unburned gases and therefore more combustible vapors were burned.

1.2.2 Phase I Computer Regression Analysis

Two methods of equating the Phase I system parameters were used in an attempt to get further insight into the explosion suppression system. The first analysis equated pressure-rise with the various system parameters in an attempt to correlate the data with the model analysis parameters. Ninety-nine test points including all initial pressures, and fuselage as well as wing tank test data were run. The equation derived from this analysis was as follows:

$$\Delta P = \frac{.00357 \, (P_1)^{3.095}}{\left(\frac{V_r}{V_c}\right)^{.2973} \left(\frac{V_f}{V_c}\right)^{.7297}}$$

where:

ΔP = Over pressure (psid)
P_1 = Initial pressure (psia)
V_r = Total volume - combustion volume (in^3)
V_f = Arrestor volume (in^3)
V_c = Combustion volume (in^3)

It can be seen from this emperical relationship that initial pressure followed by the ratios of foam volume to combustion volume and relief volume to combustion volume are the order of relevence of the test parameters included. The exponent of the initial pressure shows why normalization of the final to initial pressure in the model analysis didn't fit the data yielding an independent curve for each initial pressure.

The second computer analysis of the data equated foam volume to the other test parameters. In this analysis eighty-eight points were run again including

all initial pressures and tank configurations. The resulting empirical equation was as follows:

$$V_f = \frac{.488 \, (V_c)^{.158} \, (V_r)^{.574} \, (P_1)^{.277}}{(\Delta P)^{.025}}$$

where:

V_c = Combustion volume $(in^3)/10^4$

(V_r) = Total volume - combustion volume $(in^3)/10^4$

(V_f) = Foam volume $(in^3)/10^4$

ΔP = Overpressure (psid)

P_1 = Initial pressure (psia)

The reason for the relief volume increasing with the foam volume in this equation is that a portion of the relief volume in each system configuration is foam volume. The exponents of the variables are an indication of their importance with respect to foam volume. The exponents will not change if the 10^4 factors are removed as this procedure will only change the constant. The reason for intorducing this factor was to accommodate the computer which only fits the significant numbers.

1.2.3 Phase II Data Analysis

The data generated in this portion of the program was an attempt to evaluate the flame arresting effectiveness of a variety of materials and configurations with respect to their thermal, physical and chemical properties. Their effectiveness can only be measured with respect to system pressure rise and required thickness of material to eliminate flame propagation. For those cases where flame propagation through the arrestor material didn't occur the data correlated well with the model analysis. The divergence from the model could be taken as an indication of the arrestor effectiveness. This is a weak effect, however, whereas the required arrestor thickness with respect to combustion volume gives the stronger delineation. Unfortunately insufficient data was generated with respect to this last parameter and therefore this evaluation cannot be made.

Computer analysis of the pressure rise data with respect to the material properties was made. The best fit log-log regression analysis of the data yielded the following equation, from the 52 test conditions entered.

$$\Delta P = \frac{.054 \, (V_c)^{.9483} \, (P_1)^{1.076} \, (K)^{.1762} \, (e)^{.2536} \, (A)^{.2147}}{(C_p)^{.2164}}$$

where:

ΔP = Overpressure (psid)

P_1 = Initial pressure (psia)

V_c = Combustion volume $(in^3)/100$

C_p = Heat capacity of material $(BTU/\#-F^\circ)$

K = Thermal conductivity $(BTU-IN/\# - ^\circ F - ft^2$

ρ = Density - $(\#/ft^3)$

A = Surface area $(ft^2/\#)/10^3$

t = Thickness (2 inches constant)

The data input for this empirical analysis included a ten to one variation in combustion volume while holding the relief volume constant. In addition to this, the other system variable of initial pressure was varied by 30%. Several coatings and three basic materials and their thermophysical properties were also included. The analysis resulted in a curve fit within 10% of the experimental values.

It is apparent from this empirical relationship that by increasing the heat capacity of the arrestor while reducing its thermal conductivity and density, improved arrestor effectiveness occurs. It should be noted here, however, that increasing these parameters, their effect on ΔP decreases due to the fractional exponents. This fits well with the fact that water wet and JP-5 wet arrestors perform somewhat better than the dry specimens. Also wetting the specimen would have a tendency to reduce the microsurface area improving the performance. However, by comparing the data of those specimens which failed and thereby were not included in the analysis, the analysis of the surface area effect is somewhat questionable.

1.3 Explosion Suppression Systems/Aircraft Parameter Considerations

1.3.1 Fuel Tank Configurations

The data generated in this program indicates that the explosion suppression system configuration is dictated by the size and type of fuel tank being considered. The two types of configuration are single cell and multicell or multi-void systems. This result is quite evident by inspecting the data presented in Table 21.

1.3.1.1 Fuselage Tank

Fuselage tanks generally fall into the single cell class, however, as the cell becomes larger, the required foam volume to combustion volume increases to a point where multi-void configurations perform better than single cell configurations. In this program where the simulated fuselage tank was of 100 gallons capacity, the 10% voided lined wall configuration performed the best over the range of 0, 2 and 5 psig initial tank pressures. For this configuration, the tank void volume percents for 10 psig overpressure were, 52, 46 and 38 percent respectively. The 15-inch diameter cylinders functioned effectively up to 58% void volume, but were limited to 0 psig initial pressure.

142

1.3.1.2 Wing Tanks

The lined wall and egg crate configurations appear to be the most efficient explosion suppression systems configurations for multicell wing tanks. Again as the combustion volume gets larger the multivoid (egg crate) configuration out-performs the single void (lined wall) configuration. Voiding percentages for the (300-gallon) six-cell simulated wing tank exceeded 90% for both the egg-crate and lined wall configurations. When the cell size was doubled, (the three-cell, 300 gallon wing tank) the preferred foam configuration became the egg crate style providing up to 58% voiding for the 10 psig overpressure criterion. The lined wall configuration was only good to 43% voiding as experienced in the single cell fuselage tank. Had the system been tested with voided lined walls, the results might have been quite different, with up to 55% or larger voiding realized as indicated in the fuselage tanks with a similar foam configuration.

1.3.1.3 Advanced Materials

Substitution of the 3M felt or Scott's fire extinguishing foam evaluated in the Phase II portion of this program might well change the allowable void percentage for all of the configurations tested. Both of these materials have superior flame arresting properties at elevated initial pressures as indicated by the Phase II results. Their increased voiding, however, would have to make up for their greater displacement and absorption penalties, as discussed below, in order to compete weightwise with the 25 ppi foam systems.

1.3.2 Foam System Penalties

The results of the gross voided foam explosion suppression system configuration tests can now be converted into aircraft penalties. The penalties of concern are range penalties and gross take-off weight penalties.

1.3.2.1 Gross Voided Foam - Range Penalties

Range penalties are of greater concern in the case of a retrofit system since in new aircraft design, the direct fuel loss can be offset in the design by increasing the tank size. The retrofit range loss for the first approximation is simply the volume percent penalty. This is the sum of the percent fuel displacement and percent fuel absorption. Figure 69 shows the relationship of 10, 15 and 25 ppi foam and allowable voiding for this penalty. The values of fuel displacement and fuel retention required to plot volume and weight penalties for the 25 ppi foam were obtained in Phase II and are given in Table 19. Data for the 10 and 15 ppi foam material curves shown in Figure 69 were obtained from previously supplied Air Force test reports. It can be seen that the increase in voiding permitted by decreased pore size over shadows the weight and volume penalties incurred by material absorption and displacement.

1.3.2.2 Gross Voided Foam - Gross Take-off Weight Penalties

The gross take-off weight penalty for a new design aircraft is not shown, but is simply the weight penalty as given in Figure 69 times the growth factor for the typical fighter or cargo aircraft. Weight penalty is the percent by weight foam minus the percent by weight fuel displaced. Since both of these

factors for the smaller pore size low-density foams are equal and less than the 10 ppi standard high-density foam the advantage of 25 ppi foam need not be enhanced by the gross voiding techniques (Figure 69). However, the voiding does improve the stature of the system making it weight competitive with other inerting systems.

1.3.2.3 Additional Weight Penalties

So far the materials physical weight penalties are all that have been accessed. In the case of gross voiding, attachment of the foam or the assembling of the foam requires in some cases mechanical fasteners or adhesive-bonding which manifest themselves in an additional weight penalty. Experience has shown that bonding of this material nearly doubles the foam weight penalty. Consequently, adhesive bonding should be avoided if possible. In the case of the hollow bodies, this can be accomplished by making these forms in two or more telescoping parts. Compression packing of these bodies in the subject tank eliminates any further fastening requirement. In the case of egg crating or lined walls, interlocking foam assemblies have proven satisfactory. Where mechanical fasteners are required, lacing has been found quite satisfactory with only a 10 to 30% additional weight penalty.

1.3.3 System Effects

Another aspect of the gross voided foam system which must be addressed is its effect upon fuel system operations. With a little engineering, most problems can be handled. Plumbing, gauging and fuel transfer are the primary fuel system functions of concern. The hollow body gross voiding concept adapts quite well in that proper sizing and controlled packing provides voids between the bodies themselves and the tank walls adequate for gauging probes, pump inlets or vent valving. This is also true for the lined wall and egg crate configuration in the vertical view. Where wall plumbing comes thru a hole in the foam, proper sealing will allow the system to function quite well.

1.3.3.1 Fuel Flow

Aerial refueling represents the high rate of fuel flow seen by aircraft fuel systems. Since the absolute pressure drop is less for the gross voided foam configuration than the fully packed systems which are acceptable, no problems are anticipated. Two previously performed tests of gross voided foam installations in modern figher aircraft fuel systems bear out this conclusion. In these test, maximum refueling flow rates were imposed with and without the gross voided foam system without difficulties or increased refueling time. Fuel flow pressure drop through the smaller pore diameter foam, while greater, is not a problem since the pressure drop is a function of the thickness through which the fuel must pass. Gross voiding drastically reduces the thickness of the 25 ppi foam resulting in a lesser pressure drop than that of the much thicker larger pore diameter foam.

1.3.3.2 Fuel Level Effects

Foam distribution and placement should be designed to insure that the proper relief volume to combustion volume ratio is maintained at all fuel levels.

This is not a problem in any of the single-cell design configurations, however in the case of the multi-cell lined wall configuration, considerations of this requirement needs attention. The multi-cell system utilizes the intercommunicating openings between cells for pressure relief of the ignited cell. Fuel levels limit and in some cases totally eliminate this communication, reducing the system effectively to a single cell which requires additional relief volume, thus more foam. By proportioning the foam such that a greater percentage is located in the top (normal usage volume) of the tank, the problem disappears. Such a system has been designed and qualified on an advanced fighter aircraft.

1.3.4 Installation Considerations

Two types of installation are of concern; new aircraft and retrofit gross voided foam systems.

1.3.4.1 New Aircraft Systems

In the case of new aircraft, greater design latitude and free access to the tanks reduce the installation problems. Of the gross voided foam configurations under consideration, the lined wall and egg crate multicell (wing tank) system is the most difficult to install. Isolation of each cell requires tedious design to insure the minimum thickness of foam in all flame paths and to obtain seals around all pass through components including bracketry and gang nut channels. Fuel transfer holes and tank venting holes between compartments are particularly difficult in that the wing skins form part of the perifery of the holes and fasteners are nearly always present. These problems are not insurmountable, but do present an engineering design problem. The engineering effort is well worth it however, in that 80 to 90% voiding is possible as compared to the 40 to 60% voiding available when using hollow free bodies.

1.3.4.2 Retrofit Systems

The retrofit case is quite different. Access to tanks particularly wing tanks generally is difficult and in some cases requires major aircraft structure re-work. Here for the sake of simplicity, the hollow body configuration is particularly well suited. The hollow bodies can be compressed to pass through small openings and possibly even be strung to facilitate removal. Random hollow body orientation which occurs through this method of packing could interfere with fuel system components, but this should not be a major problem since all mechanical equipment is made accessible due to maintenance requirements. Removal of the component to place a nylon or some other material cage around the critical sites will alleviate the problem. Uniform distribution of the hollow bodies in all cells is not necessary, nevertheless, a good degree of uniformity should be strived for.

TABLE XXI
Phase I System Void Percentages

Fuselage Tanks (100 gallons)			
Configuration	0 PSIG	2 PSIG	5 PSIG
0% Lined Wall	43.0%	40.0%	37.0%
10% Voided Lined Wall	53.0%	52.0%	47.5%
15% Voided Lined Wall	47.5%	44.5%	-
25% Voided Lined Wall	44.5%	-	-
15" Dia. Cylinders	58.5%	42.0%	-
15 Dia. Cylinders Flat Ends	50.5%	35.0%	23.0%
7.5" Dia. Cylinders Hemi. Ends	50.5%	45.0%	32.5%
10% Voided Lined Wall (15 PPI)	29.0%	-	-

6 Cell Wing Tank (50 gallons each)			
Lined Wall	80.0%+	80.0%+	80.0%+
Egg Crate (1" Wall)	92.0%	87.0%	79.0%
15" Dia. Cylinders	59.0%		
7.5" Dia. Cylinders Hemi. Ends.	70.0%	40.0%	-

3 Cell Wing Tank (100 gallon each)			
Lined Wall	35-45% *	-	-
Egg Crate	40.0%+	30.0%+	50.0%+

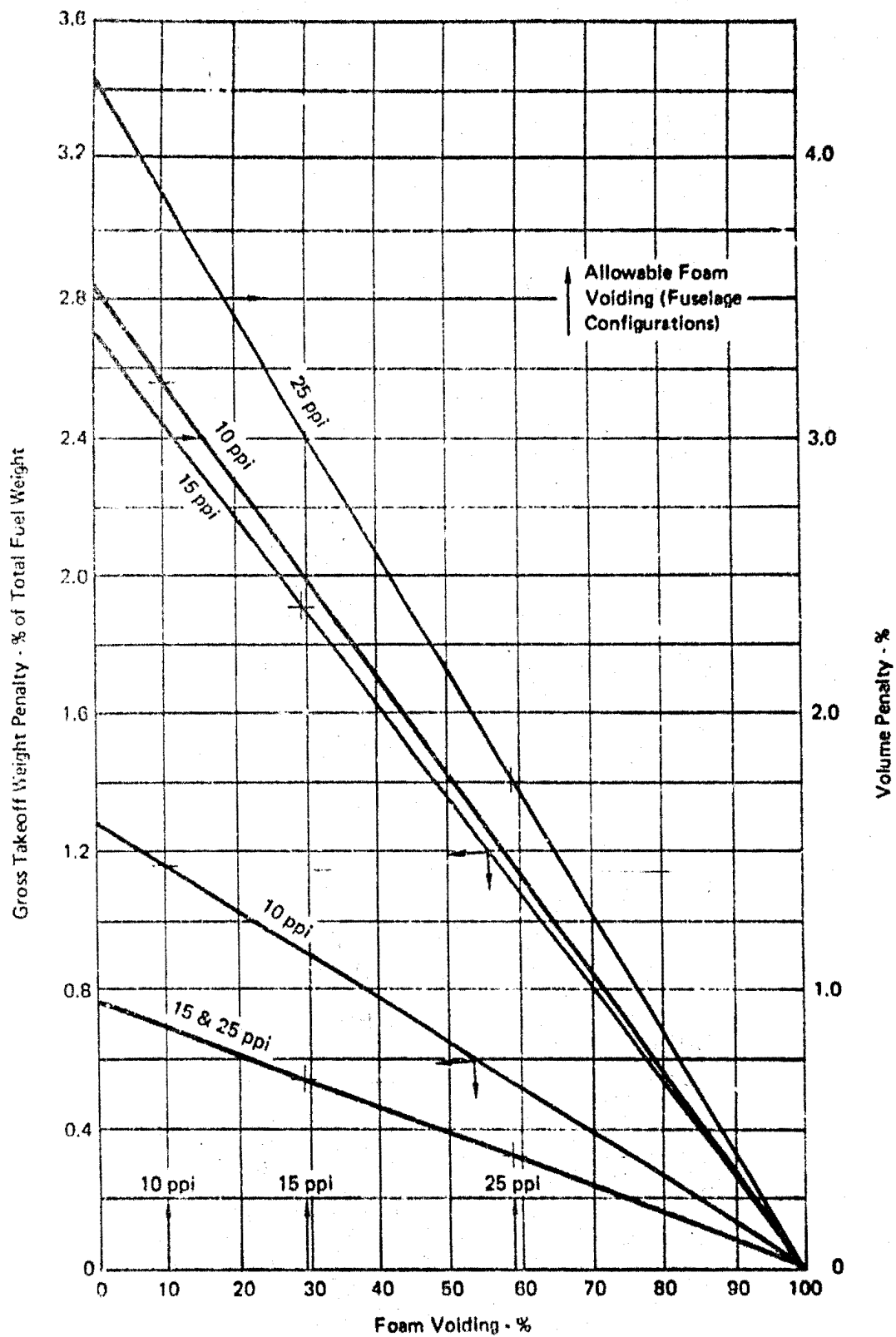Progressive Failure Press Build Up Depends on number and size of Cells.

FIGURE 69   FOAM WEIGHT AND VOLUME PENALTIES · % OF FUEL vs
FUSELAGE SYSTEM VOIDING

147

RESULTS OF THE CHROMATOGRAPHIC ANALYSIS OF PROPANE SAMPLES

Contaminants	(%)	Detection Limits (%)
Hydrogen	0.138	.0050
Acetylene	.0001	.0001
Ethane	.025	.0001
Propane	91.107	.0001
Butane	8.730	.0001